IEEE Access
Multidisciplinary | Rapid Review | Open Access Journal

SPECIAL SECTION ON MILLIMETER-WAVE COMMUNICATIONS: NEW RESEARCH TRENDS AND CHALLENGES

Received June 22, 2019, accepted July 12, 2019, date of publication July 16, 2019, date of current version September 4, 2019.

Digital Object Identifier 10.1109/ACCESS.2019.2929241

A Survey on 5G Millimeter Wave Communications for UAV-Assisted Wireless Networks

LONG ZHANG[1], (Member, IEEE), HUI ZHAO[1], SHUAI HOU[1], ZHEN ZHAO[1], HAITAO XU[2], (Member, IEEE), XIAOBO WU[3], QIWU WU[4], AND RONGHUI ZHANG[5]

[1]School of Information and Electrical Engineering, Hebei University of Engineering, Handan 056038, China
[2]School of Computer and Communication Engineering, University of Science and Technology Beijing, Beijing 100083, China
[3]China Academy of Transportation Sciences, Beijing 100029, China
[4]Department of Armaments Management and Support, Engineering University of PAP, Xi'an 710086, China
[5]Guangdong Key Laboratory of Intelligent Transportation System, School of Intelligent Systems Engineering, Sun Yat-sen University, Guangzhou 510275, China

Corresponding authors: Long Zhang (zhanglong@hebeu.edu.cn) and Hui Zhao (zhaohui_0507@hotmail.com)

This work was supported in part by the National Natural Science Foundation of China under Grant 61501406, Grant 51775565, and Grant 61802107, in part by the Research Program for Top-Notch Young Talents of Hebei Province, China, under Grant BJ2017037, in part by the Natural Science Foundation of Hebei Province under Grant F2019402206, Grant E2017402115, Grant F2017402068, and Grant F2018402198, and in part by the Natural Science Foundation of Guangdong Province under Grant 2018A030313492.

ABSTRACT In recent years, unmanned aerial vehicles (UAVs) have received considerable attention from regulators, industry and research community, due to rapid growth in a broad range of applications. Particularly, UAVs are being used to provide a promising solution to reliable and cost-effective wireless communications from the sky. The deployment of UAVs has been regarded as an alternative complement of existing cellular systems, to achieve higher transmission efficiency with enhanced coverage and capacity. However, heavily utilized microwave spectrum bands below 6 GHz utilized by legacy wireless systems are insufficient to attain remarkable data rate enhancement for numerous emerging applications. To resolve the spectrum crunch crisis and satisfy the requirements of 5G and beyond mobile communications, one potential solution is to use the abundance of unoccupied bandwidth available at millimeter wave (mmWave) frequencies. Inspired by the technique potentials, mmWave communications have also paved the way into the widespread use of UAVs to assist wireless networks for future 5G and beyond wireless applications. In this paper, we provide a comprehensive survey on current achievements in the integration of 5G mmWave communications into UAV-assisted wireless networks. More precisely, a taxonomy to classify the existing research issues is presented, by considering seven cutting-edge solutions. Subsequently, we provide a brief overview of 5G mmWave communications for UAV-assisted wireless networks from two aspects, i.e., key technical advantages and challenges as well as potential applications. Based on the proposed taxonomy, we further discuss in detail the state-of-the-art issues, solutions, and open challenges for this newly emerging area. Lastly, we complete this survey by pointing out open issues and shedding new light on future directions for further research on this area.

INDEX TERMS Millimeter wave (mmWave) communications, unmanned aerial vehicle (UAV), mmWave UAV communications, UAV-assisted wireless networks, 5G and beyond.

I. INTRODUCTION

Unmanned aerial vehicles (UAVs), popularly known as drones, refer to a class of aircrafts that operates without a human pilot aboard. The flight of UAVs can be realized with various degrees of autonomy: either under the remote control by a human operator or autonomously by the onboard sensors and computers. Due to their capability to hover, sufficient flexibility, ease of deployment, higher maneuverability, lower operating and maintenance costs, UAVs have attracted significant attention recently for both civilian and commercial applications. They are being used in a broad range of ways ranging from precision agriculture, smart logistics, law enforcement, disaster response, prehospital emergency care,

The associate editor coordinating the review of this article and approving it for publication was Zhenyu Xiao.

and mineral exploration, to personal business drone-based photography and drone racing [1]–[6]. For instance, Amazon is projected to own nearly 450,000 commercial drones in its delivery fleet by 2020 under the proposed "Amazon Prime Air" service, operating with delivery worldwide [7].

Meanwhile, the advent of a new generation of highly capable UAVs has also led to plenty of interest in the use of UAVs to provide reliable and cost-effective solutions for wireless communications in many real-world scenarios [8]–[14]. In particular, by the aid of wireless communication modules, UAVs can be rapidly deployed as flying base stations (BSs) in three-dimensional (3D) space. The aerial deployment has been regarded as a promising way to provide ubiquitous access from the sky towards ground user equipments (UEs) in specified areas during temporary events (e.g., hotspot areas and large public venues) [8], [12], [13], [15]–[18]. Compared with terrestrial static BSs, one unmatched advantage of using UAV-based flying BSs is that their positions and altitudes can be dynamically adjusted to provide on-the-fly air-to-ground (A2G) communication links. The placement of flying BSs has been viewed as an effective complement of existing cellular systems to enhance wireless capacity and coverage footprint on the ground with ultra dense traffic demands, to meet the requirements of the fifth generation (5G) and beyond 5G (B5G) cellular mobile communications. As a consequence of practical demands, several drone programs about aerial BSs[1] from industrial communities have already been initiated, e.g., AT&T's all-weather flying COW (Cell on Wings) to provide the Long Term Evolution (LTE) coverage of the fourth generation (4G) cellular systems, Verizon's Airborne LTE Operations (ALO) initiative to enable the access to wireless connectivity, Nokia Bell Labs' F-Cell (flying-cell) to enable the "drop and forget" small cell deployment anywhere, Facebook's Aquila using the solar-powered drone to blast Internet to underserved areas via laser communications, etc.

On the other hand, UAVs can be utilized as mobile relays to provide wireless connectivity for partitioned ground UEs without any direct line-of-sight (LOS) transmission links because of the blocking of physical obstacles like mountains or buildings [9], [19]. Given this scenario, the load-carry-and-deliver forwarding strategy is well tailored to the use of a single UAV to relay data packets from one source UE to another destination UE, aiming to achieve higher system throughput [20]. From the perspective of aerodynamics characteristics, the distinct features of various mainstream drones, such as flying altitude, energy resource, maximum payload, and endurance time, will necessitate the configuration of multi-tier architecture for future drone-cell networks [12], [21]–[23]. It has been further highlighted that the coordination, collaboration, and self-organizing flocking behavior of multiple UAVs under this architecture can create flying ad hoc networks (FANETs), Internet of Drones (IoD), and even drone swarm like a flock of birds which is beyond the capability of one single UAV [24]–[28]. Technically, the integration of collective intelligence into the drone swarm will ultimately bring lots of benefits for 5G cellular mobile systems, e.g., higher downlink spectral efficiency and better quality of experience (QoE) for ground UEs.

From all the above realistic applications of interest, we can observe that the widespread use of UAVs has exerted an important influence on wireless networking. The networking strategy by employing one single UAV or multiple UAVs to assist wireless networks has attracted even more attention from both academia and industry. Beyond that, several other typical applications about UAV-assisted wireless networks include wireless sensor networks (WSNs) [29], vehicle-to-everything (V2X) communications [30], Internet of Things (IoT) [31], flyMesh [32], wireless powered networks [33], caching aided wireless networks [34], mobile edge computing (MEC) [35], [36], cloud radio access networks (CRANs) [37], emergency networks [38], device-to-device (D2D) communications [19], cognitive radio (CR) networks [39], etc. In addition to the role of classic aerial BS, the part played by UAVs in these application scenarios has covered various networking entities such as aerial relay, aerial data collector, aerial caching, aerial MEC server, aerial power source, and so on. These representative applications by leveraging one single UAV or multiple UAVs to assist wireless networks are summarized in Table 1 for the ease of reference.

In the past few years, the rapid proliferation of massive number of internet-connected things (e.g., smart devices, industrial sensors, driverless cars, connected factories, etc.), and their various emerging applications (e.g., ultra-high definition video, artificial intelligence, face recognition, Tactile Internet, augmented reality (AR), virtual reality (VR), broadband kiosks, cloud gaming, autonomous driving, etc.) have propelled the explosive growth in wireless data traffic. However, radio spectrum resources in legacy cellular systems and conventional wireless local area networks (WLANs) based on IEEE 802.11 standards[2] that are all operating in the microwave frequency bands below 6 GHz frequencies have been already heavily utilized. There is more and more concern about limited spectrum available for use relative to the exponentially growing data capacity demand. Several enabling techniques have been proposed to achieve enhanced network capacity and higher spectral efficiency for future cellular systems, e.g., massive multiple-input and multiple-output (MIMO) [40], cognitive radio [41], network densification [42], non-orthogonal multiple access (NOMA) [43], advanced channel coding and modulation [44], cooperative relaying [45], etc. Neverthe-

[1]Throughout this paper, the terms "aerial BS" and "flying BS" can be used interchangeably.

[2]Here the IEEE 802.11 standards refer to the set of WLAN protocols that specifies the set of media access control (MAC) and physical layer (PHY) specifications. In this work, this set of standards does not contain the recent most expected WLAN technologies for ultra-high-speed communications, e.g., IEEE 802.11ad and IEEE 802.11ay operating at unlicensed 60 GHz mmWave frequency, which are still requesting proposals from regulators, industry and research community.

TABLE 1. Summary of typical applications of UAV-assisted wireless networks.

Typical Application Direction	Role of UAV	Achieved Function for UAV	Reference
Wireless cellular networks	Aerial BS	Ubiquitous coverage and access	[12], [15]–[17]
Wireless relay networks	Aerial relay	Wireless connectivity	[9], [19]
Multi-tier air-ground networks	Aerial BS	Higher downlink spectral efficiency	[12], [21], [22]
Flying ad hoc networks	Aerial drone swarm	Enhanced usage efficiency of single UAV	[24], [26]
Wireless sensor networks	Aerial data collector	Data collection and dissemination	[29]
V2X communications	Aerial RSU/relay/radio access	V2X applications	[30]
Internet of Things	Aerial IoT device	Intelligent applications	[31]
FlyMesh	Aerial relay	Coverage and fully connected UAV networks	[32]
Wireless powered networks	Aerial power source	Wireless power transfer	[33]
Caching aided wireless networks	Aerial caching	Reduced wireless backhaul load	[34]
Mobile edge computing	Aerial MEC server	Dynamic deployment of edges	[35], [36]
Cloud radio access networks	Aerial radio access/caching	Wireless connectivity and caching distribution	[37]
Emergency networks	Aerial BS/relay	Coverage and information relaying	[38]
D2D communications	Aerial power source	Wireless power transfer	[19]
Cognitive radio networks	Aerial cognitive device	Dynamic spectrum access	[39]

less, those advances will not be an essential step towards tackling the issue of limited available spectrum.

To overcome the spectrum crunch crisis, one potential solution has been to expand the use of higher frequencies in radio spectrum, since large amount of licensed and unlicensed spectrum bands are still available at these frequencies. As such, the expanded use of millimeter wave (mmWave) frequencies, ranging from around 30 GHz to 300 GHz, has been recognized as a promising approach for providing wide available spectrum resources and multiple Gigabit data transmission speeds [46]–[52]. With this incomparable advantage, mmWave communications are indeed more suited to 5G and B5G wireless systems with the requirements of massive data throughput, high wireless bandwidth, super-fast speeds, ultra-low latency, and increased connectivity for a networked society. They will also be dedicated to the support of a wide variety of broadband applications envisioned for Multiple Gigabit Wireless Systems (MGWS) in the frequencies around 60 GHz unlicensed industrial, scientific and medical (ISM) frequency band, and WiGig (wireless Gigabit) network as the 60 GHz Wireless Fidelity (Wi-Fi) solution [53]. In addition, the use of mmWave communications has been highlighted as a key enabler for 5G New Radio (NR) developed by the Third Generation Partnership Project (3GPP) as a unified air interface to support many user cases expected in 5G, e.g., enhanced Mobile Broadband (eMBB) and Ultra-Reliable Low Latency Communications (URLLC) [54]–[56].

Owing to the promising applications of UAVs to assist wireless networks along with the possibility of multiple Gigabit data transmissions by using 5G mmWave communications, a natural idea is to link UAV-assisted wireless networking and mmWave communications together. Fig. 1 depicts the application scenario of 5G mmWave communications for UAV-assisted wireless networks. In the typical scenario, multiple rotary-wing drones act as flying BSs, aerial radio access points, and aerial relays via A2G mmWave beams to expand wireless coverage footprint and provide multi-Gigabit transmission towards physical objects including ground UEs in 5G systems, and ground vehicles in vehicular networks via vehicle-to-vehicle (V2V) and vehicle-to-infrastructure (V2I) communications. The information exchange and transfer among several drones, e.g., fixed-wing drones and rotary-wing drones, can be achieved through multi-hop drone relaying by means of air-to-air (A2A) mmWave beams. Moreover, drones are deployed as access networks for ground D2D transmitters (TXs) and receivers (RXs) (i.e., D2D pairs) at hotspot areas to provide additional capacity without the support of terrestrial BSs.

There is no doubt that the use of mmWave frequencies will be definitely a very promising way for UAV-assisted wireless networks to sustain ultra-high-speed and real-time transmissions for future 5G and B5G wireless applications. The integration of the merits from these two techniques has inspired their respective advantages:

- MmWave communications for UAV-assisted wireless networks can support higher data rate due to higher bandwidth. It is easier to achieve the peak data rate of up to 10 Gbit/s, which is unlikely to be matched by any wireless technologies with lower microwave frequencies. Conceptually, a large amount of licensed and unlicensed mmWave frequency bands are potentially available for use in UAV-assisted wireless networks, e.g., 28 GHz licensed band and 60 GHz unlicensed ISM band [57].
- Much shorter mmWave wavelength makes it feasible to design the physically smaller mmWave circuits and antennas, which enables to build the beamforming antenna arrays with many antennas to be packed on a chip in a tiny component size [52], [58]. It is perfect for low-altitude short range UAVs with limited payloads.
- Low interference and increased security benefit from the inherently directional mmWave beams and the narrow beamwidth with a high immunity to jamming and eavesdropping [48], [59].

In spite of being advantageous, atmospheric absorption at mmWave wavelengths is a concern of 5G mmWave communications for UAV-assisted wireless networks, thus restricting their transmission range of mmWave signals

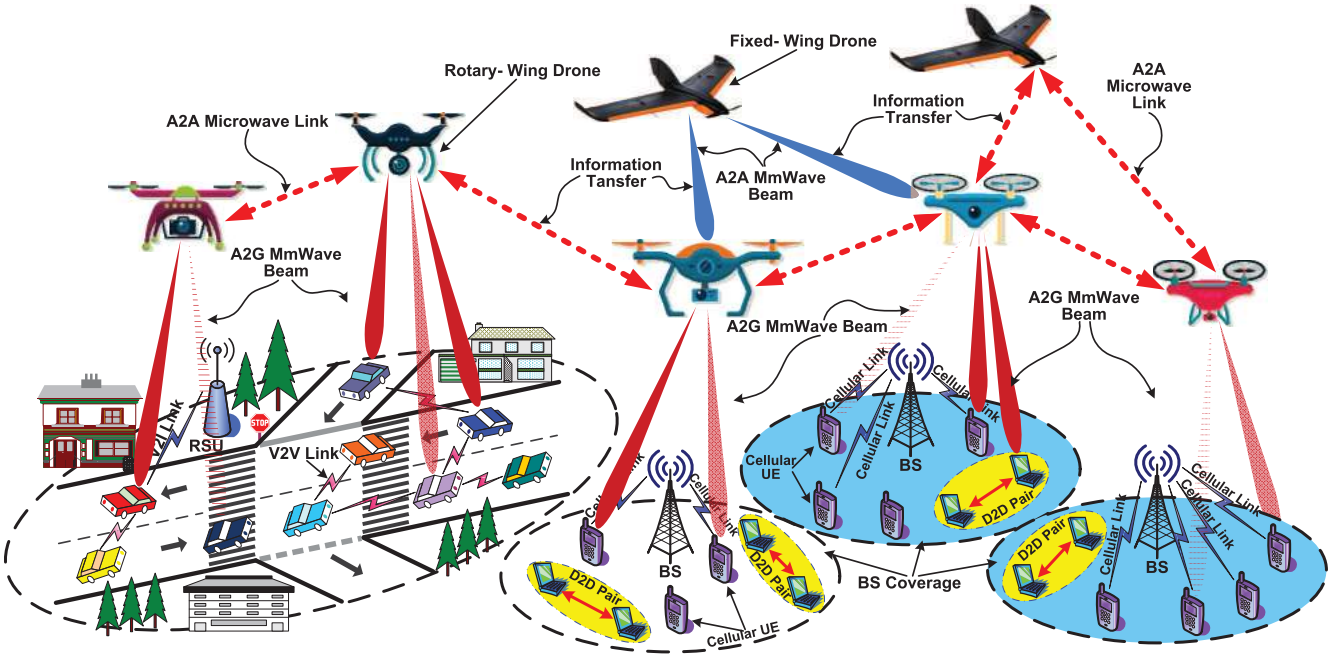

FIGURE 1. Illustration of 5G mmWave communications for UAV-assisted wireless networks.

and resulting in high propagation attenuation at higher mmWave frequencies [60], [61]. Another major technical challenge is blockage effect, when travelling mmWave signals are blocked by physical obstacles in their propagation paths. For instance, human-body blockage [62]–[65] and self-blockage [59] caused by human activity and components of UAV itself, respectively, which poses extra challenges on mmWave LOS propagation. In this paper, we focus on the scenario of the combination of 5G mmWave communications with UAV-assisted wireless networks and the emerging studies related to the integration of these two important areas.

Although UAV-assisted wireless networks and mmWave communications have been studied extensively in previous works, existing surveys and tutorials either cover UAV-assisted wireless networks and UAV communications for 5G and beyond [8], [11], [12], [24], [25], [66]–[68], or concentrate on mmWave communications for 5G and vehicular communications [48]–[50], [69]–[73]. Those existing contributions are still separated across these two important areas. To the best of our knowledge, only two existing survey papers in [10], [66] are related to mmWave communications for UAV-assisted wireless networks. Nevertheless, the work in [66] by Li *et al*. just shortly review the technology challenges and existing solutions for mmWave UAV-assisted cellular networks as one of physical layer techniques over the entire topic focused on. Although the work in [10] by Xiao *et al*. discussed the major technical challenges and possible solutions in mmWave UAV cellular systems for the first time, they did not fully cover the detailed progress of the state-of-the-art comprehensively. This motivates us to deliver a detailed survey with the objective to give a comprehensive summary of current achievements in the integration of 5G mmWave communications into UAV-assisted wireless networks, and to discuss the state-of-the-art issues, solutions, and open challenges in this newly emerging area. In this survey, a taxonomy graph to classify the related research issues based on the existing literatures is presented in Fig. 2. As displayed in Fig. 2, we will discuss seven important research issues that we would like to be targeted at: antenna technique, radio propagation channel, multiple access mechanism, spatial configuration, resource management, security strategy, and performance assessment. To the authors' best knowledge, this paper is the first comprehensive effort to review the cutting-edge solutions related with 5G mmWave communications for UAV-assisted wireless networks in a holistic way. With this survey, our objective is to provide readers with an overall understanding of what has been accomplished so far, in the area of 5G mmWave communications for UAV-assisted wireless networks, and to open up new perspectives for subsequent studies on this area.

For convenience, a list of acronyms used in this paper is provided in Table 2. The remainder of the paper is organized as follows. Firstly, existing surveys and tutorials related to UAV-assisted wireless networks and communications along with 5G mmWave communications are discussed and compared with our survey in Section II. Section III presents the brief overview of 5G mmWave communications for UAV-assisted wireless networks including key technical advantages and challenges of 5G mmWave communications, and brief Introduction to the integration

TABLE 2. List of acronyms.

Acronym	Meaning	Acronym	Meaning
2D	Two-Dimensional Space	LTE	Long Term Evolution
3D	Three-Dimensional Space	MAC	Media Access Control
3GPP	Third Generation Partnership Project	MBH	Multi-Beam Horn
4G	Fourth Generation Cellular Mobile Communications	MEC	Mobile Edge Computing
5G	Fifth Generation Cellular Mobile Communications	MGWS	Multiple Gigabit Wireless Systems
6G	Sixth Generation Mobile Systems	MIMO	Multiple-Input and Multiple-Output
A2A	Air-to-Air	MINLP	Mixed Integer Non-Linear Programming
A2G	Air-to-Ground	ML	Maximum Likelihood
AAN	Aerial Access Network	MS	Mobile Station
ALO	Airborne LTE Operations	MSE	Mean Square Error
AN	Artificial Noise	MmWave	Millimeter Wave
AoA	Angle of Arrival	NFV	Network Functions Virtualization
AoD	Angle of Departure	NLOS	Non-Line-of-Sight
AP	Access Point	NOMA	Non-Orthogonal Multiple Access
AR	Augmented Reality	NR	New Radio
AWV	Antenna Weight Vector	OFDM	Orthogonal Frequency Division Multiplexing
BBU	Baseband Unit	OMA	Orthogonal Multiple Access
BDMA	Beam Division Multiple Access	PDF	Probability Density Function
B5G	Beyond 5G Cellular Mobile Communications	PHY	Physical Layer
BS	Base Station	QoE	Quality of Experience
CCDF	Complementary Cumulative Distribution Function	QoS	Quality of Service
CDF	Cumulative Distribution Function	RF	Radio Frequency
COW	Cell on Wings	RRH	Remote Radio Head
CPS	Cyber Physical System	RSS	Received Signal Strength
CR	Cognitive Radio	RSU	Road Side Unit
CRAN	Cloud Radio Access Network	RX	Receiver
CSI	Channel State Information	SBS	Small Base Station
D2D	Device-to-Device	SDMA	Spatial-Division Multiple Access
DBF	Digital Beamforming	SINR	Signal-to-Interference-Plus-Noise Ratio
DM	Directional Modulation	SPF	Stratospheric-Platform
DoA	Direction of Arrival	TDMA	Time-Division Multiple Access
EH	Energy Harvesting	ToA	Time of Arrival
EHF	Extremely High Frequency	TR	Tensor Recovery
ELSM	Echo Liquid State Machine	TX	Transmitter
eMBB	enhanced Mobile Broadband	UAV	Unmanned Aerial Vehicle
F-Cell	Flying-Cell	UCA	Uniform Circular Array
ESN	Echo State Network	UE	User Equipment
FANET	Flying Ad Hoc Network	ULA	Uniform Linear Array
FCC	Federal Communications Commission	UPA	Uniform Planar Array
G2A	Ground-to-Air	URA	Uniform Rectangular Array
G2G	Ground-to-Ground	URLLC	Ultra-Reliable Low Latency Communications
GMT	Ground Mobile Terminal	USRP	Universal Serial Radio Peripheral
HAPS	High-Altitude Platform Station	UUV	Unmanned Underwater Vehicle
HetNet	Heterogeneous Network	V2I	Vehicle-to-Infrastructure
IoD	Internet of Drones	V2V	Vehicle-to-Vehicle
IoE	Internet of Everything	V2X	Vehicle-to-Everything
IoT	Internet of Things	VLEO	Very Low Earth Orbit
ISM	Industrial, Scientific and Medical	VR	Virtual Reality
ITU	International Telecommunication Union	WiGig	Wireless Gigabit
KNN	K-Nearest Neighbor	Wi-Fi	Wireless Fidelity
LOP	Line-of-Propagation	WLAN	Wireless Local Area Network
LOS	Line-of-Sight	WSN	Wireless Sensor Network
LSM	Liquid State Machine	XR	eXtended Reality

of 5G mmWave communications into UAV-assisted wireless networks. In Section IV, we comprehensively review the state-of-the-art research issues and challenges from the perspective of the taxonomy of the related research issues. Then Section V summarizes the current research and proposes the open issues together with the future research directions. Finally, Section VI concludes the paper. For the sake of clear presentation, the organizational structure of this paper in a top-down manner is exhibited in Fig. 3.

Notations: Throughout this paper, we use a, $\mathbf{a}$, $\mathbf{A}$, and $\mathcal{A}$ to denote a scalar variable, a vector, a matrix, and a set, respectively. The cardinality for a set $\mathcal{A}$ is denoted by $|\mathcal{A}|$. Further, $(\cdot)^*$ and $(\cdot)^H$ denote conjugate and Hermitian (conjugate transpose), respectively. We use $[a]^+$ to represent the maximum value between 0 and variable a, i.e., $[a]^+ = \max\{a, 0\}$. The set of real numbers is denoted by $\mathbb{R}$. The operator $\mathbb{E}[\cdot]$ is the expectation operation, and the operator $\mathrm{Var}[\cdot]$ is the variance operation. The distribution of a circularly symmetric complex Gaussian random variable x with mean Σ and covariance Λ is represented by $x \sim \mathcal{CN}(\Sigma, \Lambda)$, where $\sim$ stands for "distributed as". We employ $PL(d)$ to denote the free space path loss measured in dB from TX to RX over

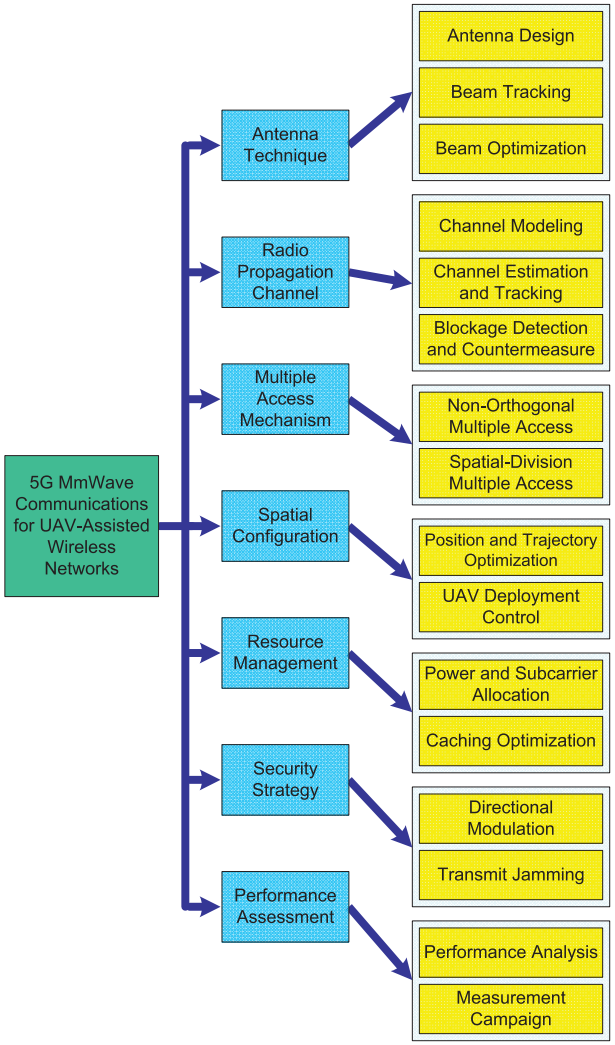

FIGURE 2. Taxonomy of related research issues in 5G mmWave communications for UAV-assisted wireless networks.

a distance d. In addition, $|\cdot|$ and $\|\cdot\|$ stand for the absolute value of a scalar variable and the Euclidean distance between the pair of vectors, respectively. Finally, $F_\zeta(\cdot)$ is the Fejér kernel of order ζ and $\Gamma(z) = \int_0^\infty x^{z-1}e^{-x}dx$ is the Gamma function.

II. REVIEW OF EXISTING SURVEYS AND TUTORIALS

In this section, we will present the existing surveys and tutorials, including UAV-assisted wireless networks and communications as well as 5G mmWave communications. Moreover, the comparison of this paper with existing surveys and tutorials will be also summarized.

A. UAV-ASSISTED WIRELESS NETWORKS AND COMMUNICATIONS

During the past few years, a number of excellent surveys and tutorials have been reported to be published in the fields of UAV-assisted wireless networks and UAV communications for 5G and B5G wireless systems. Mozaffari *et al.* [8] presented a comprehensive tutorial on UAV-enabled wireless communications and networking applications, and provided the insightful comments to some important research opportunities and challenges in flying BSs. The analytical frameworks and optimization tools were proposed to deal with the challenging open problems towards UAV communications and networking. Gupta *et al.* [25] briefly discussed the challenges to effectively design stable and reliable context-specific UAV networks according to their inherent features. The authors put more emphasis on the problems of routing, seamless handover, and energy efficiency in UAV networks. With relation to routing mechanism, Jiang and Han [74] carried out a brief survey on routing protocols for UAVs based on hop counts, i.e., single-hop and multi-hop routing. Besides, position-based routing protocols and cluster-based routing protocols for UAV networks were extensively surveyed and compared by Oubbati *et al.* [75] and Arafat and Moh [76], respectively.

By integrating UAVs into cellular networks, Fotouhi *et al.* [11] conducted a comprehensive survey on some major networking issues about UAV cellular communications, such as standardization efforts for aerial UE, deployment of aerial BSs, drone communication prototypes, security and so forth. Li *et al.* [66] presented a comprehensive survey on key techniques for UAV communication towards 5G and B5G wireless networks from three aspects involving physical layer, network layer, and joint communication, computing and caching. Particularly, mmWave communications as a key technology at physical layer of UAV-assisted cellular networks was briefly discussed. From the perspective of cyber physical system (CPS), Wang *et al.* [67] carried out a systematic review of UAV networks, with an emphasis on the impact of CPS components on the system performance of UAV networks. A survey on wireless communications, evaluation tools and applications in unmanned aerial and aquatic vehicle multi-hop networks was described in the literature by Sánchez-García *et al.* [68]. Similar to UAV multi-hop networks, Bekmezci *et al.* [24] presented a survey on communication protocols from four layers and cross-layer interactions in FANET which is typically a kind of ad hoc networks. Driven by future drone-cell networks, Sekander *et al.* [12] reviewed the existing innovations in drone networks and drone-assisted cellular networks, and proposed the multi-tier drone network architecture over the conventional single-tier drone networks.

In addition to these surveys and tutorials on UAV networks [25], [67], [68], UAV cellular networks [11], [66], UAV-enabled wireless networks [8], FANETs [24], and multi-tier drone networks [12], several other surveys have also been published on different topics with regard to UAV-related networks and communications, such as channel modeling [77], civil applications [1], [78], UAV-assisted vehicular networks [30], wireless charging techniques [79], IoT services [6], game-theoretic optimization approach [80], CR-based UAV [39], etc.

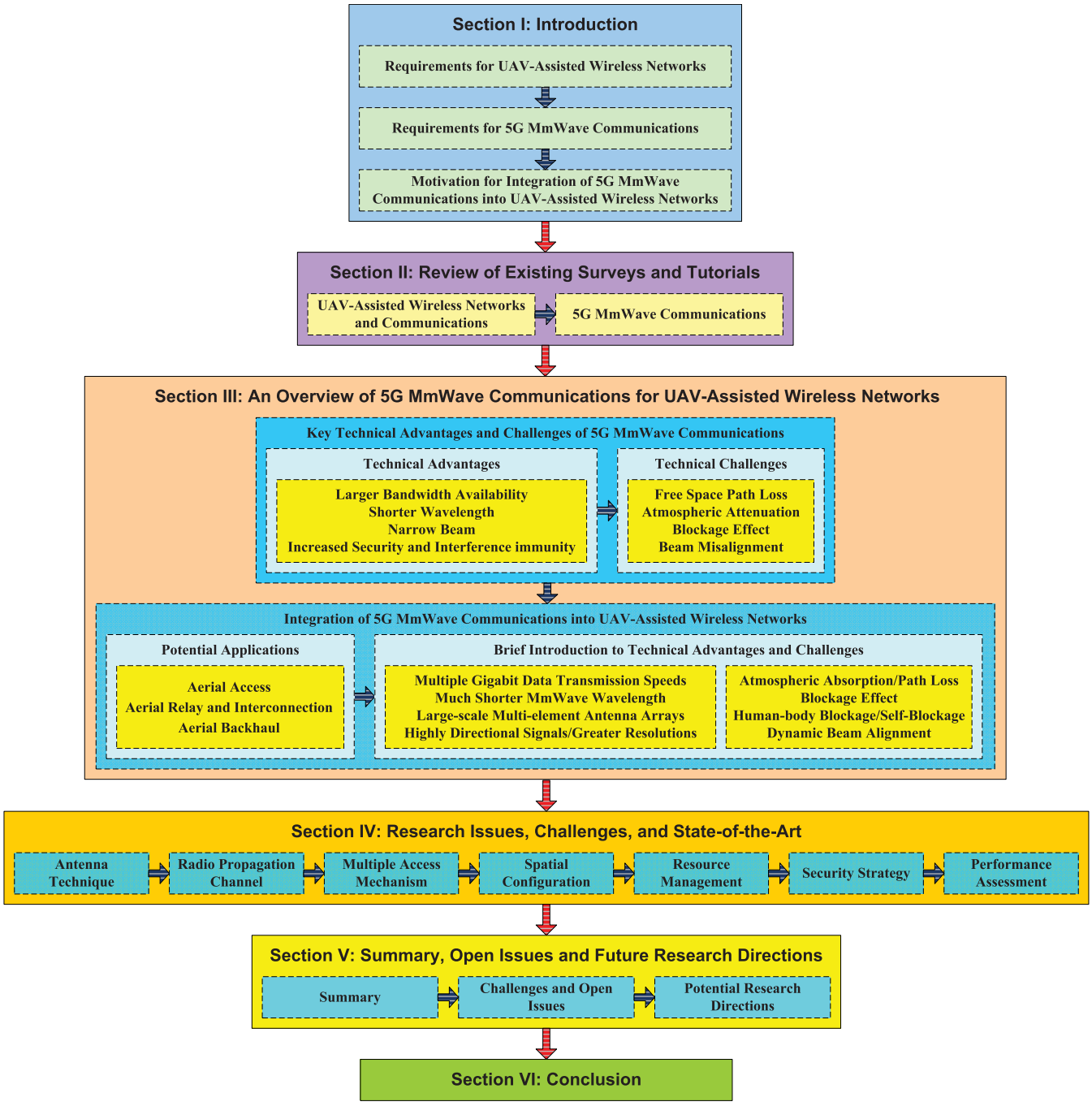

FIGURE 3. The organizational structure of this paper.

B. 5G mmWave COMMUNICATIONS

Many other existing survey papers have been dedicated to mmWave communications for 5G wireless systems and vehicular communications. By surveying the recent channel measurements of mmWave signals in urban environments, Rangan *et al.* [69] elaborated on several techniques including adaptive beamforming, multi-hop relaying, heterogeneous network (HetNet) architectures, and carrier aggregation in the context of mmWave cellular wireless networks. Xiao *et al.* [48] gave a systematic survey on main technical progress of mmWave communications for 5G and B5G mobile networks. The authors focused primarily on mmWave channel measurement campaigns and modeling, mmWave MIMO systems, multiple-access technologies, mmWave bands for backhauling, etc. Furthermore, Niu *et al.* [49] conducted a survey on existing research progress in 5G mmWave communications. The authors mainly discussed the peculiar characteristics,

TABLE 3. A brief comparison of our study with existing survey papers and tutorials.

Survey Paper	Year	Topic Focused On	Main Issues Elaborated and Addressed	MmWave-UAV
Bekmezci *et al.* [24]	2013	Flying ad hoc networks	FANET application scenarios, design characteristics, communication protocols, test beds and simulators	Not covered
Rappaport *et al.* [50]	2013	MmWave communications for 5G and B5G mobile networks	MmWave propagation measurement campaigns	Not covered
Rangan et al. [69]	2014	MmWave cellular wireless networks	Channel measurements, adaptive beamforming, multi-hop relaying, heterogeneous network architectures, and carrier aggregation	Not covered
Niu *et al.* [49]	2015	MmWave communications for 5G mobile networks	Peculiar characteristics, research challenges, and potential applications of mmWave communications	Not covered
Gupta *et al.* [25]	2016	Important issues in UAV communication networks	Routing, seamless handover, and energy efficiency	Not covered
Xiao *et al.* [10]	2016	*UAV cellular networks with mmWave communications*	MmWave channel propagation characteristics, fast beamforming training and tracking, mmWave SDMA, blockage problems, and directional user discovery	Covered
Xiao *et al.* [48]	2017	MmWave communications for 5G and B5G mobile networks	MmWave channel measurement campaigns and modeling, mmWave MIMO systems, multiple-access technologies, and mmWave bands for backhauling	Not covered
Rappaport *et al.* [71]	2017	MmWave communications for 5G and B5G mobile networks	MmWave propagation models	Not covered
Mozaffari *et al.* [8]	2018	UAV-enabled wireless communications and networks	Application scenarios, key research directions, challenging open problems, and summary of analytical frameworks	Not covered
Fotouhi *et al.* [11]	2018	UAV cellular communications	Standardization efforts for aerial UE, deployment of aerial BSs, drone communication prototypes, UAV regulations, and security	Not covered
Sekander *et al.* [12]	2018	Multi-tier drone network architecture	Potential challenges, performance optimization of drone-assisted cellular networks, and feasibility analysis of multi-tier drone-aided cellular architecture	Not covered
Wang *et al.* [67]	2018	A CPS perspective for UAV networks	Three CPS components in UAV networks, UAV networks of three CPS hierarchies, and coupling effects in UAV networks	Not covered
Hemadeh *et al.* [70]	2018	MmWave communications for 5G and B5G mobile networks	MmWave propagation characteristics, channel modeling, and design guidelines	Not covered
Sánchez-García *et al.* [68]	2018	UAV and unmanned underwater vehicle (UUV) multi-hop networks	Wireless communications, evaluation tools and application scenarios	Not covered
Zhou *et al.* [72]	2018	IEEE 802.11ay based mmWave WLANs	Channel bonding and aggregation, channel access and allocation, beamforming training and beam tracking, and single-user MIMO and multi-user MIMO beamforming	Not covered
Jameel *et al.* [73]	2019	Propagation channel modeling for mmWave vehicular communications	MmWave channel modeling approaches, channel attributes, and channel models based on three measurement scenarios including V2I, inter-vehicle, and intra-vehicle	Not covered
Li *et al.* [66]	2019	UAV communications for 5G and B5G mobile systems	Physical layer, network layer, joint communication, computing and caching, and *mmWave communications for UAV-assisted cellular networks*	Covered
This survey	2019	*5G mmWave communications for UAV-assisted wireless networks*	Antenna technique, radio propagation channel, multiple access mechanism, spatial configuration, resource management, security strategy, and performance assessment	Covered

research challenges, and potential applications of mmWave communications. Other similar surveys and tutorials on mmWave communications for 5G and B5G were also reported in recent literature [50], [70], [71]. The work of Rappaport *et al.* in [50] focused on mmWave propagation measurement campaigns conducted in New York City, NY with 28 GHz mmWave frequencies and Austin, TX with 38 GHz mmWave frequencies. Also, the surveys carried out by Hemadeh *et al.* [70] and Rappaport *et al.* [71] were both targeted at mmWave propagation characteristics and channel modeling. Faced to the challenges of ultra-high-speed WLANs, Zhou *et al.* [72] presented a comprehensive survey on MAC-related issues, especially channel access for multiple channels and beamforming for both single-user MIMO and multi-user MIMO, for mmWave WLANs based on the IEEE 802.11ay standard. Lastly, Jameel *et al.* [73] briefly discussed the mmWave propagation channel modeling from the perspective of vehicular communications.

Different from all the works as mentioned previously, Xiao *et al.* [10] combined mmWave communications with UAV cellular networks together, and presented a brief overview of key technical challenges and possible solutions in mmWave UAV cellular, including mmWave channel propagation characteristics, fast beamforming training and tracking, mmWave spatial-division multiple access (SDMA), problem of mmWave blockage effect, and directional user discovery. To sum up, as Table 3 shows, we provide a brief comparison of our study with existing survey papers outlined before mainly from three aspects, including topic focused on, main issues elaborated and addressed, and whether the integration of mmWave communications into UAV-assisted wireless networks or not. In Table 3, we use "mmWave-UAV" as the abbreviation to represent the integration of mmWave communications into UAV-assisted wireless networks due to the limited space of this table. In comparison with the aforementioned survey papers, this survey provides

a critical and systematic overview of the up-to-date activities related to research issues on 5G mmWave communications for UAV-assisted wireless networks from the point of view of literature classification.

III. AN OVERVIEW OF 5G mmWave COMMUNICATIONS FOR UAV-ASSISTED WIRELESS NETWORKS

In this section, we will present a brief overview on 5G mmWave communications for UAV-assisted wireless networks. Specifically, we will first introduce the key technique advantages and challenges of 5G mmWave communications. Then the integration of 5G mmWave communications into UAV-assisted wireless networks will be briefly discussed from two aspects, i.e., potential applications as well as main technical advantages and challenges.

A. KEY TECHNICAL ADVANTAGES AND CHALLENGES OF 5G mmWave COMMUNICATIONS

1) TECHNICAL ADVANTAGES

The mmWave communications will play an important role in 5G and B5G wireless systems, due to the ability to support orders of magnitude increases in network capacity. In what follows, we will briefly discuss the key technique advantages of 5G mmWave communications from four perspectives, i.e., larger bandwidth availability, shorter wavelength, narrow beam, and increased security/interference immunity.

a: LARGER BANDWIDTH AVAILABILITY

The mmWave range in the electromagnetic spectrum is usually considered to be the band of spectrum from around 30 GHz to 300 GHz that lies between the microwaves and the infrared waves, also called the Extremely High Frequency (EHF) range. The abundance of unoccupied bandwidth available at mmWave frequencies is one of key advantages of 5G mmWave communications compared to limited microwave spectrum resources below 6 GHz currently used by conventional wireless systems and existing 4G LTE. Particularly, the available bandwidth in mmWave frequency bands of 71 $\sim$ 76 GHz and 81 $\sim$ 86 GHz (widely known as E-band) is more than the sum total of all other licensed spectrum available for existing wireless systems [81]. It is obvious that heavily utilized microwave spectrum below 6 GHz for existing wireless systems is insufficient to attain the Gigabit data transmission speeds. However, there are still huge amount of lightly licensed and unused spectrum resources available at mmWave frequencies reserved for future applications around the world. The larger bandwidth translates to extremely high data rates, easily achieving the peak data rates of 10 Gbit/s or more with full duplex capability, which is much greater than the limit rate of 1 Gbit/s by using lower microwave frequencies [71]. This achievement of remarkable data rate enhancement has been theoretically verified through the Shannon-Hartley theorem showing that the capacity increases linearly with the bandwidth.

In light of the advantage of larger bandwidth availability, a multi-layer spectrum approach was proposed by Huawei, based on the consideration of divergent requirements of 5G services and different characteristics of related frequency bands. The 24.25 $\sim$ 29.5 GHz and 37 $\sim$ 43.5 GHz mmWave frequency bands were specifically selected for early deployment of 5G mmWave systems in accordance with the 3GPP Release 15 [82]. To provide the full-duplex Gigabit Ethernet connectivity at the data rates of 1 Gbit/s or higher, the E-band (i.e., 71 $\sim$ 76 GHz and 81 $\sim$ 86 GHz) was initially allocated by the International Telecommunication Union (ITU) as early as 1979, to support the ultra high capacity point-to-point communications [83]. The ITU and 3GPP also launched a plan for two phases of research for 5G standards, covering two mmWave frequency bands to be used with commercial needs, i.e., 40 GHz and 100 GHz [84]. In 2015, the Federal Communications Commission (FCC) proposed the flexible service rules for the mmWave frequency bands including 28 GHz, 37 GHz, and 39 GHz for licensed usage, and 64 $\sim$ 71 GHz for unlicensed usage [85]. In addition to the ongoing efforts from the regulators and industrial communities, some service providers are all fighting to establish their 5G commercial networks by using the extraordinary amount of bandwidth available at mmWave frequencies. In many instances, AT&T and Verizon have been focused on the 39 GHz and 28 GHz mmWave frequency bands, respectively, for their initial 5G deployments.

b: SHORTER WAVELENGTH

Within the range of the electromagnetic spectrum, higher frequency of electromagnetic wave implies shorter wavelength of wave, which means that more information can be transmitted per unit of time. Compared to microwave signals below 6 GHz previously used by increasingly crowded traditional cellular systems and WLANs, mmWave signals have much shorter wavelengths that span between 10 mm and 1 mm.[3] For example, mmWave signals at 28 GHz, 60 GHz, and 300 GHz have the extremely short wavelengths of 10.7 mm, 5 mm, and 1 mm, respectively. In particular, the wavelengths of mmWave signals at 28 GHz and 73 GHz are nearly 10 $\sim$ 30 times smaller than the wavelength of microwave signal at 2.5 GHz [69]. Additionally, shorter wavelengths for mmWave signals also bring about several distinct benefits:

- **Tiny component sizes**: Compared with lower microwave frequencies, the components and antennas for mmWave frequencies can be designed in tiny physical dimensions owing to smaller millimeter-long wavelengths. Thus, dozens to hundreds of antenna elements are easily packed in an array of tiny size similar to fingernail, which makes it feasible to miniaturize physically smaller circuits, modules, and equipments for 5G mmWave applications [50], [52], [58], [69]. A typical

[3]Note that the range of the wavelengths between 10 mm and 1 mm exactly corresponds to the mmWave frequencies between 30 GHz and 300 GHz. Actually, the wavelengths of the mmWave signals may be slightly larger than 10 mm due to the adopted 28 GHz mmWave frequency band.

FIGURE 4. The comparison of size scale between a one-cent coin and two QTM052 mmWave antenna modules announced in July and October 2018, respectively. (Image source: Qualcomm Technologies, Inc. [86]).

half-wave dipole at 900 MHz is 152.4 mm long, but it is only 2.5 mm at 60 GHz in free space or even less when built on a dielectric substrate [87]. More recently, Qualcomm designed and developed the world's first fully-integrated 5G NR mmWave antenna module QTM052 for next generation smartphones and mobile devices. The antenna module packs a tiny phased antenna array with a compact dimension, roughly the size of a one-cent coin, as shown in Fig. 4. With these smaller antenna modules, equipment manufacturers will have more options for antenna placement, providing them with more freedom and flexibility in the design of 5G NR devices, e.g., more space for batteries and more choices for smaller smartphones.

- **Higher antenna gains**: Based on the electromagnetics and antenna theory, shorter wavelengths of mmWave signals can obtain proportionally higher antenna gains under the given effective antenna aperture. Because of smaller physical dimensions at mmWave frequencies, the application of large-scale multi-element antenna arrays enables greater antenna gain and achieves highly directional beamforming. Through the configuration of a pair of transmit antennas with the same aperture areas and the equal transmit power, 30 dB more gain can be achieved at 80 GHz mmWave beam compared to that of 2.4 GHz microwave frequency [70]. With the fully digital processing, massive MIMO can be integrated to achieve large beamforming gains [88]–[90].

c: NARROW BEAM

By jointly combining digital precoding and analog beamforming, shorter wavelengths of mmWave signals enable the integration of massive MIMO with dozens to hundreds of antenna elements to be packed into a small space at mmWave transceivers. The antennas can steer mmWave beams rapidly in different directions. According to the electromagnetics and antenna theory, the increased frequencies result in the decreased beamwidth. As a result, highly directional steerable narrow beams can be formed for mmWave antenna arrays to direct the transmit power precisely towards the intended users along a desired direction [91]. It has been suggested that beam orientation of mmWave signals can be optimized, aiming to reduce the energy loss during transmission. Therefore, mmWave antennas with narrow directional beams can send and receive much more energy to compensate for stronger propagation attenuation and higher free space path loss of mmWave signals. These characteristics make mmWave communications be more specifically suited to ultra high capacity point-to-point transmission. Moreover, another major advantage of the formed narrow beamwidth is spatial reuse over the same spectrum to simultaneously serve multiple users with different radios within a specific small geographical area. It is further revealed that system capacity has an apparent enhancement by employing mmWave antennas with narrow beamwidth than the capacity by using wider beamwidth antennas of microwave frequencies [92].

d: INCREASED SECURITY AND INTERFERENCE IMMUNITY

In contrast to the congested spectrum and the easily intercepted signals caused by wide beams at lower microwave frequencies below 6 GHz, narrow beams of mmWave signals allow the ability to obtain highly directional signals and greater resolutions. When malicious eavesdroppers want to intercept and decode the confidential messages successfully, they need to physically be within the transmission path of mmWave signals with narrow beams. With the help of complicated and high-cost hardware equipments as well as accurate location, eavesdroppers may have the possibility to intercept mmWave signals. Obviously, the inherent benefits including highly directional beams and greater resolutions make the interception of mmWave signals much more difficult and costly because mmWave signals are only restricted to a relatively small area. Therefore, the security of mmWave communications and the privacy of mmWave users can be enhanced, by protecting the sensitive and legitimate messages from passively eavesdropping and actively jamming [48], [59], [93]. Additionally, narrow beams also make mmWave transmission highly immune to interference and noise at the receiving end due to the capability to focus their transmit power levels of mmWave signals.

2) TECHNICAL CHALLENGES

Despite many attracting technique benefits and potentials for 5G mmWave communications, there still have several challenges and limitations that we should try to overcome for mobilizing mmWave.

a: FREE SPACE PATH LOSS

The free space path loss is the loss in signal strength of a signal in terms of radio energy when it travels between the feedpoints of two antennas through free space (i.e., unobstructed LOS channels in the air) [94]. The signal strength of a signal can be measured as the transmitter power output received by a receiving antenna at a transmission distance from the transmitting antenna. We generally employ the Friis transmission equation as follows to calculate the power (denoted by P_R) received from a receiving antenna with gain G_R, when

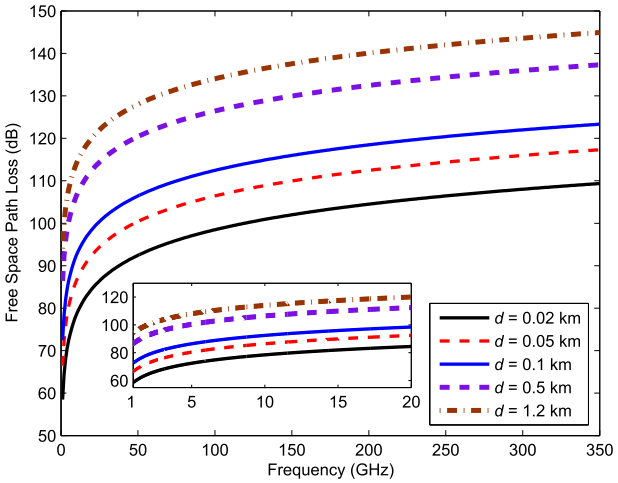

FIGURE 5. The free space path loss at microwave and mmWave frequencies under different transmission distances.

transmitted from the transmitting antenna with gain G_T [95]:

$$\frac{P_R}{P_T} = G_T G_R d^{-n} \left(\frac{\lambda}{4\pi}\right)^2, \quad (1)$$

where P_T is the transmit power, λ is the signal wavelength, d is the transmission distance between the TX and RX antennas, and n is the path loss exponent. For free space scenario, $n = 2$ [95]. We also note that n usually has different values that depend on radio propagation channels for various complex environments [96], e.g., $n \in [2.7, 4.0]$ for normal urban area cellular radio and $n \in [1.6, 1.8]$ for indoor LOS scenarios. According to (1), free space path loss can be expressed by $PL^{FS} = \left(\frac{4\pi d}{\lambda}\right)^2 = \left(\frac{4\pi df}{c}\right)^2$, where f is the signal frequency and c is the speed of light. We can actually use PL^{FS} to predict the signal strength of a signal at a given distance d of interest. For the typical applications of wireless communications and networking, PL^{FS} can be described through a convenient way in unit of dB by adopting f in GHz and d in km:

$$PL^{FS} = 20\log_{10}(d) + 20\log_{10}(f) + 92.45 \quad (2)$$

Based on (2), PL^{FS} can be obtained in direct proportion to signal frequency and transmission distance. Compared to microwave signals below 6 GHz, free space path loss is much higher for mmWave signals at higher frequencies under the condition of the same transmission distance and antenna configurations. With different transmission distances, free space path loss at microwave and mmWave frequencies is depicted in Fig. 5. As the signal frequency increases, free space path loss will raise as well. From the figure, it is also clearly revealed that free space path loss will increase for both microwave and mmWave frequencies with the growth of transmission distance between the TX and RX antennas. This demonstrates that the use of mmWave frequencies limits the transmission distance, e.g., 60 GHz indoor short-range broadband communications at 3.5 Gbit/s over a range of 5 m [97]. However, to extend the communication distance, several advanced solutions, e.g., distance-adaptive design at physical layer, ultra-massive MIMO, reflectarrays, and HyperSurfaces, have been proposed with the improved transmission distance up to 100 m in both LOS and NLOS areas at 60 GHz [98]. Recent field trial jointly carried out by Huawei and NTT DoCoMo has further attained the long-distance transmission with 5G high data speed at 39 GHz in both stationary and mobility scenarios [99]. In addition, the path loss of mmWave NLOS links is more larger than the free space path loss of mmWave unobstructed LOS links. For instance, based on the measurement campaigns at 60 GHz, the NLOS path loss is 147.4 dB which is obviously higher than the LOS free space path loss with the value 119.3 dB under the transmission distance 200 m [100].

b: ATMOSPHERIC ATTENUATION

The free space path loss just reflects only a kind of signal attenuation which occurs while traveling in the ideal vacuum environment. But beyond that, mmWave signals traveling in free space are also effected by frequency-related atmospheric attenuation. In principle, the propagation of mmWave signals is typically influenced by interaction of atmospheric molecules in the form of oxygen, water vapor, rain, fog, cloud, etc, within the Earth's atmosphere. The atmospheric attenuation is primarily caused by the vibrating attribute of atmospheric molecules when they interact with mmWave propagation. More precisely, these molecules can absorb a certain portion of signal energy of mmWave propagation and vibrate with a strength proportional to signal frequency [70], [101], [102]. The atmospheric effect below 10 GHz is relatively low and can be also measured by using the Friis transmission equation [103], however atmospheric attenuation for mmWave frequencies and higher increases significantly, specially at certain frequencies. Hence, atmospheric effects on mmWave propagation not only restrict the transmission distance of mmWave signals, but also affect the utilization of 5G mmWave communications.

With the varying frequencies from 1 GHz to 350 GHz, atmospheric attenuation per kilometer generated by atmospheric oxygen and water vapor at sea level is displayed in Fig. 6. We can observe from this figure that atmospheric gases make the signal attenuation very high at mmWave frequencies, especially for the water vapor density of 7.5 g/m^3. Moreover, there are three attenuation peaks of atmospheric absorption in the frequency bands approximately 60 GHz, 120 GHz, and 180 GHz, wherein the attenuation reaches the maximum values, namely, 14.65 dB/km, 2.0 dB/km, and 27.77 dB/km, respectively. Specifically, atmospheric oxygen absorption is particularly high at 60 GHz and 120 GHz, and water vapor absorption is especially high at 180 GHz. These attenuation peak points are caused by absorption resonances of atmospheric molecules such as oxygen and water vapor at those frequencies.

In addition to atmospheric absorption by oxygen and water vapor, rain attenuation can be regarded as the most significant propagation impairment for mmWave frequencies. The

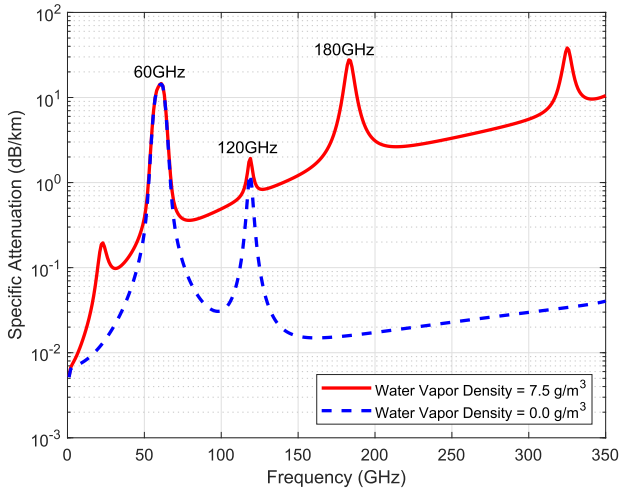

FIGURE 6. The specific attenuation caused by atmospheric oxygen and water vapor at microwave and mmWave frequencies under whether there has water vapor with the density of 7.5g/m^3 or not. Here, atmospheric pressure $P = 101.325$kPa, temperature $T = 20°$C, and distance $d = 1$km.

raindrops are approximately the same order of the size as the wavelengths of mmWave signals. Therefore, the rainfall causes additional attenuation due to the scattering and absorption of electromagnetic waves by rain particles. Theoretically, rain attenuation has a bearing on raindrop shape, raindrop size distribution, rain rate, signal polarization and frequency, etc [102], [104], [105]. The impact of rainfall intensity on rain attenuation per kilometer at sea level under the varying frequencies between 1 GHz and 350 GHz is further shown in Fig. 7. As can be observed, rain attenuation at mmWave frequencies is much higher than that of microwave frequencies. On the other hand, as the rain rate increases, the attenuation will also become greater. Despite the inevitable rain attenuation, there are also a number of frequency windows wherein atmospheric attenuation is significantly smaller. In consequence, these windows at mmWave frequencies provide the opportunity for mobilizing mmWave.

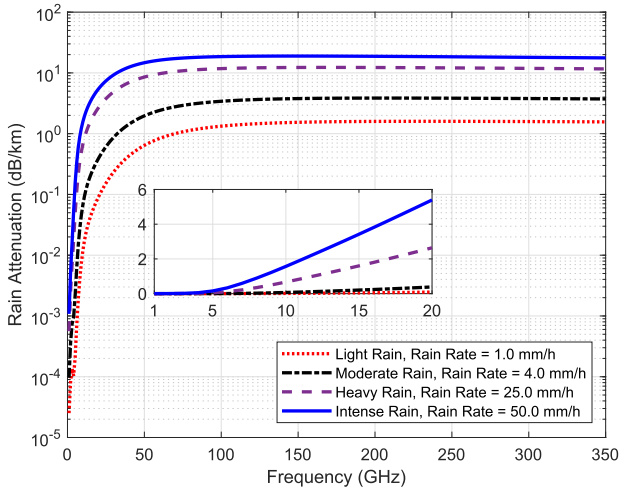

FIGURE 7. The rain attenuation at microwave and mmWave frequencies under different rainfall intensities in terms of rain rates. Here, distance $d = 1$ km.

c: BLOCKAGE EFFECT

Although mmWave communications own the capability to provide ultra-high-speed indoor wireless transmission, wireless backhaul, small cell access, cellular access, etc, mmWave bands are not robust enough and the system performance degrades significantly due to the sensitivity of mmWave links to blockages, e.g., static, dynamic, and self-blockage [106]. Typically, the propagation of mmWave signals is rather susceptible to blockage effect due to severe penetration loss and higher reflection/diffraction loss [106]–[108]. These losses of mmWave signals are caused by different materials or surfaces of the physical obstacles and even foliage penetration while traveling in their propagation paths blocked by the obstacles. It should be admitted that several factors including shape, dimension, and material type of the obstacles have a dramatic impact on blockage effect at mmWave bands. In many instances, the attenuation of mmWave signals at 60 GHz for drywall with the thickness of 2.5 cm and mesh glass with the thickness of 0.3 cm reaches 6.0 dB and 10.2 dB, respectively [107]. Even more serious, mmWave signals cannot penetrate most solid materials compared to microwave signals. With respect to the duration of blockage with 0.2 s, the blockage of human body can result in the reduction of signal strength of mmWave signals at 60 GHz by 20 dB, much greater than at microwave frequencies [109]. As a consequence, frequent blockages of mmWave LOS links and large blockage duration lead to performance degradation of 5G mmWave communications. Fortunately, traveling signals still have the alternative ways to reach the RX side by the aid of diffraction, reflection and scattering, in spite of the blockages of mmWave LOS links [110].

d: BEAM MISALIGNMENT

The narrow beams of mmWave signals allow the ability to achieve highly directional beams and greater resolutions along the desired directions. We can utilize the highly directional antennas to focus their power of steerable narrow beams on the intended users. With the large-scale antenna arrays, highly directional beamforming can be leveraged to compensate for stronger atmospheric attenuation and higher free space path loss at mmWave frequencies. In order to fully take advantage of highly directional mmWave transmission or reception, the beams between TX and RX sides need to be well steered and aligned [111]–[114]. Efficient beam alignment policies, e.g., beam tracking, beam training, hierarchical beam codebook design, accurate estimation of the channel, etc, are required to reduce the delay overhead with or without a priori knowledge of the TX and RX locations [115]–[118].

Nevertheless, due to the decrease of beamwidth of mmWave signals and the mobility of UEs, it will become more and more difficult to effectively align the beams between TX and RX sides [111], [119]. To this end, beam misalignment between TX and RX sides is unavoidable from practical view points. The misalignment of beams not only reduces the probability of successful transmission and

reception for TX and RX sides, but also degrades the network performance, such as severe delay spread, reduced system throughput, and significant loss of beamforming gain. Based on the measurements, beam misalignment can cause additional propagation loss of mmWave links that is almost symmetric with respect to the misaligned angle [120]. For instance, in the mmWave system with the beamwidth of 7°, the beam misalignment of 18° results in the link budget drop by about 17 dB, which further generates the maximum throughput reduction by up to 6 Gbit/s or leads to the entire link interruption [121].

B. INTEGRATION OF 5G mmWave COMMUNICATIONS INTO UAV-ASSISTED WIRELESS NETWORKS

1) POTENTIAL APPLICATIONS

As has been mentioned before, the use of 5G mmWave communications can bring multiple benefits including larger bandwidth availability, shorter wavelength, narrow beam, increased security/interference immunity, etc. Meanwhile, UAVs are being used to provide a promising solution to reliable and cost-effective wireless communications from the sky. On the one hand, they can be deployed as flying BSs to enable aerial access to ground UEs in target areas. On the other hand, UAVs can serve as aerial relays for partitioned ground UEs, and can even create multi-tier architecture for FANETs or connected drones. As such, the application of UAVs has been considered as an alternative complement of legacy cellular systems, with the potentials to achieve higher transmission efficiency, enhanced wireless coverage, and improved system capacity. To meet the exponentially growing data capacity demand of future 5G and beyond wireless applications, an intuitive way is to integrate UAV-assisted wireless networking with mmWave communications. With this integration of two promising techniques, three kinds of typical applications can be summarized as follows:

a: AERIAL ACCESS VIA A2G/G2A MmWave LINKS

As previously introduced, UAVs can be used to provide aerial access from the sky to ground UEs in a certain area of interest. As summarized in Table 1, we can deploy the UAVs as many forms of aerial access equipments, e.g., aerial BS, aerial RSU, aerial data collector, and even aerial MEC server and caching, to achieve on-the-fly wireless access. To keep up with the exponentially growing data capacity demand, a promising idea is to link aerial access in UAV-assisted wireless networks with mmWave communications together. Particularly, bidirectional mmWave links are allowed to be properly designed for aerial access applications in our considered scenario. To be precise, depending on the transmission direction between UAVs and ground UEs, bidirectional mmWave links consist of the A2G links (i.e., downlink) and the ground-to-air (G2A) links (i.e., uplink). In many instances, typical applications for aerial access using A2G and G2A mmWave links include downlink NOMA transmission to serve ground UEs simultaneously [122], flying cache-enabled remote radio heads (RRHs) by deploying cache storage units at UAVs [37], flying BSs with multiple transmit antennas to provide wireless access to ground legitimate receivers [123], etc.

b: AERIAL RELAY AND INTERCONNECTION VIA A2A MmWave LINKS

UAVs can further serve as aerial relays to provide wireless connectivity towards ground UEs without direct transmission links. Given this scenario, data packets from source UE are first sent to an initial UAV via aerial access, and then transferred to other UAVs in a multi-hop fashion by means of UAV interconnection in FANETs or directly to destination UE through UAV relay using the load-carry-and-deliver forwarding mechanism. To meet the requirement of the sustainable increase of transmission capacity and data traffic, it will be far more realistic to apply higher mmWave frequencies instead of lower microwave frequencies to design the A2A communication links for both aerial relay and multi-hop interconnection. Additionally, as exhibited in Fig. 1, information exchange and transfer among the UAVs can be also achieved through multi-hop drone interconnection based on the A2A mmWave links. By using multiple antenna arrays to obtain multiple beams, each UAV can establish the directional mmWave links with its neighboring UAVs in the mmWave flyMesh architecture [32].

c: AERIAL BACKHAUL VIA A2G/G2A MmWave LINKS

With the ultra dense small cell deployment in 5G wireless systems, the backhaul between BS and core network is traditionally connected by optical fiber or coax in terrestrial networks, to support multiple Gigabit data transmissions. However, it will not be flexible, easier to deploy, and cost-effective for massive deployment of small cells [49], [124]. In comparison with wired backhaul, UAVs can serve as aerial BSs and RRHs to provide wireless backhaul due to flexibility, ease of deployment, and lower operating and maintenance costs. With the heavy data traffic burdens for small cells, UAV based aerial backhaul via A2G/G2A links by using mmWave frequencies has been proposed as a potential solution to attain Gigabit data transmission speeds. Moreover, ultra-high-speed wireless backhaul by integrating UAVs and mmWave communications will further improve the flexibility and apparently reduce the costs of wired backhaul in terrestrial networks [8]. For instance, the mmWave flyMesh has been proposed to provide ultra-high-speed wireless backhaul between mmWave flyMesh and relay BS [32].

2) BRIEF INTRODUCTION TO TECHNICAL ADVANTAGES AND CHALLENGES

Inspired by the technique benefits and potentials for 5G mmWave communications, UAV-assisted wireless networks with mmWave communications still have some inherited merits:

- Multiple Gigabit data transmission speeds can be guaranteed for UAV-assisted wireless networking with

mmWave communications, due to the abundance of unoccupied bandwidth available at mmWave frequencies. To be precise, the peak data rate of 10 Gbit/s or more can be easily achieved with the help of full-duplex Gigabit A2G mmWave connectivity. This attracting peak data rate is much greater than the limit rate of 1 Gbit/s by using traditional wireless technologies operating at lower microwave frequencies. A large amount of licensed and unlicensed mmWave frequency bands are potentially available for usage in UAV-assisted wireless networks including 28 GHz licensed band and 60 GHz unlicensed ISM band [57]. From the perspective of policymakers, FCC has adopted rules for wireless broadband operations at frequencies above 24 GHz [125], and approved the unlicensed V-Band use of 57 $\sim$ 64 GHz mmWave bands to enhance wireless backhaul [126]. These mmWave bands will be the candidate for A2G and G2A links in UAV-assisted wireless networking scenarios.

- Much shorter mmWave wavelength (ranging form 1 mm to 10 mm) makes it feasible to miniaturize physically smaller circuits, modules, and equipments for mmWave applications in UAV-assisted wireless networks. In particular, hundreds of mmWave antennas can be easily integrated as a beamforming array on a chip in a tiny component size [50], [52], [58], [69]. This advantage makes mmWave antenna arrays and other related modules and equipments very suitable for low-altitude short range UAVs with limited payloads. Thereby, we can offer more choices for placing antennas, and more freedom and flexibility in system design and optimization for computing, memory, and communications of UAV payloads.
- Large-scale multi-element antenna arrays can be potentially applied into UAV-assisted wireless networking with mmWave communications. It has been demonstrated that greater antenna gain and highly directional 3D beamforming will be easily designed and achieved under this scenario [10], [127], [128]. By adopting the 3D beamforming, the beamforming gain can be markedly concentrated in the target area due to ubiquitous access from the sky [127]. The spatial beamforming gain enhancement can effectively combat stronger atmospheric attenuation and higher free space path loss at mmWave frequencies. This will bring better system performance in UAV-assisted wireless networks with mmWave communications.
- Highly directional signals and greater resolutions can be achieved owing to narrow beams of mmWave signals by integrating mmWave communications into UAV-assisted wireless networks. On the one hand, highly directional transmission that is similar to optical-like propagation can enable low interference and increased security [59]. It will further help to protect the sensitive and legitimate messages for ground UEs from passively eavesdropping and actively jamming, especially for A2G mmWave links under the scenario of aerial BSs enabled cellular systems. On the other hand, narrow directional beams can concentrate much more wireless energy on target area, to compensate for stronger propagation attenuation and higher free space path loss of mmWave signals.

Although there exist many attracting advantages, mmWave communications also pose several technique challenges and limitations towards the integration of mmWave communications with UAV-assisted wireless networking:

- Propagation behavior and characteristics at mmWave frequencies, i.e., severe atmospheric absorption and higher path loss, have restricted the transmission distance for all the potential application scenarios as mentioned above. This requires us to consider short distance of mmWave links for UAV deployment no matter in aerial access or aerial backhaul. In addition, for actual system design, we should avoid using three attenuation peaks of atmospheric absorption in the frequency bands approximately 60 GHz, 120 GHz, and 180 GHz. Within these mmWave bands, atmospheric attenuation can reach the maximum values, which may further affect the system performance. This in turn tells us that we can take full advantage of several frequency windows with relatively smaller atmospheric attenuation, to achieve mmWave communications in UAV-assisted wireless networks.
- It has been highlighted that the propagation of mmWave signals is more susceptible to blockage effect along the propagation channel because of severe penetration loss and higher reflection/diffraction loss as stated previously. Compared with terrestrial static BSs, UAV-based flying BSs are characterized by dynamic time-varying positions and altitudes. This kind of high flexibility for UAV deployment together with the use of mmWave frequency bands make mmWave signals more vulnerable to the blockage problem. The typical blockage primarily includes human-body blockage incurred by human activity [62]–[65] and self-blockage caused by components of UAV itself [59]. The self-blockage of mmWave signals along the propagation channel is especially related with the scenario of UAV-assisted wireless networks, due to the components of UAV itself, e.g., the rotating propeller. Despite the impact of self-blockage, UAV-assisted wireless networks are more practical and applicable towards mmWave transmission owing to the easily established A2G LOS links.
- UAV-based aerial BSs can provide ubiquitous access from the sky owing to the typical characteristic of sufficient flexibility and high mobility with dynamic time-varying positions and altitudes. In addition, narrow mmWave beams and possible mobility of ground UEs make it very difficult to properly steer and align the highly directional beams for mmWave antenna arrays at the side of UAVs or ground UEs [10], [32]. Apparently, it will be far more realistic to dynamically adjust

directional beams according to current instant time in practical dynamic environment. As such, achieving dynamic beam alignment between UAVs and ground UEs with lower overhead and computational complexity will be incredibly complicated and challenging.

IV. RESEARCH ISSUES, CHALLENGES, AND STATE-OF-THE-ART

From the perspective of the taxonomy of the state-of-the-art research advances, we will give readers a comprehensive summary of key topics on 5G mmWave communications for UAV-assisted wireless networks in this section, including antenna technique, radio propagation channel, multiple access mechanism, spatial configuration, resource management, security strategy, and performance assessment.

A. ANTENNA TECHNIQUE

As an important component of UAV-assisted wireless networks with 5G mmWave communications, the antenna acts as wireless interface to transmit and receive mmWave signals for UAVs and ground UEs. In this regard, the antennas can be figuratively described as the "eyes and ears" of advanced wireless communication systems. Due to the extension from conventional microwave frequency bands to mmWave frequency bands, there will be much higher propagation attenuation and severe free space path loss under the same communication distance and antenna gains. Compared with traditional user devices, high mobility and physical structures of UAVs also pose extra challenges on accurate tracking of dynamic mmWave beam directions. Thus, the design of high gain and high-efficiency antennas is of great importance for realization of UAV-assisted wireless networks with mmWave communications. As shown in Fig. 8, recent efforts and solutions on the antenna-related research including antenna design [129]–[132], beam tracking [10], [32], [133], [134], and beam optimization [135] will be summarized in the following subsection.

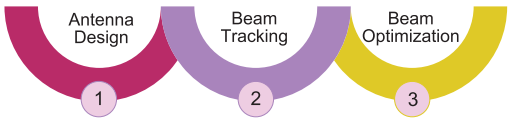

FIGURE 8. The classification of antenna technique solutions for UAV-assisted wireless networks with mmWave communications.

1) ANTENNA DESIGN

The success deployment of UAV-assisted wireless networks with 5G mmWave communications has given fresh impetus to the development and design of wireless antennas, complying to the requirements of mmWave frequency bands, propagation characteristics, circuit components, gain rating, geometries of mounting devices, transceiver architecture, communication system performance, and so on. Based on the state-of-the-art solutions about antenna design in our considered scenario, we will present the existing research efforts on the design issues and solutions of two representative antennas, i.e., array antennas and beam antennas.

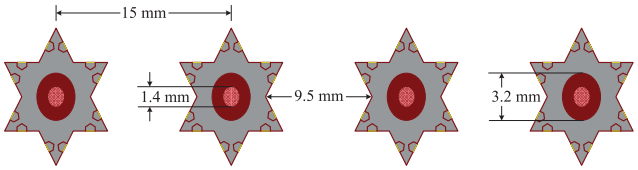

FIGURE 9. Illustration of the top view of the devised 1 × 4 star shaped antenna array.

a: ARRAY ANTENNA

The use of UAVs flying at a high altitude of about 20 km to build up the high-altitude platform station (HAPS) system and the stratospheric-platform (SPF) system has been recognized as a low-cost and flexible method for future wireless infrastructure. Compared to the outermost layer of the atmosphere in which the satellites orbit the earth, the deployment of UAVs at the layer of the atmosphere has many advantages, such as free-space like channel, lower transmit power similar to terrestrial systems, reduced propagation delay, etc. Based on this insight, Tsuji *et al.* [129] conducted the experiments to test the performance of digital beamforming (DBF) antenna and multi-beam horn (MBH) antenna for mmWave frequency band under the stratospheric conditions. To be specific, as for array antenna design, the authors proposed an electronically controlled mmWave DBF antenna for HAPS. In particular, this kind of array antenna was mounted on the helicopter, and was operating under the stratospheric conditions where the temperature was below −60 °C and the atmospheric pressure is 1/20 of that on the earth. Based on this setting, the performance of the devised mmWave DBF antenna under the stratospheric conditions was tested to examine the optimal forming of antenna beams for mmWave SDMA. More precisely, the contents of the experiments included beam-tracking performance, beam compensation, measurement of antenna beam patterns, and transmission of data packets. According to the experimental results, despite the harsh conditions of low temperature and low pressure, mmWave DBF antenna system can still work properly.

Bandwidth enhancement and miniaturization for microstrip antenna are one of the major challenges towards the design of conventional compact antenna. Especially, for the application scenario with mmWave communications, tiny component size of mmWave circuits and increased bandwidth result in lower antenna gain, which can be improved by building large antenna arrays. Under this background, the dual-band mmWave printed microstrip antenna patch was designed by Siddiq *et al.* [130] for UAV applications. The devised antenna array with coaxial feed resonated at 29 ∼ 30 GHz and 57 ∼ 66 GHz mmWave bands. Beyond this, the shape of the structure of UAV's wing was based on the size of 1250 mm × 350 mm × 50 mm by using the star shaped printed microstrip antenna. Specifically, the authors put forward two kinds of star shaped antenna arrays, i.e., 1 × 2 array and 1 × 4 array. Fig. 9 illustrates the top view

TABLE 4. The comparison of main features between the DBF antenna and the MBH antenna.

Main Feature	DBF antenna	MBH antenna
Array configuration	16 elements (4×4 square array)	3 elements (TX , RX, respectively)
Bandwidth	About 4 MHz	> 300 MHz
Type of antenna	Microstrip antenna	Corrugate horn
Antenna gain	15.7 dBi	28.4 dBi
MmWave frequency	28.2 GHz (TX), 31.1 GHz (RX)	$47.2 \sim 47.5$ GHz (TX), $47.9 \sim 48.2$ GHz (RX)
Total weight	74.2 kg (TX+RX)	62.2 kg (TX+RX)
Beamwidth	About 13 °C	—
Number of beams	Optional (3) (TX), Optional (3) (RX)	—
Stratospheric conditions	Low temperature (-60 °C), low pressure ($1/20$ on the earth)	Low temperature (-60 °C), low pressure ($1/20$ on the earth)

of the 1×4 star shaped antenna array with core parameters. It should be admitted that antenna gain can increase for both antenna arrays with the growth of frequency, and 1×4 array can achieve more gain than that of 1×2 array.

In addition to the advantage that the positions and altitudes are dynamically adjusted to match the requirement of ground users, UAV-based flying BSs can be also deployed with the characteristic of directional mobility and quasi-stationary hovering. How to improve the directivity of flying BS and facilitate better beam-steering resolution and lower cross-beam interference is an important issue we need to resolve. Fortunately, phased array antenna is a good choice to tackle this problem. Huo and Dong [131] proposed a uniform rectangular based phased array beamforming model for flying BSs with mmWave communications. The proposed phased array antenna employed a dimension of 2×8 antenna elements to realize the 3D beamforming. In order to provide a broad coverage towards ground users, the elevation radiating direction of main lobe (i.e., main beam) was required to host sufficient wide beamwidth, and the azimuth radiation pattern of main lobe should require narrow beamwidth. Through the field trial tests, it is observed that the measurement results for both single user and multiple users can obtain multiple Gigabit data transmissions over flying BSs with mmWave communications.

b: BEAM ANTENNA

In the context of UAV-enabled HAPS system and SPF system with mmWave communications, Tsuji *et al.* [129] also developed an mmWave MBH antenna that can achieve high-speed transmission at 47 GHz and 48 GHz. To be specific, the antenna direction of mmWave MBH antenna was devised to own three control modes: i) fixed mode: MBH antenna cannot adjust the direction; ii) inclination adjustment mode: the direction of beam was adjusted as the helicopter changes its inclination; iii) inclination/position adjustment mode: the footprint can be controlled in the same spot. Furthermore, mmWave MBH antenna was demonstrated to possess several advantages in controlling the antenna beams, such as broad bandwidth, low development cost and low power consumption. Similar to the experiments for mmWave DBF antenna in [129], MBH antenna was also installed on the helicopter to test its performance over the HAPS system. The measurement mission included beam tracking, beam pattern,

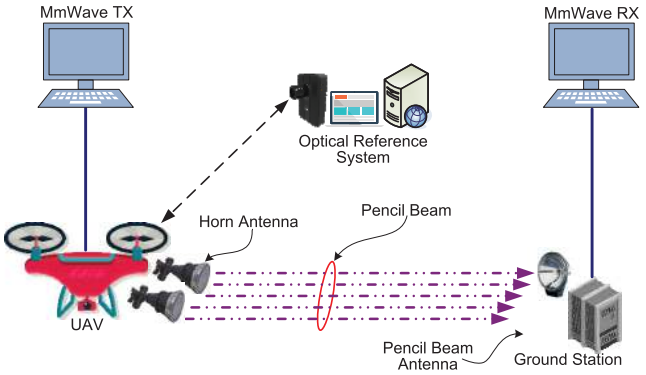

FIGURE 10. The experiment configuration for verifying the mmWave link at 28.5 GHz with the bandwidth of 800 MHz. Here, the mmWave TX and RX connect the UAV and the ground station, respectively.

and quality of communication signals. Finally, experiment results showed that the system can work properly and further demonstrated that highly directional beams can solve the disadvantage of UAV-assisted wireless networks, which becomes a major component of mmWave UAV communications for 5G and beyond. The main features of the devised antennas in [129] are summarized in Table 4.

With the help of 3D beamforming and tracking antennas, the advantage of using highly directional mmWave antennas at TX and RX sides is that a continuously maintained antenna gain can be obtained, although there exist higher free space path loss and severe atmospheric attenuation caused by higher mmWave frequencies. Motivated by that, Heimann *et al.* [132] performed an experimental verification by implementing the mmWave link at 28.5 GHz with the bandwidth of 800 MHz between a fixed ground station equipped with an active antenna (i.e., pencil beam antenna) and a lightweight UAV equipped with a passive antenna (i.e., lightweight horn antenna). As shown in Fig. 10, a mmWave TX-RX scheme was designed by sending from the UAV based platform to the static infrastructure side including ground station and mmWave RX. From Fig. 10, the optical reference system was used to obtain the accurate position and orientation information of UAV for tracking performance evaluation. Based on this setup, the author carried out three tests: i) pencil beam alignment in static UAV environment, ii) precise tracking of UAV in dynamic environment, and iii) effect of the tracking precision. Based on the insightful

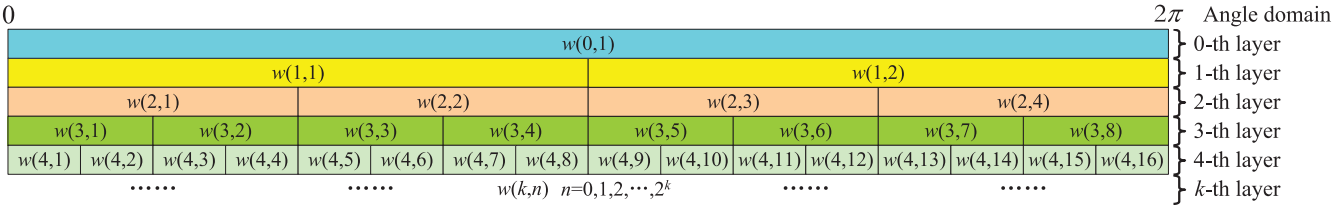

FIGURE 11. The hierarchical beam codebook for beamforming training under a tree structure, where $w(k, n)$ stands for the n-th codeword in the k-th layer, for $n = 1, 2, \cdots, 2^k$ and $k = 0, 1, 2, \cdots$.

discussions and tests, the authors analyzed the performance of beam tracking in UAV communications at mmWave band according to signal strength, quality and throughput for different antenna tapers, tracking algorithms and mobility patterns.

2) BEAM TRACKING

Beamforming, also known as spatial filtering, is a signal processing technique that has been already used in Wi-Fi routers with multiple antennas, to dramatically improve Wi-Fi performance, smoothing the path to the next generation IEEE 802.11ac standard and beyond. In practice, beamforming technology concentrates the signal energy over a narrow beam by means of highly directional signal transmission or reception to improve the spectral efficiency. By applying the beamforming technology into mmWave communications, it is efficient to compensate for higher free space path loss and stronger atmospheric attenuation at mmWave frequencies [136]. Evidently, signal interference will be severe when many people gather in small space to access wireless networks. Fortunately, beamforming technology achieves the equivalent ''bunching'' wireless signal into a rope, which can effectively reduce the cumulative signal interference to obtain better signal-to-interference-plus-noise ratio (SINR) at RX.

However, due to the fast-moving objects (e.g., vehicles, drones, and trains) under the context of 5G mmWave communications for UAV-assisted wireless networks, significant challenge of beamforming application is how to achieve fast and accurate tracking of dynamic mmWave beam directions with low computational complexity and overhead. To deal with this problem, Li *et al.* [133], [134] developed a recursive analog beam tracking algorithm for tracking dynamic beams in mmWave communications using analog beamforming. The beam tracking error minimization problem was formulated as a constrained sequential control and estimation problem by jointly optimizing both the analog beamforming vectors and the beam direction estimators. To resolve this problem, the authors relaxed the dynamic scenario into a static beam tracking scenario. In this scenario, the devised recursive mmWave beam tracking algorithm was focused on two stages: i) coarse beam sweeping, and ii) recursive beam tracking. Moreover, the lower bound of the variance of beam direction estimator using the mean square error (MSE) converges quickly to the minimum Cramér-Rao lower bound by optimizing among all the analog beamforming vectors. However, in the dynamic scenario, beam direction maybe changes over time. In order to keep track of the changing mmWave beam direction, the step-size parameter α_n within the n-th time slot was proved to be subject to:

$$\alpha_n = \frac{\lambda}{\sqrt{M}\,(M-1)\,\pi d}, \tag{3}$$

where λ is the mmWave wavelength, M is the number of antennas at the linear antenna array receiver, and d is the distance between neighboring antennas. Compared with three reference algorithms (i.e., IEEE 802.11ad, least square, and compressed sensing) through simulations, the proposed algorithm simultaneously can achieve faster tracking speed, higher tracking accuracy, low complexity, and low pilot overhead.

Due to high mobility of UAVs, the time to complete the beamforming training is more stringent. In the meantime, the overall mmWave beam search time is excessively costly for the exhaustive search algorithm because of a large number of candidate beam directions. To reduce the beamforming training time and mmWave beam search overhead, Xiao *et al.* [10] proposed to adopt a hierarchical beam search scheme based on the tree-structured beamforming codebook which covers the whole search space in angle domain. As shown in Fig. 11, there are k layers in the typical tree-structured codebook, and there are also M^k codewords with equal beamwidth and different steering angle in the k-th layer, where M is a positive integer which denotes the degree of tree-structured codebook, for $M \geq 2$. It suffices to mention that the mmWave beam search overhead of hierarchical beam search scheme is greatly lower than the exhaustive search scheme. On the basis of this advantage, the authors further designed the hierarchical coarse codebook based on a binary tree like structure wherein there are $\log_2 N + 1$ layers and the k-th layer contains 2^{k-1} best beams or known as antenna weight vectors (AWVs), for $k = 1, 2, \cdots, \log_2 N$ [137]. We wish to remark that the AWVs of the last layer in the coarse codebook can hold the narrowest mmWave beam under the given number of antennas N. It is also revealed that the beam coverage of the AWVs of the last layer can be characterized as the sum of the AWVs of the next layer.

In order to improve the efficiency of mmWave beam tracking and training, Xiao *et al.* [10] further pointed out two important strategies: i) priori information with respect to the

distribution range of beamforming angles, and ii) hierarchical tree structure of the beamforming codebooks. According to the potential position relations between UAVs and ground UEs, the distribution range of beamforming angles can be actually predicted as a priori knowledge. Moreover, the candidate beam directions can be also obtained in advance through mmWave beam training process. Apparently, these strategies can also significantly reduce the overhead for mmWave beam tracking and training.

Owing to flexible configuration and mobility nature, UAVs can be not only deployed as aerial BSs, but also serve as aerial relays to form the flyMesh aiming at achieving a fully connected UAV networks. However, as for the flyMesh with mmWave communications, frequent movement of UAVs at different altitudes causes the mmWave beam misalignment between UAVs or between UAV group leader and relay BS. Even worse, one of the UAVs will not work properly, and the nearby UAVs have to detect another one to establish the mmWave links. To address this challenge, Zhou *et al.* [32] proposed a fast mmWave beam tracking mechanism by employing the beam tracking policy of IEEE 802.11ad and IEEE 802.11ay standards, in order to find the suboptimal solution of the beam alignment maximization problem in mmWave flyMesh. This adopted mechanism can infer the directions of the relative movement relations between UAVs or between UAV group leader and relay BS according to the variations of SINR values obtained by beam tracking. To be specific, it is noticeable that the mmWave link for beam pair was not good enough if the SINR-based link quality was below a given threshold. Then the beam tracking initiator thus triggered the transmit beam tracking in order to select the best beam as the new transmit beam for subsequent data transmission. Through the analytical derivation, the overhead of the proposed fast beam tracking mechanism was further formulated as a function of the beam offset angle and the beamwidth. Simulation results indicated that the performance in terms of tracking overhead of the proposed fast beam tracking approach was superior to that of the method by using the IEEE 802.11ay standard.

3) BEAM OPTIMIZATION

In practice, intra-group interference involving data transmission from other UAVs and mmWave signal reflections and scattering has a bearing on the system performance of mmWave UAV group communications. As a consequence, it is of paramount importance to investigate the performance of beam anti-interference through a kind of beam optimization. In this context, Zhong *et al.* [135] elaborated the beam interference through the beam optimization based on window function and codebook design for the antenna with uniform linear arrays (ULA), and also established the interference model of mmWave UAV group communications. Fig. 12 shows the specific structure of the adopted ULA antenna under this scenario. On the basis of this structure of the ULA antenna, the mmWave beam response towards the incoming wavefront signal with the angle of arrival (AoA) denoted by θ was calculated as follows:

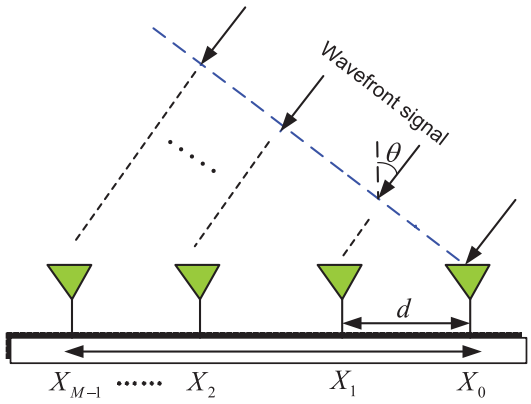

FIGURE 12. Illustration of antenna structure with uniform linear arrays wherein θ is the AoA of the incoming wavefront signal, d is the distance between two adjacent array elements, and X_m is the m-th antenna array element for $m = 0, 1, 2, \cdots, M-1$.

$$p(\theta) = \mathbf{w}(\theta)\,\alpha(\theta) = \sum_{m=0}^{M-1} w_m e^{j\frac{2\pi}{\lambda} md\sin\theta}, \tag{4}$$

where $\mathbf{w}(\theta)$ is the mmWave beam weight vector, $\alpha(\theta)$ is the array response for the AoA, M is the number of the antenna array elements, w_m is the beam weight of the m-th antenna array element, and λ is the mmWave wavelength.

As for the beam optimization based on window function, the target is to suppress the side lobes by designing the mmWave beam weight vector $\mathbf{w}(\theta)$ of weighting functions. Through the window function optimization, the sidelobes of the incoming wavefront signal can be effectively inhibited and the main lobe gain can be also been greatly improved. As for the beam optimization based on codebook design, Zhong *et al.* [135] further presented an improved N-phased codebook design scheme to optimize the weight vector $\mathbf{w}(\theta)$. Lastly, simulation results suggested that the phase adjustment of the beam can be realized by using this codebook design and the sidelobe interference by using N-phased codebook was greatly smaller than that of IEEE 802.15.3c codebook.

4) SUMMARY AND LESSONS LEARNED

Due to the important role of antenna in 5G mmWave communications for UAV-assisted wireless networks, we have reviewed the recent efforts and solutions about the antenna-related research from three perspectives, i.e., antenna design, beam tracking, and beam optimization. With relation to antenna design, array antenna and beam antenna have been discussed, respectively. Based on the classification of antenna design, key parameters and main features for DBF antenna and MBH antenna have been compared and summarized in Table 4. By considering the narrow directional beams of mmWave signals, we have then surveyed the existing beam-related issues in terms of beam tracking and beam optimization. The important lessons learned from the review

of the antenna-related research issues are summarized as follows:

- The design of array antenna typically benefits from the feature of tiny physical dimensions, and the development of beam antenna actually relies on the attribute of highly directional mmWave beams. We can obtain higher antenna gain by increasing the number of antenna elements, utilizing the 3D beamforming, and taking advantage of the highly directionality of mmWave beams.
- The fast and accurate tracking of dynamic mmWave beam directions is very important for successful transmission and reception of data packets. Generally, beam tracking mechanism and algorithm with low computational complexity and overhead are required to maintain the beam alignment and improve the system performance. To deal with the interference problem of adjacent mmWave beams, we can employ the window function and codebook design to optimize the beams for mmWave UAV group communications.

B. RADIO PROPAGATION CHANNEL

The radio propagation channels in mmWave frequencies are significantly different from the channels in lower microwave frequencies due to shorter mmWave wavelengths. Besides, atmospheric absorption at the mmWave wavelengths is very serious, which further leads to higher propagation attenuation and reduced transmission range. Also, the propagation channels of mmWave signals are susceptible to the blockage problem that affects the design of LOS propagation links. Correspondingly, modeling the radio propagation channel and capturing the propagation characterization of mmWave signals for UAV-assisted wireless networks with 5G mmWave communications are of paramount importance to design and optimization of UAV-enabled A2G and A2A mmWave communications. Moreover, mmWave channel sparsity in angular domain necessitates the efficient and accurate channel estimation and tracking technique, aiming to obtain better and stable system performance. Another significant technical challenge is how to detect the blockage of mmWave propagation channel. In the light of the above issues and challenges as already stated, we will summarize these related studies in the subsection in terms of channel modeling [10], [37], [57], [58], [64], [65], [122], [123], [134], [138]–[145], channel estimation and tracking [58], [141], [146], [147], and blockage detection and countermeasure [59], [142].

1) CHANNEL MODELING

To fully capture perfect knowledge and understanding of actual propagation behavior and characteristics of mmWave signals, several state-of-the-art efforts have been made to solve major problems targeted at mmWave channel measurement and modeling techniques under the environment of UAV-assisted wireless networks. Based on those efforts, we will provide a detailed description and discussion about recent advances in mmWave channel modeling solutions for UAV-assisted wireless networks with mmWave communications from three categories, namely, propagation measurement, empirical channel modeling, and analytical channel modeling, as depicted in Fig. 13.

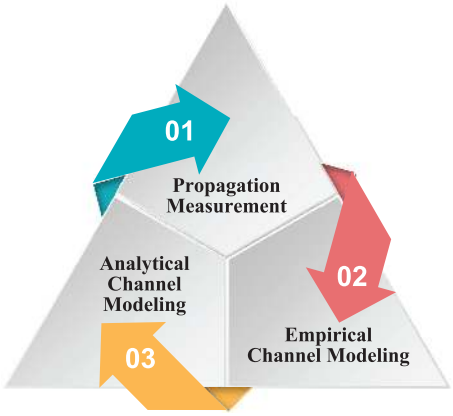

FIGURE 13. The classification of channel modeling solutions for UAV-assisted wireless networks with mmWave communications.

a: PROPAGATION MEASUREMENT

Realistic propagation behavior and characteristics at mmWave frequencies can be better captured by carrying out real-world measurement campaigns in frequency domain or time domain over the target environments. The commonly used channel measurement tools include channel sounder and vector network analyzer [148]. As for the environment of UAV-assisted wireless networks with mmWave communications, propagation measurements generally focus more on communication types, operational frequency bands, flight dynamics of UAV, propagation physical scenarios, antenna configuration, TX/RX placement, channel sounding process, etc.

To understand and analyze the characterization of A2G mmWave channels for UAV communications, Khawaja *et al.* [57] utilized the Remcom Wireless InSite ray tracing software to conduct the ray tracing simulations in frequency domain for capturing the behavior of A2G mmWave bands at 28 GHz and 60 GHz frequencies. In the A2G ray tracing simulations, four different scenarios were adopted, i.e., urban, suburban, rural, and over sea. Besides, three key factors about the scatterers (i.e., number, material, and height) were also incorporated into the involved scenarios of the simulations. Under this setting, the authors analyzed two performance metrics, namely, the received signal strength (RSS) and the root mean square delay spread of multipath components, for mmWave frequencies of 28 GHz and 60 GHz, respectively. It is observed that the fluctuation rate of the RSS versus the distance between UAV and ground station at 60 GHz was higher than that of 28 GHz. Furthermore, the behavior of root mean square delay spread of multipath components highly depended on the height of UAV along with the density/height of the scatterers around UAV.

On the basis of the A2G ray tracing simulations, Khawaja *et al.* [57] presented a preliminary framework of A2G channel sounding for mmWave UAV channels. To be even more concrete, a lightweight and compact A2G mmWave channel sounder was built up based on the high-performance software defined radio platform of the universal serial radio peripheral (USRP) X310 and the 60 GHz TX/RX development system PEM009-KIT from the product of Pasternack. The objective for the channel sounder development was to more accurately characterize the A2G mmWave propagation features via the propagation measurements at 60 GHz frequency.

As the continuation of the work about the characterization of A2G mmWave channels for UAV communications, Khawaja *et al.* [138] also performed the ray tracing simulations by taking advantage of the Remcom Wireless InSite ray tracing software to study the small-scale temporal and spatial characteristics of A2G mmWave LOS channels at 28 GHz frequency. For the simulations, four different scenarios including dense-urban, suburban, rural, and over sea, were further created and classified in terms of the number, distribution and dimensions of the buildings. Especially, the vertically polarized half-wave dipole antennas were mounted at both TX and RX with the omnidirectional pattern in azimuth direction. In the context of simulation setup, the ray tracing results for the UAV trajectories were characterized over sea and dense-urban scenarios. Moreover, the power variation of multipath components was observed to be dependent on the scatterer properties and the RX sensitivity. Meanwhile, the small-scale temporal and spatial characteristics of A2G propagation channels were validated to be subject to the constraint of the scatterer properties.

To study the impact of human-body blockage on mmWave links of flying BSs with mmWave communications as depicted in Fig. 14, Gapeyenko *et al.* [64] used the distance-based path loss model to characterize the A2G mmWave LOS and NLOS links. Conceptually, this kind of path loss model can be deemed to satisfy a standard linear model with respect to the Euclidean distance between flying BS and RX side. In order to determine key parameters of this estimated model (i.e., the least square fits of floating intercept and slope over the given distance), Akdeniz *et al.* [139] carried out the real-world measurements of mmWave outdoor cellular propagation at 28 GHz and 73 GHz frequencies in New York City, NY. Particularly, extensive measurements were performed by employing the highly directional horn antennas at both TX and RX sides under microcellular type deployments, aiming to obtain both the bulk path loss and the spatial structure of mmWave channels. What's more, the power measurements were performed at various angular offsets from the strongest angular locations. Through the measurements, the authors in [139] provided a scatter plot of the approximate omnidirectional path losses which can be easily observed as a function of the distance between TX and RX. Table 5 gives the list of key parameter values in the estimated path loss models through the realistic measurements

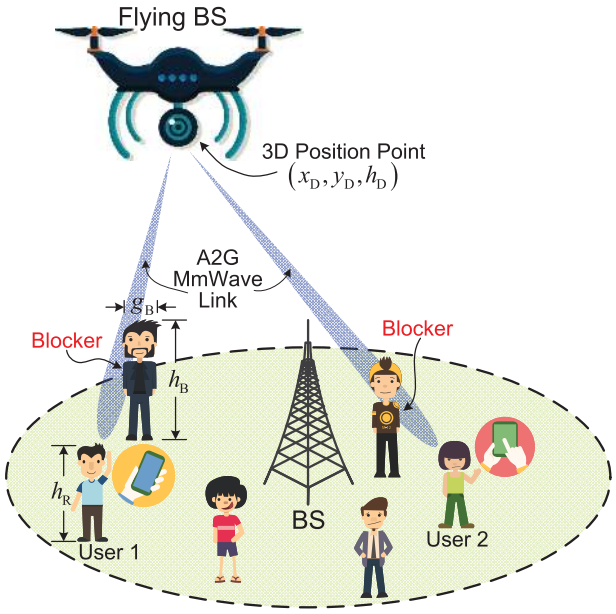

FIGURE 14. Illustration of human-body blockage on mmWave links of a flying BS with mmWave communications. Here, the flying BS is currently located at a 3D position point (x_D, y_D, h_D), and user 1 and user 2 are blocked by two human-body blockers. The user is located at the height of h_R, and the blocker is located at the height of h_B and the diameter of g_B.

in [139]. From the results of measurements, it should be also admitted that the theoretical free space path loss based on the Friis transmission equation can exhibit a good fit for the measurement data of mmWave LOS links.

b: EMPIRICAL CHANNEL MODELING

Actual radio propagation behavior of the channel in realistic environments is generally too complex to model accurately. Nevertheless, empirical channel models can be developed based on a large amount of statistical data collected from the in-situ channel observations and measurement campaigns. In what follows, we will give a review of empirical channel modeling for UAV-assisted wireless networks with 5G mmWave communications from the perspective of fading types for mmWave propagation channel.

Small-scale fading is characteristic of radio propagation resulting from the presence reflectors and scatterers that give rise to multiple components of transmitted signal while traveling [149]. At RX, the combination of these different components through multipath propagation may cause rapid amplitude fluctuations of the received signal over a small travel distance or time interval. To characterize the small-scale fading, statistical models have been used to describe the empirical fading distribution of amplitude of the received signal along the radio propagation channel, e.g., Nakagami-*m* model, Rayleigh model, Rician model, Weibull model, etc [150]. The probability density function (PDF) is generally employed to give the quantitative analysis about this kind of fading distribution.

TABLE 5. List of key parameter values in the estimated path loss models obtained from the realistic measurements.

Path Loss Model	Key Parameter Value at 28 GHz	Key Parameter Value at 73 GHz
LOS: $PL^{\mathrm{LOS}}(d) = \alpha_{\mathrm{LOS}} + 10\beta_{\mathrm{LOS}} \log_{10}(d) + \chi_{\mathrm{LOS}}$, $\chi_{\mathrm{LOS}} \sim \mathcal{CN}(0, \sigma^2_{\mathrm{LOS}})$	$\alpha_{\mathrm{LOS}} = 61.4$, $\beta_{\mathrm{LOS}} = 2$, $\sigma_{\mathrm{LOS}} = 5.8\,\mathrm{dB}$	$\alpha_{\mathrm{LOS}} = 69.8$, $\beta_{\mathrm{LOS}} = 2$, $\sigma_{\mathrm{LOS}} = 5.8\,\mathrm{dB}$
NLOS: $PL^{\mathrm{NLOS}}(d) = \alpha_{\mathrm{NLOS}} + 10\beta_{\mathrm{NLOS}} \log_{10}(d) + \chi_{\mathrm{NLOS}}$, $\chi_{\mathrm{NLOS}} \sim \mathcal{CN}(0, \sigma^2_{\mathrm{NLOS}})$	$\alpha_{\mathrm{NLOS}} = 72$, $\beta_{\mathrm{NLOS}} = 2.92$, $\sigma_{\mathrm{NLOS}} = 8.7\,\mathrm{dB}$	Case 1 (Combined two antenna heights at RX): $\alpha_{\mathrm{NLOS}} = 86.6$, $\beta_{\mathrm{NLOS}} = 2.45$, $\sigma_{\mathrm{NLOS}} = 8\,\mathrm{dB}$ Case 2 (Only one kind of antenna height at RX): $\alpha_{\mathrm{NLOS}} = 82.7$, $\beta_{\mathrm{NLOS}} = 2.69$, $\sigma_{\mathrm{NLOS}} = 7.7\,\mathrm{dB}$

Under the scenario of UAV-based flying BSs with mmWave communications, Zhu *et al.* [123] modeled the amplitude of the received A2G mmWave signal as Nakagami-*m* fading distribution for both the LOS and NLOS propagation conditions at mmWave frequency bands. Based on this A2G channel modeling, their target was to explore the secrecy rate performance at physical layer for UAV-enabled wireless networks using mmWave communications. The Nakagami fading parameter m is a shape factor of Nakagami distribution, which can be specifically expressed by $m = \frac{(\mathbb{E}[R^2])^2}{\mathrm{Var}[R^2]}$, where $R \geq 0$ is the amplitude of received signal. Especially, parameter m can be empirically estimated, for $m \geq 1/2$. In [123], the authors used m_{L} and m_{N} to describe Nakagami-*m* fading model for mmWave LOS link and mmWave NLOS link, respectively.

Rayleigh fading is regarded as a reasonable statistical model to describe the distribution of the envelope amplitude of received signal, which is made up of the multipath reflected and scattered waves as well as the significant LOS component. Under the scenario of next generation drone-assisted HetNets with mmWave communications, Meng *et al.* [140] characterized the radio propagation channel for information exchange between the BSs and the lead drone as Rayleigh fading model at mmWave frequency bands. As a special case, Nakagami-*m* fading model includes Rayleigh fading model when we set $m = 1$. Thus, we can use a PDF $f(R; \Omega)$ to quantify Rayleigh fading model, where $\Omega = \mathbb{E}\left[R^2\right]$ is the average fading power. On the basis of this fading model, the authors focused on the problem of drone swarm formation control for enhancing the formation strength of drones during flight control.

In comparison with small-scale fading, large-scale fading or shadowing is usually used to describe the average signal-power attenuation and path loss of the received signal strength at RX after traveling over a large travel distance [151]. Large-scale signal-power attenuation caused by shadowing of obstacles has been shown to follow a log-normal distribution. We generally employ the path loss model $PL(d)$ in dB to analyze this kind of fading distribution, where d is the distance between TX and RX.

Under the context of the proactive deployment of cache-enabled UAVs in cloud radio access network (CRAN), Chen *et al.* [37] formulated the mmWave propagation channel between UAVs serving as the RRHs and ground mobile users as the standard log-normal shadowing model using path loss metric. By choosing the specific channel parameters, the standard log-normal shadowing model was exploited to characterize the mmWave LOS and NLOS links under the constraint of the given 3D position $\mathbf{w}_k = (x_k, y_k, h_k)$ of the k-th UAV (h_k is the altitude of the k-th UAV) and 2D position $\mathbf{w}_i = (x_i, y_i)$ of the i-th ground user. More precisely, the channel parameters include the path loss exponents n_{LOS} and n_{NLOS} for LOS link and NLOS link, respectively, and the shadowing random variables $\chi_{\sigma_{\mathrm{LOS}}}$ and $\chi_{\sigma_{\mathrm{NLOS}}}$ for LOS link and NLOS link, respectively. With the 800 MHz broadband sliding correlator channel sounder, measurement campaigns for outdoor cellular channels at 38 GHz were conducted to obtain the measured data, aiming to quantify these channel parameters [152]. In Table 6, we provide the comparison among three adopted empirical channel models for UAV-assisted wireless networks with 5G mmWave communications. As shown in Table 6, the quantitative description about each empirical channel model is given in detail in terms of PDF or path loss.

c: ANALYTICAL CHANNEL MODELING

In contrast to empirical channel models, analytical channel modeling is used to characterize the radio propagation behavior of the channel through the way of conceptually and mathematically convenient simplifications. This kind of model is very popular for predicting the dedicated propagation phenomena by devising simplified models based on the analytical results. In the meantime, the effect of radio propagation channel on the performance of communication system can be also analyzed by leveraging the analytical models under the given channel parameters.

In the light of UAV-based MIMO system with mmWave communications, Zhao *et al.* [58] formulated the A2G channel between flying BS and ground UE as a 3D geometry-based model. In the considered system, UAV-based flying BS was equipped with $M \times N$ uniform rectangular arrays (URA), and the variation of mmWave propagation channel mainly generated from UAV movements. Under this setting, apart from the state parameters of UAV movements

TABLE 6. The comparison of empirical channel models for UAV-assisted wireless networks with mmWave communications.

Reference	Scenario	Communication Type	Adopted Channel Model	Fading Type	Quantitative Description
[123]	Aerial BS	A2G (downlink: UAV→ground RXs)	Nakagami-m fading model	Multipath fading: small-scale fading	**PDF**: $f(R;m,\Omega)=\frac{2m^m R^{2m-1}}{\Gamma(m)\Omega^m}\exp\left(-\frac{mR^2}{\Omega}\right)$, where $R\geq 0$ is the amplitude of received signal, and $\Omega=\mathbb{E}\left[R^2\right]$ is the average fading power, for $\Omega>0$. **Key parameter**: For mmWave LOS link, Nakagami fading parameter $m=m_{\mathrm{L}}=3$; For mmWave NLOS link, Nakagami fading parameter $m=m_{\mathrm{N}}=2$.
[140]	Swarm Formation Control	A2G (downlink: UAV→terrestrial BS) G2A (uplink: terrestrial BS→UAV)	Rayleigh fading model	Multipath fading: small-scale fading	**PDF**: $f(R;\Omega)=\frac{2R}{\Omega}\exp\left(-\frac{R^2}{\Omega}\right)$, where $R\geq 0$ is the amplitude of received signal, and $\Omega=\mathbb{E}\left[R^2\right]$ is the average fading power, for $\Omega>0$. **Key parameter**: —
[37]	Cache-enabled flying RRH	A2G (downlink: UAV→ground mobile users)	Log-normal shadowing model	Multipath fading: large-scale fading	**Path Loss for mmWave LOS link**: $PL_{k,i}^{\mathrm{LOS}}(d_{k,i})=PL(d_0)+10n_{\mathrm{LOS}}\log(d_{k,i})+\chi_{\sigma_{\mathrm{LOS}}}$, **Path Loss for mmWave NLOS link**: $PL_{k,i}^{\mathrm{NLOS}}(d_{k,i})=PL(d_0)+10n_{\mathrm{NLOS}}\log(d_{k,i})+\chi_{\sigma_{\mathrm{NLOS}}}$, where $d_{k,i}=\|\boldsymbol{w}_k-\boldsymbol{w}_i\|=\sqrt{(x_k-x_i)^2+(y_k-y_i)^2+h_k^2}$ is the distance between the k-th UAV and the i-th ground users, and $PL(d_0)$ is the free space path loss given by $20\log\left(\frac{4\pi d_0 f_c}{c}\right)$ with the free-space reference distance d_0, the carrier frequency f_c, and the speed of light c. **Key parameter**: For mmWave LOS link, $n_{\mathrm{LOS}}=2$ and $\chi_{\sigma_{\mathrm{LOS}}}=5.3\,\mathrm{dB}$; For mmWave NLOS link, $n_{NLOS}=2.4$ and $\chi_{\sigma_{\mathrm{NLOS}}}=5.27\,\mathrm{dB}$; $d_0=5\,\mathrm{m}$; $f_c=38\,\mathrm{GHz}$.

in 3D space, the adopted channel model was designed based on the steering vector of URA antenna and channel parameters, e.g., small-scale fading/large-scale fading coefficients, Doppler frequency, etc. It should be noted that the state parameters of UAV movements can be obtained through the sensor fusion of the flight control system of UAV, and the channel parameters can be estimated by means of the pilot transmission.

Under the condition of multi-user MIMO system wherein multiple UAVs serving as aerial users communicate with UAV-based aerial BS via the A2A mmWave communication links, Rodríguez-Fernández *et al.* [141] characterized the A2A channel between aerial BS and aerial user by a *D*-delay model. Each aerial user was equipped with a hybrid MIMO architecture, and also employed a hybrid analog precoder to transfer the data streams denoted by a vector to aerial BS within each channel slot. In addition, aerial BS and aerial users were equipped with the uniform planar arrays (UPA). Particularly, the authors used the d-th delay tap channel matrix for each aerial user under the given channel slot to describe the *D*-delay channel model. Some representative parameters for mmWave channel and antenna array were incorporated into the adopted channel model, e.g., the array response vector of the UPA, the azimuth angle of departure (AoD)/AoA, the elevation AoD/AoA, etc.

By jointly considering the LOS and NLOS components of the propagation in mmWave hybrid UAV communications with blockage problem, Zhao and Jia [142] utilized the Saleh-Valenzuela channel model to describe the propagation channel between flying BS and ground user. Each UAV was equipped by N ULA antennas with uniform spacing d. Due to the hybrid precoding scheme, the number of radio frequency (RF) chains for each UAV (denoted by N_{RF}) should be much smaller than the number of antennas with ULA, i.e., $N_{\mathrm{RF}}\ll N$. The proposed channel model underlined not only the multipath channel vector for the scenario of multiple ground users (i.e., the NLOS component), but also the LOS component of each ground user with the given complex gain. Additionally, both the LOS and NLOS components of the propagation depended on the ULA's steering-response vectors that were related with the physical direction of arrival (DoA) of each path between flying BS and ground user. It is implicitly understood that the NLOS component strongly characterized the radio propagation behavior in mmWave communications.

Under the downlink mmWave-NOMA transmission scenario where one UAV-based flying BS equipped with an M element of ULA array serving multiple ground users with single antenna, Rupasinghe *et al.* [122], [143]–[145] used the simplified channel vector to model the LOS propagation channel between UAV and ground users. Different from the Saleh-Valenzuela channel model, the authors just incorporated the LOS component into the simplified channel model because they believed that the effect of LOS path is dominant compared to the NLOS path due to relatively high hovering altitudes of UAV. In addition, Xiao *et al.* [10] analyzed the propagation characteristics of mmWave channels in UAV-assisted cellular systems with mmWave communications, and discussed some challenges for mmWave channel modeling, e.g., multipath components caused by first- and second-order reflections and sparse AoDs and AoAs in angle domain. Based on these observations

TABLE 7. The comparison of analytical channel models for UAV-assisted wireless networks with mmWave communications.

Reference	Scenario	Communication Type	Adopted Channel Model	Quantitative Description
[58]	Aerial BS with MIMO communi-cations	A2G (downlink: UAV→ground UEs)	3D geometry-based channel model	**Channel vector** (at time slot with length t): $\mathbf{h}_k(t) = \frac{\alpha_k}{(D_k)^\gamma} e^{-j(2\pi f_\mathrm{d} t T_\mathrm{s} \cos\varphi_k + \delta_k)} \mathbf{a}(\phi_k, \theta_k)$, where α_k is the small-scale fading coefficient for the k-th UE, γ is the large-scale fading coefficient, D_k is the distance between the antenna-1 of UAV and the k-th UE, f_d is the maximum Doppler frequency, T_s is the sampling period, φ_k is the angle between uplink transmitted signal and the motion direction of the k-th UE, δ_k is the initial phase, and $\mathbf{a}(\phi_k, \theta_k)$ is the steering vector of URA.
[141]	Multi-user MIMO communi-cations	A2A (aerial users→aerial BS, aerial BS→aerial users)	D-delay channel model	**Channel matrix** (for the d-th delay tap, the n-th channel slot and the u-th aerial user): $\mathbf{H}_{u,d}^{(n)} = \sqrt{\frac{N_\mathrm{R} N_{\mathrm{T},u}}{L_u}} \sum_{l=1}^{L_u} g_{u,l}^{(n)} \kappa \left(dT_s - \tau_{u,l}^{(n)}\right) \mathbf{f}_\mathrm{R}\left(\phi_{u,l}^{(n)}\right) \mathbf{f}_{\mathrm{T},u}^{*}\left(\theta_{u,l}^{(n)}\right)$, where L_u is the number of channel paths, $N_{\mathrm{T},u}$ the number of transmit antennas of the u-th UAV, N_R is the number of receive antennas of aerial BS, $g_{u,l}^{(n)}$ is the complex gain of the l-th channel path, κ is the combined effects of pulse shaping and analog filtering, T_s is the sampling period, $\tau_{u,l}^{(n)}$ is the delay of the l-th channel path, $\mathbf{f}_\mathrm{R}\left(\phi_{u,l}^{(n)}\right)$ is the array response vector of receive UPA, and $\mathbf{f}_{\mathrm{T},u}\left(\theta_{u,l}^{(n)}\right)$ is the array response vector of transmit UPA.
[142]	MmWave hybrid UAV communi-cations with blockage	A2G (downlink: UAV→ground users)	Saleh-Valenzuela channel model	**Channel vector** (between the m-th UAV and the k-th ground user): $\mathbf{h}_{m,k} = \beta_{m,k}^{(0)} \mathbf{a}\left(\phi_{m,k}^{(0)}\right) + \sum_{l=1}^{L} \beta_{m,k}^{(l)} \mathbf{a}\left(\phi_{m,k}^{(l)}\right)$, where $\beta_{m,k}^{(l)}$ is the complex gain for both LOS and NLOS component, $\beta_{m,k}^{(0)} \mathbf{a}\left(\phi_{m,k}^{(0)}\right)$ is the LOS component of the k-th user, $\beta_{m,k}^{(l)} \mathbf{a}\left(\phi_{m,k}^{(l)}\right)$ is the l-th NLOS component of the k-th user, for $l = 1, 2, \cdots, L$, L is the total number of the NLoS path, and $\mathbf{a}\left(\phi_{m,k}^{(l)}\right)$ is the $N \times 1$ steering vector of the k-th user served by the m-th UAV.
[122], [143]–[145]	mmWave-NOMA transmis-sion	A2G (downlink: UAV→ground users)	Simplified channel model	**Channel vector** (between the UAV and the k-th ground user): $\mathbf{h}_k = \sqrt{M} \frac{\alpha_k \mathbf{a}(\theta_k)}{\sqrt{PL\left(\sqrt{d_k^2 + h^2}\right)}}$, where M is the number of antennas in ULA array, α_k is the small-scale gain of the LOS path which is circularly symmetric complex Gaussian distributed with $\mathcal{CN}(0,1)$, $PL\left(\sqrt{d_k^2 + h^2}\right)$ is the path loss between the UAV and the k-th user, and $\mathbf{a}(\theta_k)$ is the steering vector with AoD θ_k for ULA.
[10]	MmWave UAV cellular	G2A (uplink: ground UEs→UAV)	Wideband time-varying continuous channel model	**Channel matrix** (at time t for wideband time-varying continuous): $\mathbf{H}(t) = \sqrt{N_\mathrm{UE} N_\mathrm{BS}} \sum_{l=1}^{L(t)} \lambda_l(t)\, p(t - \tau_l(t))\, \mathbf{a}(\psi(t))\, \mathbf{a}^H(\Omega_l(t))$, where N_UE is the number of UE's antennas, N_BS is the number of antennas of flying BS, $L(t)$ is the number of multipath components, $\lambda_l(t)$ is the complex coefficient of the l-th multipath component, $p(t)$ is the raised cosine pulse, $\tau_l(t)$ is the relative delay of the l-th multipath component, $\mathbf{a}(\psi(t))$ is the steering vector with AoA $\psi(t)$ for flying BS, and $\mathbf{a}(\Omega_l(t))$ is the steering vector with AoD $\Omega_l(t)$ of the l-th multipath component from the UE.
[10]	MmWave UAV cellular	A2G (downlink: UAV→ground UEs)	Narrowband discrete channel model	**Channel matrix** (narrowband discrete): $\mathbf{H} = \sqrt{N_\mathrm{UE} N_\mathrm{BS}} \sum_{l=1}^{L} \lambda_l \mathbf{a}(\psi)\, \mathbf{a}^H(\Omega_l)$, where L is the number of multipath components, λ_l is the complex coefficient of the l-th multipath component, $\mathbf{a}(\psi)$ is the steering vector with AoA ψ for flying BS, and $\mathbf{a}(\Omega_l)$ is the steering vector with AoD Ω_l of the l-th multipath component from the UE.

and challenges, the authors proposed to employ two channel models for mmWave UAV cellular, i.e., the wideband time-varying continuous channel model and the narrowband discrete channel model. Beyond that, Li *et al.* [134] and Gapeyenko *et al.* [65] exploited the multipath channel model to characterize the propagation channel for UAV-assisted wireless networks with mmWave communications. Similar to [10], [141], [142], the multipath model in [65], [134] was formulated bearing in mind the assumption that there are multiple alternative paths (i.e., multipath components) between TX and RX. It is noted that each path was featured by some metrics such as delay, path loss, AoA, AoD, etc. Tables 7 summarizes the above mentioned analytical channel models and compares the quantitative descriptions for each models in terms of channel vector or channel matrix.

2) CHANNEL ESTIMATION AND TRACKING

The technical challenges including high propagation attenuation, atmospheric absorption, limited shadowing and diffraction of mmWave communications can lead to the issue of

mmWave channel sparsity in angular domain. That is, only a limited number of mmWave channels can be used as feasible and effective propagation paths between TX and RX. By taking advantage of the channel sparsity of mmWave communications, Talvitie *et al*. [146] proposed a method to accurately estimate the channel parameters, such as AoD, AoA and time of arrival (ToA) of UE, in mmWave MIMO system by employing a distributed compressed sensing method known as the simultaneous orthogonal matching pursuit algorithm. Note that the considered MIMO system contained a terrestrial BS with known position and antenna orientation, and a UE with unknown position and antenna orientation. An iterative refinement algorithm was presented to improve the estimation accuracy with the reasonable complexity in comparison with the large dictionary based approach. Most important of all, this proposed method can be extended to the tracking scenario of UAV networks by replacing UE with UAV.

Under the scenario of multi-user A2A mmWave MIMO system with the hybrid architecture, Rodríguez-Fernández *et al*. [141] devised a channel estimation and tracking algorithm by using the priori information of the trajectory of each UAV (i.e., aerial user) in order to reduce both overhead and computational complexity. In this case, during a training stage, UAV-based aerial BS was required to estimate the multi-user mmWave MIMO channel matrices by taking the priori trajectory information of aerial users into consideration. To estimate these channel matrices, the maximum likelihood (ML) estimator assisted with prior information was utilized, and the optimal ML estimator of the frequency-selective mmWave MIMO channel was further derived for multi-user scenario. Moreover, the upper and lower bounds of the azimuth and elevation AoA and AoD for different uplink channels were obtained. Simulation results showed that the proposed channel estimation and tracking algorithm can achieve lower estimation errors under low overhead and low SINR regime.

Due to the essential attribute of high mobility of UAVs in UAV-assisted wireless networks with mmWave communications, one fundamental challenging task is how to accurately track a large number of dynamic propagation paths while incurring lower pilot overhead. In the meantime, the overhead of channel estimation can be also reduced with the help of an effective channel tracking technique, i.e., tracking the temporal variations of channel parameters [153], [154]. Motivated by this observation, Zhao *et al*. [58] designed an efficient channel tracking method for flight control system in UAV-based MIMO system with mmWave communications. The problem of UAV channel tracking was transformed into the track of state information of UAV movements, and the estimate of unrelated parameters of UAV movements. Besides, sensor fusion was adopted to obtain the UAV movement information. Due to the fact that the UAV channel tracking was a typical nonlinear procedure, unscented Kalman filter as a widely recognized nonlinear filter was used for nonlinear estimation. Compared with the traditional channel tracking method, the proposed method required a much lower training overhead.

By investigating the mmWave UAV communications with beam squint effect, Zhao and Jia [147] proposed an efficient channel tracking strategy under the comb-type orthogonal frequency division multiplexing (OFDM) structure (i.e., pilot-data-multiplexed OFDM structure). In this context, the channel tracking problem was transformed into the parameter estimate of the channel vector such as DOA, Doppler shift, and uplink/downlink channel complex gain. Simulation results demonstrated that the complexity of the downlink channel tracking was obviously reduced by making efficient use of both the angle reciprocity and the Doppler reciprocity.

3) BLOCKAGE DETECTION AND COUNTERMEASURE

One of the major technical challenges for UAV-assisted wireless networks with mmWave communications is blockage effect over the propagation channel, namely, travelling mmWave signal is blocked by physical obstacles in their propagation paths. Different from the other blockage patterns that most of work discussed, Bao *et al*. [59] placed more emphasis on self-blockage problem of mmWave signals incurred by the components of UAV itself, i.e., the rotating propeller of UAV, as illustrated in Fig. 15. In order to confirm that there indeed exists this kind of self-blockage, the authors conducted the experiments to identify the blockage effect of UAV propeller based on hardware testbed. This kind of testbed consisted of the mmWave TX/RX modules with horn antennas at 60 GHz frequency and the fine-tuned propulsion system. In particular, the blockage loss measurement and the blockage pattern identification were carried out. Experimental results verified that self-blockage effect of

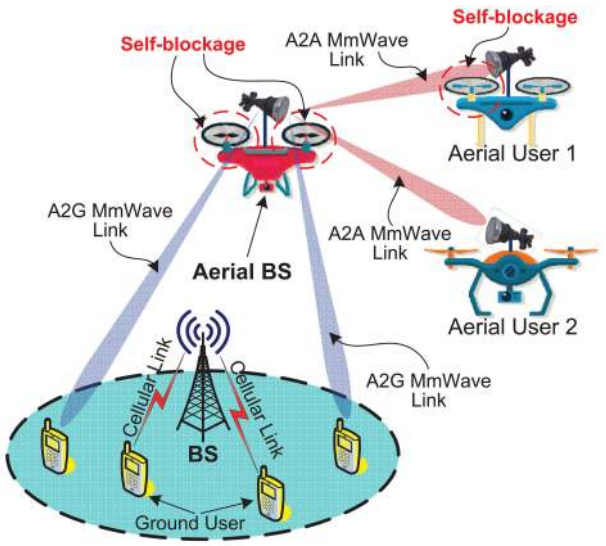

FIGURE 15. Illustration of self-blockage of mmWave signals incurred by the rotating propeller of UAV. Here, UAV-based aerial BS with the lightweight horn antenna can communicate with ground users and aerial users via A2G mmWave links and A2A mmWave links, respectively.

UAV propeller was obvious, which can severely deteriorate the system performance.

On the basis of the experiments for blockage effect, the authors in [59] further presented a sequential quickest change detection strategy to identify the blockage pattern characterized by three parameters, i.e., beginning time, time duration, and SINR drop. Specifically, the detection of blockage pattern was formulated as a multi-channel quickest detection for identifying the change of distribution in random process by utilizing multiple series of observations. Moreover, the Holm procedure was employed to determine whether a significant change of channel occurred. Simulation results showed that the proposed blockage detection approach can accurately identify the blockage with a modest blockage loss.

To deal with the blockage problem in mmWave UAV communications with hybrid structure, Zhao and Jia [142] further provided the corresponding countermeasure proposal by devising an angle domain channel transmission scheme. In this scheme, the DoA of LOS path with the most power can be regarded as the optimal transmission direction. Meanwhile, the deployment of multiple UAVs was also presented by taking deployment diversity into account, aiming to reduce the probability of blockage. A user scheduling mechanism to maximize the achievable sum rates was also proposed based on the water-filling algorithm.

4) SUMMARY AND LESSONS LEARNED

We have surveyed the existing efforts on channel modeling, channel estimation and tracking, and blockage detection and countermeasure for UAV-assisted wireless networks with 5G mmWave communications. In particular, channel measurement and modeling techniques have been reviewed and discussed from three aspects, i.e., propagation measurement, empirical channel modeling, and analytical channel modeling. The detailed comparisons of estimated path loss models based on realistic measurements, empirical channel models, and analytical channel models have been summarized in Table 5, Table 6, and Table 7, respectively. The important lessons learned from the review of research issues and solutions related to radio propagation channel are summarized as follows:

- Through the realistic measurement campaigns within indoor or outdoor environments, we can use channel sounder and vector network analyzer as effective tools to obtain the measurement results of propagation behavior and characteristics of mmWave signals along the bidirectional mmWave links. The distance based free space path loss model can be properly employed to characterize the mmWave LOS and NLOS channels by choosing the key parameters (e.g., α, β, and σ) reasonably.
- For empirical channel models, we need to give more insights into the current fading types (i.e., small-scale or large-scale fading) of A2G and G2A mmWave propagation channels when we apply them into our scenario. We should also pay attention to what kind of PDFs or path loss models can be utilized to describe fading distribution. For the application of analytical models, we ought to take the antenna and its associated parameters into account. Moreover, channel vector or channel matrix are required to be properly formulated to characterize the propagation behavior of mmWave channels between UAVs and ground UEs.
- To overcome the challenge of mmWave channel sparsity in angular domain, channel estimation and tracking approach should be well designed to achieve lower overhead and higher estimation accuracy. The commonly used methods that we learned include compressed sensing, priori information based policy, Kalman filter, etc. The blockage effect of mmWave propagation channel not only covers conventional blockage caused by physical obstacles, but also includes self-blockage due to UAV itself. The latter one is a novel scenario for further research on the blockage problem.

C. MULTIPLE ACCESS MECHANISM

The UAVs acting as flying BSs can provide aerial access to ground UEs during temporary events, e.g., hotspot areas and large public venues, where a large number of UEs straining the available wireless resources. Consequently, much more spectrally efficient multiple access techniques are required for enabling multiple UEs to share the same available wireless resources, to support massive connectivity while maintaining the requirements of different quality of service (QoS). Recently, NOMA has been regarded as an effective multiple access solution for 5G to improve spectral efficiency and support many thousands of UEs [43], [155]–[157]. In addition, with the advanced multiple antenna technique, SDMA as the channel-based multiple access mechanism has also attracted increasing research interests, especially for inherently directional A2G mmWave beams under our considered scenario. In the following subsection, we will summarize the related research on NOMA [122], [143]–[145] and SDMA [10], [158] for UAV-assisted wireless networks with mmWave communications.

1) NON-ORTHOGONAL MULTIPLE ACCESS

To increase the spectral efficiency and serve more ground users simultaneously, Rupasinghe *et al.* [122], [143], [144] proposed a downlink NOMA transmission mechanism at UAV-based flying BS operating in mmWave frequency bands. By maximizing the achievable mmWave-NOMA sum rates under the constraint of the given hovering altitude of UAV, a beam scanning strategy was introduced to identify the best physically radiated region of mmWave beam due to the partial coverage of user region by downlink beam. According to the constraint that the transmit power allocation of mmWave-NOMA TX to ground users was based on channel quality between ground user and flying BS, each ground user should send its feedback information about channel quality back to mmWave-NOMA TX. More precisely, the transmit power allocation towards each ground user via the NOMA

transmission should be conducted in a way inversely proportional to its channel quality.

By considering that full channel state information (CSI) would generate more link overheads, Rupasinghe *et al.* also [145] presented two limited feedback schemes in terms of user distance and user angle instead of full CSI feedback. The authors pointed out that both user distance and user angle were changing much slowly compared with full CSI. The summary of three feedback schemes to measure the channel quality used in [122], [143]–[145] is provided in Table 8. In addition, an analytical framework was developed to optimize the outage probability of each ground user and the outage sum rates based on the user distance feedback policy. The authors noted that mmWave-NOMA with distance feedback can exhibit better outage sum rates compared to conventional orthogonal multiple access (OMA).

TABLE 8. Summary of the channel quality feedback schemes used in the proposed mmWave-NOMA transmission mechanism.

Feedback Scheme	Measurement Metric
Full CSI	$\frac{\lvert\alpha_k\rvert^2}{M\times PL\left(\sqrt{d_k^2+h^2}\right)}\left\lvert\frac{\sin\left(\frac{\pi M(\bar{\theta}-\theta_k)}{2}\right)}{\sin\left(\frac{\pi(\bar{\theta}-\theta_k)}{2}\right)}\right\rvert^2$
Ground user distance	d_k
Ground user angle	$F_M\left(\pi\left[\bar{\theta}-\theta_k\right]\right)$
Parameter description: α_k: small-scale gain of single LOS path between the k-th user and flying BS, which is given by circularly symmetric complex Gaussian distributed with $\mathcal{CN}(0,1)$; M: number of antennas in uniform linear antenna array; d_k: horizontal distance between the k-th user and flying BS; h: hovering altitude of flying BS; $PL\left(\sqrt{d_k^2+h^2}\right)$: path loss between the k-th user and flying BS; θ_k: AoD of LOS path between the k-th user and flying BS; $\bar{\theta}$: beamforming azimuth AoD of flying BS beam; $F_M(\cdot)$: Fejér kernel with M antennas in uniform linear antenna array.	

2) SPATIAL-DIVISION MULTIPLE ACCESS

With the aid of the inherently directional A2G mmWave beams from flying BS, multiple ground users using different spatial beams can access the channel with the same set of frequencies concurrently. Based on this insight, Xiao *et al.* [10] explored the use of SDMA or known as beam division multiple access (BDMA) in UAV-assisted cellular systems with mmWave communications, as illustrated in Fig. 16. To reach this goal, ground users should be dynamically divided into several different parallel spatial user groups or clusters according to the entire range of AoDs of ground users, and each user group must be identified by a beamforming codeword pair. In particular, the beamforming codeword pair of the i-th ground user was characterized by $\{w_i, f_i\}$, where w_i denotes the beam combining codeword for the i-th ground user at the side of BS, and f_i refers to the beamforming codeword for the i-th ground user at the side of mobile station (MS) on the ground. It is worth noting that codewords w_i and f_i were both obtained from the predefined codebook. Compared to conventional UAV cellular operating at lower microwave frequencies, UAV-assisted cellular systems with mmWave-SDMA strategy demonstrated a superior

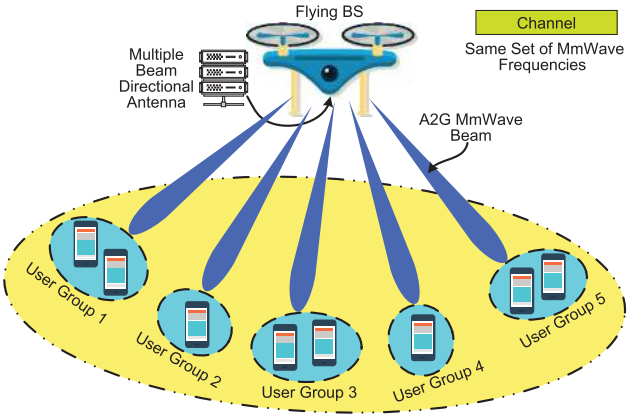

FIGURE 16. Illustration of the SDMA technique in UAV-assisted cellular systems with mmWave communications. Here, flying BS is equipped with a smart (or adaptive) antenna (e.g., multiple beam directional antenna), and each ground user is equipped with a single antenna. Each A2G mmWave beam from flying BS should correspond to only one user group, and the number of beams is equal to the number of transceivers of flying BS using the smart antenna system.

performance in terms of the total achievable rate of uplink transmission and multi-user capacity.

Considering that the ULA antenna would lead to huge physical size of the transceiver of UAV, Tan *et al.* [158] adopted the uniform circular arrays (UCAs) for phased array antennas to be deployed at flying BS in UAV-based MIMO systems under Ricean fading channel. With the only knowledge of the CSI at the transceiver of UAV, a statistical-eigenmode mmWave-SDMA approach was used in the downlink transmission for two ground users with single-antenna. Furthermore, a suboptimal beamforming precoder was exploited to maximize the SINR of each ground user. Based on this setting, the authors constructed a general theoretical framework to analyze the achievable rate of UAV-based MIMO systems. Based on the suboptimal beamforming precoder, a closed-form expression of achievable rate was rigorously derived, which was a function of the number of antennas, the radius of UCA configuration, and the azimuth and elevation AoDs. Moreover, it has been shown that the achievable sum-rate of the systems was quite close to a fixed saturation value when SINR was larger than 20 dB.

3) SUMMARY AND LESSONS LEARNED

We have provided a review on existing works about two kinds of multiple access techniques for mmWave downlink transmission, i.e., NOMA and SDMA, for UAV-assisted wireless networks with 5G mmWave communications. Three feedback schemes to measure the channel quality used in downlink NOMA transmission mechanisms have been summarized in Table 8. The important lessons learned from the review of related research on NOMA and SDMA are summarized as follows:

- The proposed NOMA and SDMA mechanisms all fall into the category of mmWave downlink transmission, wherein UAV-based flying BS serves as the TX side of

multiple access. Due to the effect of channel quality on transmit power allocation, feedback information about channel quality should be sent back to flying BS in mmWave NOMA transmission. We need to turn our attention to the use of feedback information, because different feedback information determines different link overheads.

- The SDMA approach, also known as BDMA, is well suited to our considered scenario, owing to the spatial attribute for inherently directional A2G mmWave beams. The difficult is how to adaptively and effectively assign ground users into different parallel spatial clusters.

D. SPATIAL CONFIGURATION

Due to the capability to hover, sufficient flexibility, ease of deployment, higher maneuverability, rapid reconfiguration, etc, UAVs can be effectively deployed at any positions of interest in 3D space, to serve as the aerial relay/BS/access point. For the rotary wing UAVs, their real-time positions are relatively fixed and static over a given geographic area. However, the spatial positions will be in the dynamic time-varying states for the fixed-wing UAVs according to current instant time. For such insight about UAV spatial configuration, one important problem for the design of UAV-assisted wireless networks with mmWave communications is to determine and optimize the spatial positions and trajectories of UAVs, to comply with the requirement of system performance. Additionally, except for spatial deployment in regard to the optimization of positions and trajectories, another challenge is how to effectively control the multi-UAV deployment, e.g., UAV clustering and UAV swarm formation. In the following, as shown in Fig. 17, we will review the existing studies about spatial configuration of UAVs in terms of position and trajectory optimization [37], [64], [159]–[162] as well as UAV deployment control [17], [140], [163].

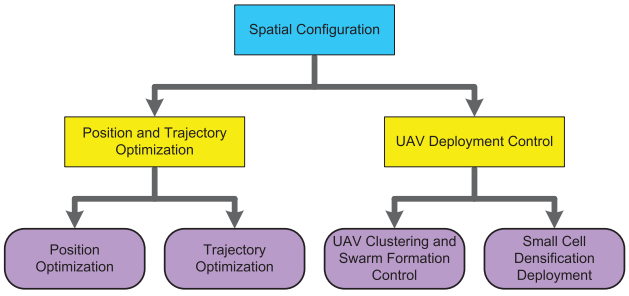

FIGURE 17. The classification of spatial configuration solutions for UAV-assisted wireless networks with mmWave communications.

1) POSITION AND TRAJECTORY OPTIMIZATION

For the position and trajectory optimization, the objective is to reconfigure UAV's position and trajectory in order to fulfill the requirements of system performance and resource optimization. As described in Fig. 17, we will provide readers a review of related work about position optimization and trajectory optimization of UAVs in the context of UAV-assisted wireless networks with mmWave communications.

a: POSITION OPTIMIZATION

To find and determine the optimal position of UAV as an aerial relay accurately and quickly is an extremely challenging task in mmWave UAV relay systems. This is because UAV generally has no priori knowledge about its optimal position. In this context, Kong *et al*. [159] proposed an Autonomous Relay solution to tackle this problem. The main idea of the Autonomous Relay is to apply compressive sensing technique into online measurement and estimate of link quality of mmWave beam in 3D space. To describe the link quality, the authors constructed a 3D matrix $\mathbf{Q} \in \mathbb{R}^{n_1 \times n_2 \times n_3}$, aiming to take advantage of compressive sensing for 3D Matrix, where n_1, n_2, and n_3 are the coordinate scales of the 3D space position point. Specifically, link quality was defined as the product of the receiving quality $R_o(i,j,k)$ at the 3D point with coordinate (i,j,k) from the mmWave TX o (origin point) and the receiving quality $R_c(i,j,k)$ at the 3D point (i,j,k) from the mmWave RX c, i.e., $\mathcal{Q}(i,j,k) = R_o(i,j,k) \times R_c(i,j,k)$. In order to find the optimal position point $\left(p_x^*, p_y^*, p_z^*\right)$ for UAV relay so that link quality $\mathcal{Q}\left(p_x^*, p_y^*, p_z^*\right)$ was maximized, link quality matrix update procedure was formulated as a matrix recovery problem by using MatrixUpdate method.

Based on the work by Kong *et al*. [159], Thomas and Chandran [160] reviewed the Autonomous Relay approach specialized for quick and accurate determination of mobile relay's position in mmWave communications. With the help of this approach, link qualities of mmWave beams can be sampled while UAV is moving. According to the real-time sampling results, UAV adjusted its trajectory to further reach its optimal position. It has been shown that the Autonomous Relay approach can obtain more accurate relay position and can also generate more stable results than existing classic methods including the K-nearest neighbor (KNN) and the tensor recovery (TR).

By taking the use of the caching in UAVs and the user-centric information on the ground into account, Chen *et al*. [37] investigated the proactive deployment issue of cache-enabled UAVs to optimize the QoE of ground mobile users in the CRAN. In this work, UAVs acted as the flying cache-enabled RRHs and the A2G communication links between UAVs and ground users employed mmWave frequencies in the CRAN system. However, G2A communication links (i.e., wireless fronthaul links) between terrestrial baseband units (BBUs) and UAVs employed traditional licensed cellular bands at microwave frequencies. In particular, a realistic mobility model for users was leveraged by considering the periodic, daily, and pedestrian mobility patterns, and the QoE metric was defined as the concrete human-in-the-loop metric that captures data rate, delay, and device type of each user. Under this setup, their goal was

to find an effective deployment (i.e., optimal positions) of cache-enabled UAVs to improve each user's QoE while minimizing the transmit power of UAVs. Specifically, this optimization problem can be expressed by:

$$\underset{\mathcal{C}_k,\mathcal{U}_{\tau,k},w_{\tau,t,k}}{\text{minimize}} \sum_{\tau=1}^{T}\sum_{k\in\mathcal{K}}\sum_{i\in\mathcal{U}_{\tau,k}}\sum_{t=1}^{F}\left(2^{\delta_{i,n}^{\mathrm{R}}\frac{|\mathcal{U}_{\tau,k}|}{B_{\mathrm{V}}}}-1\right)\sigma^2 10^{\frac{\bar{l}_{t,ki}}{10}} \tag{5a}$$

$$\text{subject to } h_{\min}\le h_{\tau,k},\ k\in\mathcal{K}, \tag{5b}$$

$$i\neq j,\ i,j\in\mathcal{C}_k,\mathcal{C}_k\subseteq\mathcal{N},k\in\mathcal{K}, \tag{5c}$$

$$0<P_{\tau,t,ki}^{\min}\le P_{\max},\ i\in\mathcal{U},k\in\mathcal{K}, \tag{5d}$$

where $\mathcal{U}$ is the set of ground users, $\mathcal{N}$ is the set of popular contents, $\mathcal{K}$ is the set of UAVs, $\mathcal{C}_k$ is the set of C cached contents in the storage units of the k-th UAV, $\mathcal{U}_{\tau,k}$ is the set of ground users served by the k-th UAV at the τ-th time slot, $w_{\tau,t,k}$ is the coordinate of the k-th UAV with altitude of the k-th UAV denoted by $h_{\tau,k}$ at the τ-th time slot, $h_{\min}$ is the minimum altitude of UAV, T is the number of time slots, F is the number of intervals in each time slot, $\delta_{i,n}^{\mathrm{R}}$ is the minimum rate that is required to maximize the QoE of user, B_{V} is the total bandwidth available for each UAV, σ^2 is the noise power spectral density, $\bar{l}_{t,ki}$ is the average path loss from the k-th UAV to i-th user at the t-th interval, $P_{\tau,t,ki}^{\min}$ is the minimum transmit power required to ensure the QoE requirement of the i-th user receiving the n-th content at the t-th interval within time slot τ, and $P_{\max}$ is the maximum transmit power of UAV.

To solve this problem, Chen *et al.* [37] proposed a prediction algorithm by taking advantage of machine learning framework of the conceptor-based echo state networks (ESNs), aiming to find the optimal positions of UAVs as well as the user-UAV association and the content caching at UAVs. In this case, the optimal positions of UAVs were the 3D points where UAVs were serving their associated ground users with minimum transmit power. The algorithm to find the optimal position of each UAV just had the runtime complexity $O(|\mathcal{K}|)$ in linear time. It is also observed via simulations that the proposed algorithm can achieve better performance gains in respect of the minimum transmit power of UAVs compared to the traditional ESN methods.

Considering the impact of human-body blockage on the LOS links of flying BSs by using mmWave communications as shown in Fig. 14, Gapeyenko *et al.* [64] explored the optimized deployment problem of mmWave-based flying BS, which captures the optimal altitude, coordinate, and coverage radius of flying BS. An approximate A2G mmWave path loss model was exploited for quasi-stationary flying BS with rotary wing, which combines the LOS and non-line-of-sight (NLOS) transmission links at mmWave frequencies together. Thus, the 3D position point $(x_{\mathrm{D}}, y_{\mathrm{D}}, h_{\mathrm{D}})$ of mmWave-based flying BS was associated with the adopted path loss model, where $(x_{\mathrm{D}}, y_{\mathrm{D}})$ is the two-dimensional (2D) space position of flying BS over the horizontal plane coordinate and h_{D} is the altitude of flying BS. To obtain the optimal 3D position point $\left(x_{\mathrm{D}}^*, y_{\mathrm{D}}^*, h^*\right)$ of flying BS, the authors formulated a 3D placement problem of flying BS as follows:

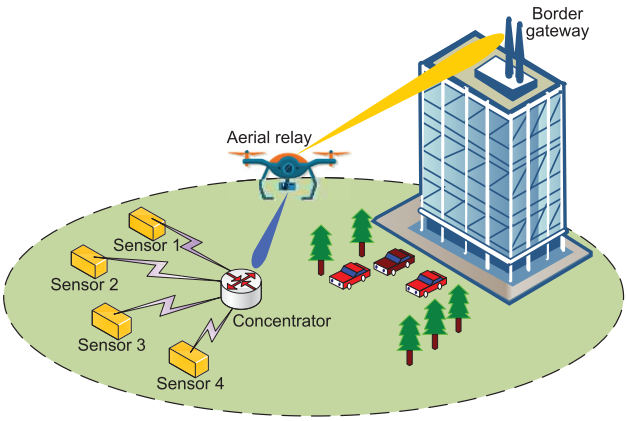

FIGURE 18. Illustration of dynamic aerial relay used for data collection in WSNs.

$$\underset{x_{\mathrm{D}},y_{\mathrm{D}},h,\{m_i\}}{\text{maximize}} \sum_{i\in\mathcal{M}} m_i \tag{6a}$$

$$\text{subject to } m_i\sigma_i\ge m_i Q,\ i\in\mathcal{M}, \tag{6b}$$

$$\sum_{i\in\mathcal{M}} m_i\le N,\ i\in\mathcal{M}, \tag{6c}$$

$$x_l\le x_{\mathrm{D}}\le x_u, y_l\le y_{\mathrm{D}}\le y_u, h_l\le h\le h_u, \tag{6d}$$

$$m_i\in\{0,1\},\ i\in\mathcal{M}, \tag{6e}$$

where $\mathcal{M}$ is the set of ground users, m_i is a binary variable indicating whether the i-th user is covered or not, $h=h_{\mathrm{D}}-h_{\mathrm{R}}$ (h_{R} refers to the height of the users), σ_i is the SINR of the i-th user, Q is the target SINR level, N is the maximum number of users that flying BS can concurrently serve, and the subscripts u and l stand for the upper and the lower limits of available positions in 3D space. Through the analytical derivations by solving the 3D placement problem, the authors demonstrated their theoretical results can provide a tight match with those obtained by using the interior-point optimization method through the MOSEK optimization software.

Conventionally, highly capable sensor node with large transmit power is generally chosen as the relay in WSNs. In contrast to this static placement of relay, Fu *et al.* [161] used a single UAV operating at mmWave frequency in 3D space as the dynamic aerial relay between ground sink node (i.e., concentrator) and terrestrial BS (i.e., border gateway) over WSNs as shown in Fig. 18. The authors attempted to find the optimal position of UAV by minimizing the system power consumption. Under such circumstance, the authors defined the system power consumption denoted by P_{Total} as the sum of the transmit power P_{S} of sink node and the transmit power P_{U} of the UAV, i.e., $P_{\mathrm{Total}}=P_{\mathrm{S}}+P_{\mathrm{U}}$. Thus, their objective was to minimize the total of system power consumption, which can be further formulated as:

$$\text{minimize}\ \ \frac{\sigma_{\mathrm{S}}^2}{|h_{\mathrm{S}}|^2}\left(2^{\frac{C}{B_{\mathrm{S}}}}-1\right)+\frac{\sigma_{\mathrm{U}}^2}{|h_{\mathrm{U}}|^2}\left(2^{\frac{C}{B_{\mathrm{U}}}}-1\right), \tag{7}$$

where σ_S^2 and σ_U^2 denote the noise power spectral density at UAV and terrestrial BS, respectively, $|h_S|^2$ and $|h_U|^2$ refer to the wireless channel gain from sink node to UAV and from UAV to terrestrial BS, respectively, B_S and B_U stand for the wireless bandwidth of sink node and UAV, respectively, and C represents the traffic capacity for transmission. Based on this optimization problem, the algorithm to determine the optimal position of UAV was proposed, and the performance of UAV based relay in WSNs was also verified by comparing with traditional wireless transmission without relay.

b: TRAJECTORY OPTIMIZATION

As stated previously, the obstacles to the use of mmWave communications pose additional challenges on optimizing the operations of UAVs operating at mmWave frequencies for various communication tasks while minimizing energy consumption and service time. Faced to these challenges, Ghazzai *et al.* [162] devised a generic optimization framework to smartly assign UAVs as aerial relays to serve some pairs of transceivers. More precisely, each UAV can support the dual-band communication module operating at both mmWave and microwave bands to complete data transmission for pairs of transceivers. For each pair of transceiver, TX or RX may be located on the ground or in the air. Thus, three path loss models were adopted for microwave band in terms of A2G, A2A, and ground-to-ground (G2G) communication links, and two path loss models were also applied for mmWave band according to A2G and A2A links. To quantify the total energy consumption of each UAV, the authors characterized the hover and transition energy required for its movement, and the communication energy needed to perform the relaying of the transceiver's data. Given this scenario, the authors formulated the service time $S_{n,d}$ that is required to serve the n-th pair of transceivers by the d-th UAV as follows:

$$S_{n,d} = \sum_{m \in \mathcal{N} \setminus \{n\}} p_{m,n,d} S_{m,d} + \sum_{m \in \mathcal{N} \setminus \{n\}} p_{m,n,d} T^{\mathrm{f}}_{m,n,d} + T^{\mathrm{c}}_{n,d} \left(\sum_{m \in \mathcal{N} \setminus \{n\}} p_{m,n,d} \right), \quad (8)$$

where $\mathcal{N}$ is the set of the pairs of transceivers, $p_{m,n,d}$ is a binary variable indicating whether the d-th UAV is directly serving the n-th pair of transceivers after the m-th pair, and $T^{\mathrm{f}}_{m,n,d}$ is the flying time of the d-th UAV to move from the position where it serves the m-th pair of transceivers to the position where it serves the n-th pair. It should be noted that the first term of the right hand side of (8) is the service time of the previous m-th pair of transceivers served by the d-th UAV, and the second term of the right hand side of (8) is the time where the d-th UAV flies from the 3D position $\mathbf{x}_m$ to the 3D position $\mathbf{x}_n$, and the last term of the right hand side of (8) is the communication time of the d-th UAV to complete the relaying of the transceiver's data. For D UAVs denoted by a set $\mathcal{D}$, the service time of the n-th pair of transceivers can be further calculated as $S_n = \sum_{d \in \mathcal{D}} \left(\sum_{m \in \mathcal{N}} p_{m,n,d} \right) S_{n,d}$.

The proposed framework by Ghazzai *et al.* [162] was aimed at optimizing the trajectories of UAVs such that a weighted sum of service times of all pairs of transceivers was minimized. By considering both the communication time of UAVs to relay the data and the flying time of UAVs, this objective problem was formulated as a mixed non-linear programming problem, which was optimally solved to determine the trajectory of each UAV based on a hierarchical iterative approach. It is important to emphasize that the iterative approach comprised four steps with the aim to determine: i) the potential 3D relaying positions of UAVs by solving the unconstrained non-convex problem, ii) the trajectories of UAVs by converting the proposed objective problem into a mixed integer non-linear programming problem (MINLP) and solving the MINLP problem, iii) the adjustment of UAV stops by using the 3D hierarchical search, and iv) the algorithm convergence. Simulation results were presented to demonstrate the performance of the proposed approach and to evaluate the trajectories of UAVs by adjusting the system parameters.

2) UAV DEPLOYMENT CONTROL

According to Fig. 17, related studies for UAV deployment control generally focus on three directions, i.e., construction of UAV cluster within a predefined cylinder space, formation control of drone swarm to enhance the network capacity, and small cell densification via UAV deployment.

a: UAV CLUSTERING AND SWARM FORMATION CONTROL

The use of the energy harvesting (EH) enabled caching UAVs in terrestrial cellular networks brings about two major advantages: i) to ease the fronthaul congestion by directly providing the cached popular contents at UAVs towards the ground mobile terminals (GMTs), and ii) to prolong the operational duration of UAVs by harvesting the energy from ambient environment such as wind and solar. However, the intermittent energy arrival through EH and the uncertainty of caching poses additional challenges on the robust connectivity and the ubiquitous coverage in UAV-assisted wireless cellular networks. In response to this challenge, Wu *et al.* [17] discussed the problem of coordination and cooperation between UAVs and ground BSs under this scenario. Moreover, a user-centric cooperative UAV clustering scheme was proposed aiming to offload GMTs from BSs to UAVs within the predefined cylinder space. The core of the cooperative UAV clustering was to construct the cylinder $B(o, \chi)^+$, where o is the 2D space projection position centered on a target GMT with the content requirement over the horizontal plane coordinate and χ is the radius of the cylinder, as depicted in Fig. 19. Once the cylinder was determined, a candidate UAV can be selected to send its cached contents that a target GMT requested, which must be subject to three necessary conditions simultaneously as follows:

- The candidate UAV was under a flight condition with a minimum altitude $H_{\min}$ and a maximum altitude $H_{\max}$,

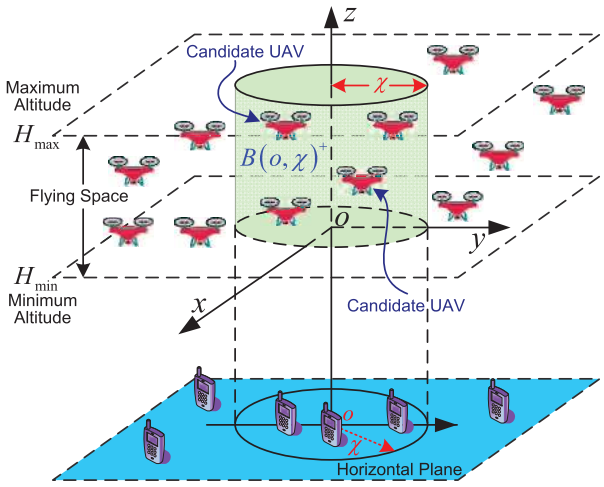

FIGURE 19. The cooperative UAV clustering based on the cylinder $B(o, \chi)^+$.

and also owned enough energy including the harvested energy and the onboard energy to support the wireless communication modules.

- The candidate UAV had the cached contents that should match the requirement of target GMT.
- The connection capacity (i.e., cell loads) of the UAV was more than the number of other candidate UAV serving GMTs or the number of other candidate UAV serving GMTs was much greater than the connection capacity of the UAV.

Based on those necessary conditions, several candidate UAVs constituted the cooperative UAV cluster. On the basis of the cooperative UAV clustering, the explicit expressions of successful transmission probabilities for a typical GMT were further obtained with the help of the Gamma approximation for the distributions of aggregated signal strength.

To effectively control and manage the drone swarm by terrestrial BSs in the deployment of low power ground nodes for next generation HetNets, Meng *et al.* [140] proposed a robust drone swarm formation control approach to raise the formation strength of drones during flight control. Their target was to enhance the network capacity in traffic hotspots by taking into account the use of mmWave communications during information exchange between terrestrial BSs and lead drone. Due to the constraints of traditional shape of antenna such as limited angles and inconvenience for deployment on flying objects, the authors presented a novel barrel antenna shape of antenna to be deployed for drone swarm formation. Especially, ray tracing model along with the receiver spatial distribution theory were employed in the design of the barrel antenna. The advantage of this kind of antenna was to improve the quality and the received power of mmWave signals between terrestrial BSs and lead drone. In the proposed approach, the drones equipped with the adopted antenna structure can fly around the given regions in which the lead drone transmitted its position signals to terrestrial BS as the backhauling and received the fronthaul signal from terrestrial BS simultaneously.

b: SMALL CELL DENSIFICATION DEPLOYMENT

In order to overcome the limitation of blockage effect of mmWave communications, the technique of small cell densification (i.e., network densification) is a good choice for design of 5G system architecture. The reason is that the application of small cell densification can raise the probability of LOS transmission conditions due to the increased number of access points (APs). To enable the small cell densification, Khosravi *et al.* [163] applied the UAVs as the mmWave APs which were deployed in a Manhattan grid manner as the typical urban scenarios, aiming to reduce the probability of blockage. The effect of the UAV-mounted mmWave APs on the throughput of ground UEs and the coverage probability in the case of a non-uniform load was investigated. Through the simulations, the authors showed that the presence of flying UAV APs with mmWave communications under the given urban scenarios can lead to ping-pong effects, where the throughput performance was found to fluctuate because of frequent handovers of UE access between UAVs and nearest APs. This would cause the overall per UE throughput performance deterioration.

3) SUMMARY AND LESSONS LEARNED

We have presented a detailed review of the state-of-the-art related to UAV spatial configuration in UAV-assisted wireless networks with 5G mmWave communications. Especially, optimization of positions and trajectories as well as how to effectively control the deployment of multiple UAVs have been reviewed. The important lessons learned from the review of existing studies about UAV spatial configuration are summarized as follows:

- No matter position optimization or trajectory optimization, the target is to achieve system performance improvement and optimal allocation of wireless resource, while satisfying a certain metric. In order to obtain the optimal position of UAV, we can take the prediction algorithm into account, such as prediction of link quality of mmWave beam via the Autonomous Relay, and machine learning framework of ESNs. The trajectory optimization of UAV is always associated with mathematical optimization problem under the given starting and ending positions of UAV. It's a general idea for designing effective algorithm to obtain the optimal or suboptimal trajectories.
- For the UAV deployment control, the essential issue is to deploy and control multiple UAVs according to specific design requirements. We can construct the UAV cluster consisting of multiple candidate UAVs within a cylinder space. The aim of this clustering is to carry out the theoretical analysis of system performance, e.g., the successful transmission probabilities.

E. RESOURCE MANAGEMENT

The integration of numerous emerging services and applications into UAV-assisted wireless networks with mmWave communications requires a fundamental understanding on

design principles and control mechanisms, to fulfill the requirements of various optimization criteria, e.g., QoS, energy efficiency, throughput maximization, etc. Under these requirements, one of the main challenges for design principles and control mechanisms is how to efficiently manage and schedule network resources, such as transmit power, radio spectrum, transmission rate, computing capability, subcarrier, backhaul capacity, storage availability, content caching, etc. The problem of resource management has been broadly involved in several network scenarios [36], [164]–[168], but not well explored in UAV-assisted wireless networks with mmWave communications. In what follows, the related research progress on resource management in our considered scenario will be summarized from two aspects according to what kind of network resources to be managed, i.e., power and subcarrier allocation [169], [170] and caching optimization [37], [171].

1) POWER AND SUBCARRIER ALLOCATION

In order to efficiently exploit the advantages of 5G HetNets assisted by UAVs, Chakareski *et al.* [169] and Naqvi *et al.* [170] envisaged a novel HetNet architecture that employed the dual operational frequency bands in comparison with traditional HetNets. Specifically, the HetNet architecture consisted of a macro ground BS operating at microwave band, multiple dual-mode small ground BSs operating at two kinds of mmWave bands, and multiple UAV-based flying small BSs operating at microwave band. Additionally, ground users can be served by three kinds of cases: i) microwave ground macro BS, ii) microwave flying small BSs (SBSs), and iii) ground SBSs with lower mmWave bands represented by L and higher mmWave bands denoted by H.

Under this scenario of interest, Chakareski *et al.* [169] and Naqvi *et al.* [170] designed an efficient radio resource management optimization framework for mmWave 5G HetNets empowered by flying SBSs. For the case of microwave ground macro BS, joint optimization of achievable rate and energy efficiency of all ground users was formulated as an optimization problem to maximize the sum rate and minimize the total power consumption for ground users simultaneously, while satisfying the minimum QoS and the maximum transmit power constraints. Mathematically, the presented optimization problem was expressed as follows:

$$\underset{p^{\mathrm{BS}}_{m,n}}{\text{maximize}} \quad \phi \frac{\sum_{m\in\mathcal{M}^{\mathrm{BS}}}\sum_{n\in\mathcal{N}^{\mathrm{BS}}} \kappa_{m,n} r^{\mathrm{BS}}_{m,n}}{R_{\mathrm{norm}}} - (1-\phi)\frac{\sum_{m,n} p^{\mathrm{BS}}_{m,n}}{P_{\mathrm{norm}}} \tag{9a}$$

$$\text{subject to} \sum_{m\in\mathcal{M}^{\mathrm{BS}}}\sum_{n\in\mathcal{N}^{\mathrm{BS}}} p^{\mathrm{BS}}_{m,n} \le P^{\mathrm{BS}}_{\max}, \ \forall m, \forall n, \tag{9b}$$

$$\sum_{m\in\mathcal{M}^{\mathrm{BS}}}\sum_{n\in\mathcal{N}^{\mathrm{BS}}} \kappa_{m,n} r^{\mathrm{BS}}_{m,n} \ge R^{\mathrm{BS}}_{\min}, \ \forall m, \forall n, \tag{9c}$$

$$p^{\mathrm{BS}}_{m,n} \ge 0, \ \forall m, \forall n, \tag{9d}$$

$$\kappa_{m,n} \in \{0, 1\} \ \forall m, \forall n, \tag{9e}$$

where $p^{\mathrm{BS}}_{m,n}$ is the power allocated to the m-th ground user on the n-th subcarrier by ground macro BS, $r^{\mathrm{BS}}_{m,n}$ is the achievable rate of the m-th ground user on the n-th subcarrier associated with ground macro BS, $\mathcal{M}^{\mathrm{BS}}$ is the set of ground users associated with ground macro BS, $\mathcal{N}^{\mathrm{BS}}$ is the set of subcarriers available for ground macro BS, $\kappa_{m,n}$ is the binary variable indicating whether the n-th subcarrier is assigned to the m-th ground user, P_{norm} is the maximum transmit power of ground macro BS, and R_{norm} is the maximum achievable rate under the constraint of P_{norm}. By using the Lagrangian function, the optimal power allocated to the m-th ground user on the n-th subcarrier can be derived via the Lagrangian multipliers which was further obtained through the sub-gradient method. Based on the optimal power allocation solution, the optimal subcarrier allocation can be also computed by using the Hungarian method.

For the case of microwave flying SBSs, the maximum interference threshold constraint was introduced to guarantee QoS to ground users associated with macro ground BS. Thus, the transmit power on a reused subcarrier by flying SBSs should be subject to the minimum rate requirement. Finally, for the case of dual-mode ground SBSs, the authors in [169], [170] proposed a step-wise algorithm for subcarrier allocation and user association to a specific mmWave band by using the Time-division multiple access (TDMA) scheme for subcarrier access. Numerical results demonstrated that the proposed optimization framework outperformed the conventional approaches in terms of maximizing the system sum rate or minimizing the system power consumption.

2) CACHING OPTIMIZATION

Caching the popular contents at the edge of networks closer to end users during off peak hours, has emerged as a promising alternative to mitigate the burden of backhaul links in core networks, enhance the capacity of the bandwidth constrained fronthaul links, and improve the QoE of end users. Motivated by these advantages, Chen *et al.* [37] explored the proactive deployment problem of cache-enabled UAVs to optimize the QoE of ground mobile users in the CRAN by proactively downloading and caching the popular contents at UAVs during off peak hours. The UAVs as the flying cache-enabled RRHs can directly deliver the caching contents to the requested ground users via A2G mmWave frequencies. Additionally, the QoE metric was characterized by the concrete human-in-the-loop metric that captures data rate, delay, and device type of each user. Based on this setup, an optimization problem was formulated as a UAV's transmit power minimization problem in (5) while satisfying the QoE metric constraint for each ground user. To solve this problem, a prediction algorithm by using the conceptor ESN was proposed to generate the content request distribution and the mobility pattern of each ground user. In this way, the user-UAV associations were determined via the K-mean clustering approach, and the optimal contents to be cached by each UAV

was further obtained. Particularly, within time duration T, the optimal set of contents $\mathcal{C}_k$ to be cached by the k-th UAV can be calculated by:

$$\mathcal{C}_k = \arg\max_{\mathcal{C}_k} \sum_{j=1}^{\frac{T}{H}} \sum_{\tau=1}^{H} \sum_{i\in\mathcal{U}_{\tau,k}} \sum_{n\in\mathcal{C}_k} \left(p_{j,in}\Delta P_{j,\tau,ki,n}\right), \quad (10)$$

where H is the number of time slots to collect user mobility, $p_{j,in}$ is the content request distribution of the i-th user during the j-th time period, and $\Delta P_{j,\tau,ki,n}$ is the reduction of UAV's transmit power by caching the contents during the j-th time period. Simulation results showed that the deployment of the cache-enable UAVs can greatly reduce the rate required for reaching the QoE metric threshold of each ground user with the low wireless fronthaul rate for each ground user. Furthermore, compared with two cases without cache and without optimizing the locations of UAVs, the proposed prediction algorithm via the conceptor ESN can achieve 40% and 25% of the reduction of the average transmit power of ground users, respectively.

Recently, the emerging VR technology has enjoyed both technological advances and widespread adoption to merge physical and virtual environment in real time. However, existing cellular networks cannot match the 360° VR content transmission due to limited backhaul and fronthaul capacity. Faced to this problem, Chen *et al.* [171] presented a framework of content caching and visible content transmission for UAV-assisted wireless VR networks, aiming to reduce the data traffic burden of the backhaul and enable the ground VR users to achieve the application requirements of low latency. In this scenario, as shown in Fig. 20, UAVs firstly collect VR contents with visible format and 360° format that the VR users request, and then send the collected contents to the cache-enabled SBSs through wireless downlink backhaul links at mmWave frequencies. In the meantime, the SBSs can directly transmit the caching contents to VR users via traditional licensed cellular bands. With this in mind, joint content caching and visible content transmission was formulated as an optimization problem with the goal to maximize the reliability of VR user. The reliability of VR user was defined as the probability of the VR user's successful transmission, which indicated that the content transmission delay of VR user should satisfy the target of the VR delay requirement.

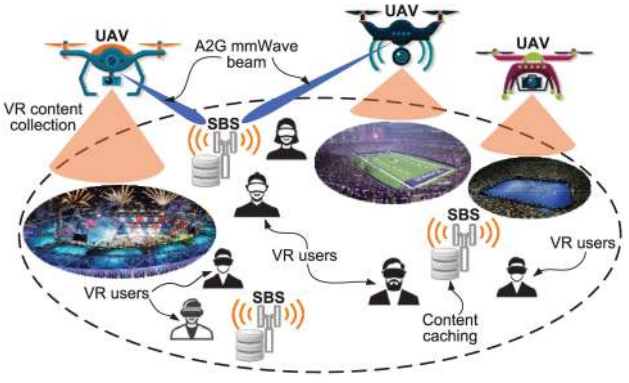

FIGURE 20. Illustration of the UAV-assisted wireless VR networks.

To maximize the reliability of VR user so as to find the optimal contents to cache and content transmission format, Chen *et al.* [171] further proposed a deep learning framework known as echo liquid state machine (ELSM) by combining the neural network concepts of the liquid state machine (LSM) and the ESN together. Specifically, the LSM was used to adjust the association policy of VR user, the cached contents and the cache content format according to the VR user's content request. Due to the higher complexity of training the traditional LSM, the ESN serving as the output function of the LSM was presented. The proposed ELSM algorithm can record large number of historical information and use it to predict the future output. Furthermore, compared with the ESN algorithm, the total reliability gains of the proposed ELSM algorithm can reach 14.5% and 25.4%, respectively. Simulation results showed that the ELSM algorithm can achieve 14.7% and 20.2% reliability gains, respectively, in comparison with the ELSM algorithm with random caching and the ESLM with random transmission format.

3) SUMMARY AND LESSONS LEARNED

We have pointed out the importance of efficiently managing and scheduling network resources. The related research progress on resource management in our considered scenario has been summarized based on what kind of network resources to be managed. The important lessons learned from the review of research issues and solutions about resource management are summarized as follows:

- Generally, the target of resource management is to efficiently and optimally allocate network resources, e.g., transmit power, subcarrier, caching, computing capability, etc. As such, resource allocation problem can be formulated as a mathematical optimization problem, while complying with one or more optimization criteria, e.g., QoE, energy efficiency, total power consumption, throughput maximization, and so on.
- Compared with the power and subcarrier allocation, the optimization of the cached popular contents at the network edge is an emerging hot topic in UAV-assisted wireless networks with mmWave communications. In essence, caching optimization together with other resource allocation can be initially formulated as a joint optimization problem. We can take advantage of machine learning framework, e.g., conceptor ESN, ELSM, multi-agent deep reinforcement learning, to design efficient algorithm for allocating the cached contents.

F. SECURITY STRATEGY

The broadcast nature of radio propagation of mmWave signals makes wireless transmissions be open and accessible to both legitimate users and unauthorized users (i.e., malicious eavesdroppers and attackers) in UAV-assisted wireless

networks with 5G mmWave communications. The open transmission environment and the lack of physical protection lead to serious security risk of malicious attacks and wiretapping under our considered scenario, e.g., passive interception of sensitive information and disruption of legitimate transmission via active jamming [172]. To combat the attacks, efficient security mechanism needs to be designed to enable the legitimate receivers to successfully obtain the confidential messages from the transmitter, while preventing the eavesdroppers from interpreting the legitimate transmission. The traditional key-based cryptographic techniques generally focus on applying the encryption and decryption at the higher layers such as network layer and application layer to secure wireless transmissions [11]. Alternatively, by taking advantage of physical characteristics of radio propagation, information theoretic security can be also achieved at the physical layer to provide direct secure communications in UAV-assisted wireless networks [173]–[176]. By integrating mmWave communications into UAV-assisted wireless networks, there also have been some recent studies on physical layer security that are focused on directional modulation [177]–[179] and jamming transmission [123]. In the following subsection, we will give a summary about these related studies.

1) DIRECTIONAL MODULATION

Owing to the inherent directional mmWave beams, it goes without saying that there exists the line-of-propagation (LOP) channels (i.e., LOS propagation channels) in UAV-assisted wireless networks with mmWave communications. As an important physical layer security technique, directional modulation (DM) [177], [179]–[183] has attracted considerable attention from both academia and industry to provide an efficient solution for secure wireless communications, especially for the LOP channel scenarios. Compared with conventional cryptographic methods at the upper layers, DM has the potential to enhance the security at the physical layer in UAV-assisted wireless networks with mmWave communications, based on the feature of spatial direction-dependent signal-modulation-formatted transmission.

As we all know, in conventional modulation, malicious eavesdroppers have the chance to eavesdrop on the captured messages from the receiving modulated signals, because the only difference among the received messages from different directions lies in the signal power for traditional wireless transmitter. However, DM is typically a transmitter side security technique due to its ability to project the modulated signals of confidential messages into one or more desired spatial directions in the definite constellation patterns. At the same time, in all the other spatial directions, the constellation patterns of the same modulated signals will be purposely distorted in the phase and amplitude such that the eavesdroppers cannot intercept and decode the confidential messages successfully. As a result, the directional angles of the desired receiver and eavesdroppers (i.e., the DoAs of the modulated signals) are greatly important for the DM transmitter, in that DM can achieve high performance gain by beamforming technique in the desired spatial directions. From a practical view point, the desired spatial directions can be defined in advance as a priori information for the DM transmitter and the legitimate receiver.

The typical DM system with QPSK modulation under the scenario of UAV-assisted wireless networks with mmWave communications is illustrated in Fig. 21, where there are one UAV with the multi-beam antenna array in the air as a DM transmitter, one ground legitimate receiver, and two ground eavesdroppers. At the side of the DM transmitter, the QPSK modulated signals with four phase-dependent unique symbols of confidential messages are generated in mmWave frequency by using the 3D beamforming technology. For the legitimate receiver, the modulated signal of the confidential messages is projected into the a priori spatial direction denoted by the DOA θ which owns a definite constellation pattern as shown on the top left corner of Fig. 21. For the eavesdroppers, the constellation patterns of the same modulated signal are specially scrambled along all the directions other than θ, which also means the artificial noise (AN) projection. The joint operation of beamforming and AN projection at the physical layer makes the eavesdroppers very difficult to intercept the confidential messages, which can further enhance the security of the system.

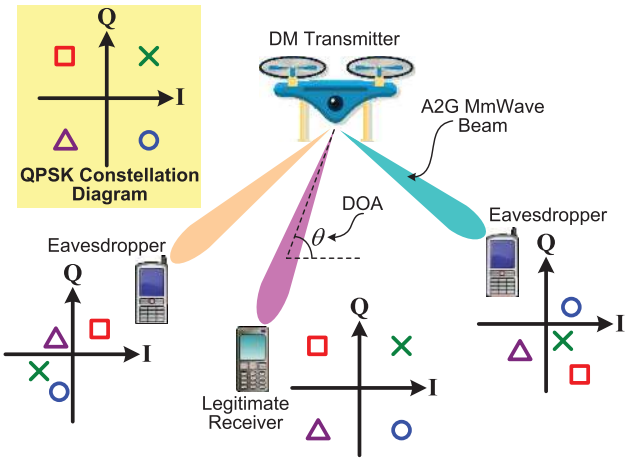

FIGURE 21. Illustration of DM system with QPSK modulation in UAV-assisted wireless networks with mmWave communications.

However, when the eavesdropper moves inside the direction of main beam of the desired receiver, and the eavesdropper can also intercept the confidential messages. To solve this problem, a new concept of secure and accurate wireless transmission was proposed by Shu *et al.* [177]–[179], in which DM, random frequency diversity, and phase alignment were incorporated. Particularly, a DOA measurement method based on Bayesian learning was presented, and the precoding vector and the artificial noise projection matrix at the DM transmitter were further designed. Compared to the single-snapshot measurement without machine learning, the proposed DOA measurement approach can generate

a substantial secrecy rate performance gain. Additionally, the Bayesian learning based method can improve the DOA measurement precision with fully-digital structure. To be specific, when the size of the training data set was increasing, the root mean squared error decreased and the DOA measurement precision was also improved. Moreover, the secrecy rate can increase with the growth of the SINR of system using the DM technique, but the secrecy rate gain would gradually decrease when the SINR increased.

2) TRANSMIT JAMMING

In consequence of the broadcast nature of the A2G wireless links, UAV-assisted wireless networks are particularly susceptible to the eavesdropping threats. Faced to the challenges of the security vulnerabilities, Zhu *et al*. [123] employed the physical layer security technique to analyze the secrecy performance of UAV-assisted wireless networks with mmWave communications. In this scenario, UAVs serving as the flying BSs with multiple transmit antennas were used to provide wireless access from the sky to ground legitimate receivers, in coexistence with multiple ground eavesdroppers. To guarantee the minimum safety distance between the randomly deployed UAVs, the Matérn hardcore point process was leveraged to implement the UAV deployment. The average secrecy rate between the associated UAV and the typical ground legitimate receiver was also evaluated, in terms of the complementary cumulative distribution function (CCDF) of the average rate between the associated UAV and the typical legitimate receiver, and the cumulative distribution function (CDF) between the associated UAV and the most detrimental eavesdropper. Even more important, as a core idea of applying the physical layer security strategy, a part of the UAVs of all the deployed UAVs was utilized as the jammers in the air to transmit the jamming mmWave signals to the eavesdroppers, as shown in Fig. 22. Based on the incorporation of the UAV jammers into the scenario, the improved average achievable secrecy rate for the jamming-aided UAV transmission was further characterized by:

$$R_{\mathrm{Sec}}^{(\mathrm{J})} = \left[\frac{1}{\ln 2} \int_0^{\infty} \frac{P_{\mathrm{cov,R}}^{(\mathrm{J})}(\gamma) + F_{\mathrm{E}^*}^{(\mathrm{J})}(\gamma) - 1}{1+\gamma} d\gamma \right]^+, \quad (11)$$

where $\gamma > 0$ is the threshold, $P_{\mathrm{cov,R}}^{(\mathrm{J})}(\gamma)$ is the CCDF of the SINR at the typical receiver, and $F_{\mathrm{E}^*}^{(\mathrm{J})}(\gamma)$ is the CDF of the SINR at the most detrimental eavesdropper. Simulation results showed that optimizing the jamming factor (i.e., the percentage of UAVs that transmit the jamming mmWave signals) can quite improve the secrecy rate. Furthermore, the use of the proper number of UAVs to transmit the jamming mmWave signals can reduce the eavesdropper's rate more than the typical receiver's rate.

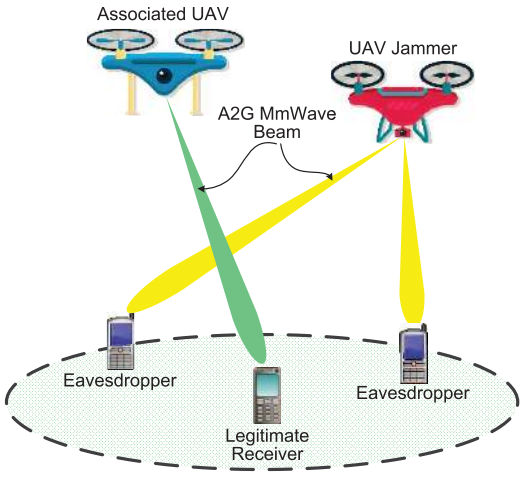

FIGURE 22. Illustration of the coexistence scenario of the associated UAV and the UAV jammer to to transmit the jamming mmWave signals to the ground eavesdroppers.

3) SUMMARY AND LESSONS LEARNED

We have presented a summary of recent studies on physical layer security that are focused on directional modulation and jamming transmission. The important lessons learned from the review of research issues and solutions about physical layer security are summarized as follows:

- The directional modulation depends on the feature of spatial direction-dependent signal-modulation-formatted transmission to enhance the security at the physical layer. Typically, directional angles of the desired receiver and eavesdroppers should be different to distinguish the constellation patterns of modulated signals. In particular, directional angles can be defined previously as a priori spatial direction that owns a definite constellation pattern. Therefore, directional angles are quite similar to the frequency hopping sequence in frequency-hopping spread spectrum system.
- For the jamming transmission, the primary idea is to apply the partial portions of UAVs as the jammers to proactively transmit the jamming mmWave signals to the eavesdroppers. Through this kind of method to transmit jamming signals, the average achievable secrecy rate between the associated UAV and the ground legitimate receiver can be improved.

G. PERFORMANCE ASSESSMENT

The assessment of the performance of UAV-assisted wireless networks with 5G mmWave communications plays a significant role in guiding us to design network protocols, optimize networking structures, analyze system parameters, diagnose performance issues, and so forth. The commonly used methods to evaluate the performance of UAV-assisted wireless networks with mmWave communications include theoretical performance analysis [65], [184]–[186] and simulation tool based measurement campaign [187]. Both of the methods can be exploited to quantitatively and qualitatively assess the network performance and provide some valuable data, metrics, models, approaches, frameworks, and mechanisms to improve the network performance. In the following,

we will review the recent studies that apply performance analysis and measurement campaign into the performance assessment of UAV-assisted wireless networks with mmWave communications.

1) PERFORMANCE ANALYSIS

Considering the importance of evaluating the performance of UAV-assisted wireless networks, especially for mmWave scenarios, Yi *et al.* [184] proposed a unified 3D spatial framework to theoretically assess the network performance by employing the tractable blockage model and the sectorized antenna pattern. In this scenario, UAV acting as the flying BS was deployed to provide the wireless link for ground users during the entire transmission process consisting of uplink phase and downlink phase. For the downlink phase, the authors analyzed the coverage performance of downlink transmission by considering the distance distributions of UAVs and the Laplace transform of interference in Poisson point processes. The losed-form expression for the downlink coverage probability at the typical BS was further derived, to enhance the evaluation efficiency. For the uplink phase, the coverage performance of uplink transmission was also analyzed by characterizing the distance distributions in the corresponding or other clusters and the Laplace transform of interference in Poisson cluster processes. Moreover, the general expression for the uplink coverage probability at the corresponding UAV was rigorously obtained. Based on the coverage probabilities of uplink and downlink phases, the system coverage probability was formulated as the function of SINR thresholds for downlink and uplink phases. Simulation results indicated that a large number of antenna elements had the capability to improve the coverage performance.

Under the scenario of the low-altitude UAVs deploying alongside the ground BS, Galkin *et al.* [185] proposed to utilize the stochastic geometry method to analyze the backhaul performance of ground stations serving the low-altitude UAV network in the urban environment. In particular, the authors analyzed the directional antenna alignment in 3D space between a typical UAV in the scenario and the ground stations including the associated backhaul ground station of UAV and other interfering ground stations. The antenna array was equipped by each ground station, and the 3D beamforming was used to concentrate the highly directional beam towards UAV, which forms the backhaul link operating at both 2 GHz LTE and mmWave frequencies. Additionally, by setting the SINR threshold, analytical expression for the probability of successfully establishing the backhaul link was obtained. The expected data rate over the backhaul link was further derived based on the backhaul probability. Compared with the interference-limited LTE signals, the mmWave signal was the noise limited signal which can generate a higher backhaul probability for UAV. Numerical results showed that the backhaul probability can increase monotonically with the growth of the height of the ground station, which also demonstrated that the backhaul performance was improved by deploying the ground station as high as possible above the ground.

The inherent challenges including multipath propagation of urban environments and dynamic blockage of mmWave links impose additional constraints and requirements for the mmWave backhaul connections in UAV-assisted wireless networks. To address these challenges, Gapeyenko *et al.* [65] adopted the flexible and reconfigurable backhaul architecture in UAV-assisted wireless networks, for the purpose of achieving the capability to dynamically reroute the backhaul links due to the unreliable blockage-prone mmWave links. The typical mathematical framework was presented by capturing the 3D multipath mmWave channel model, the heterogeneous mobility of UAVs and blockers, and the dynamic blockage effects. Based on this framework, the authors theoretically carried out the performance assessment of the flexible mmWave backhaul operation in the case of the crowded urban deployments, aiming to explore the spatial and temporal characteristics of the mmWave backhaul. The evaluation of the mmWave backhaul performance specifically covered two metrics of interest, i.e., time-averaged and time-dependent metrics. Numerical results demonstrated that both the outage probability and the spectral efficiency were improved with the growth of the intensity of UAV-BS traversals. In terms of the flight speed, the decrease of the UAV-BS speed presented an obvious positive effect on the mmWave backhaul performance.

As one major challenge, blockage effect for mmWave signal along the LOS propagation path between the drone-enabled aerial access point and the UE poses the additional constraints on the design of the analytical model for drone-based mmWave communications. Based on the extension of conventional stochastic geometry method, Kovalchukov *et al.* [186] proposed a 3D analytical model for drone-based mmWave communications by jointly capturing the random heights of communicating entities (i.e., drone-enabled aerial access points and UEs) and the high directionality of transmission. Their objective was to analyze the performance of drone-based mmWave communications through joint consideration of the above factors for the 3D analytical model. Furthermore, both the mean interference and the SINR were derived as explicit expressions. The system performance was assessed with the emphasis on the impact of the vertical dimension in aerial mmWave connectivity. Numerical results showed that capturing the vertical exposure probability along with the random altitude of communicating entities and UEs to access the aggregate interference were of great importance to the accurate performance assessment.

2) MEASUREMENT CAMPAIGN

In addition to the performance assessment using the theoretical analysis, simulation tool based measurement campaign can be also conducted to evaluate the performance of UAV-assisted wireless networks with mmWave communications. By utilizing the existing analytical models for free

space path loss, spatial consistency, and small-scale fading, Vasiliev *et al.* [187] assessed the end-to-end efficiency of UAV-assisted LTE-like mmWave cellular networks in the crowded area with the aid of NS-3 simulation tool. Owing to the deployment of antenna arrays and the high throughput, the 28 GHz band was used for mmWave communications. For the node layout, ground BS and UE were located in the opposite corners of the simulation area, and UAV as the aerial relay was located in the middle of the area. Two simulated scenarios including the source-destination case and the source-UAV-destination case were selected in the measurement campaign. On the basis of this setting, end-to-end performance in terms of the QoS metric, i.e., the average goodput and the goodput gain, was measured for these two kinds of scenarios with different parameters of free space path loss and blockage density. The results via the measurement campaign showed that the performance of the source-UAV-destination case was more efficient than that of the source-destination case in terms of average goodput and goodput gain. Especially, more than 80% of goodput gain was obtained by using the UAV as aerial relay with high blockage density.

3) SUMMARY AND LESSONS LEARNED

We have provided readers a survey of existing research efforts related with the performance assessment of UAV-assisted wireless networks with mmWave communications. To be more concrete, performance analysis and measurement campaign have been reviewed and discussed, respectively. The important lessons learned from the review of recent studies on the performance assessment are summarized as follows:

- The performance analysis of UAV-assisted wireless networks with mmWave communications focuses more on analyzing and assessing one or more performance metrics from a theoretical perspective, e.g., coverage performance, backhaul performance, and the effect of multiple factors on system performance. The main factors influencing the system performance include blockage effect of mmWave propagation channels, antenna patterns, vertical heights of communicating entities, and aggregate interference.
- Compared to the performance assessment using the theoretical analysis, we can also conduct the simulation tool based measurement campaign to verify the system performance. The major problem of using the simulation tool (e.g., NS-3 network simulator) is how to initialize the network parameters that are in accordance with the actual environments.

V. SUMMARY, OPEN ISSUES AND FUTURE RESEARCH DIRECTIONS

Many research efforts have been devoted to the development of 5G mmWave communications for UAV-assisted wireless networks. In the previous section, we have presented a comprehensive summary of current achievements in the integration of 5G mmWave communications into UAV-assisted wireless networks, and have also discussed the state-of-the-art issues, solutions, and open challenges in the newly emerging area. The survey has covered and highlighted seven different research issues that we would like to focus on, i.e., antenna technique, radio propagation channel, multiple access mechanism, spatial configuration, resource management, security strategy, and performance assessment. Based on the current great research efforts in the literature, in this section, we will summarize the existing research works in the way of comparison, and outline the open research issues along with the potential directions that need to be well investigated to encourage future research studies on this area.

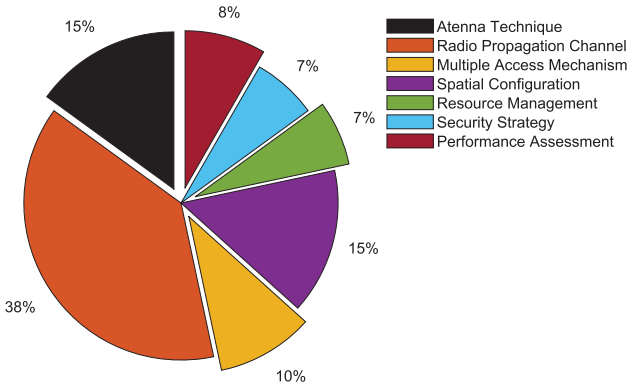

FIGURE 23. The comparison of the percentage of existing research works in 5G mmWave communications for UAV-assisted wireless networks.

A. SUMMARY

The key research information related to existing research works in the area of 5G mmWave communications for UAV-assisted wireless networks has been summarized in Fig. 23 and Fig. 24. From Fig. 23, the percentage of existing research works in terms of seven important research issues is vividly described as a pie chart. As can be observed, the majority of existing research works, close to 40%, are aimed at modeling the radio propagation channel and capturing the propagation characterization of mmWave signals for UAV-assisted wireless networks with 5G mmWave communications. This is because that the propagation channels in mmWave frequencies steeply differ from the channels in traditional microwave frequencies due to the technique challenges caused by higher frequencies, e.g., higher atmospheric attenuation and severe free space path loss. Correspondingly, the study and analysis on the radio propagation channel including channel modeling, channel estimation and tracking, and blockage detection and countermeasure, have great theoretical significance and applicable value. From this figure, we can also find that the percentage of other research issues occupies a comparatively small proportion, which indicates a potential research opportunity. In addition, Fig. 24 illustrates the time distribution of existing research works. From Fig. 24, it is clearly revealed that almost all of existing research works are distributed in the last three years. These research efforts appear a continually increasing trend, although six months have passed in 2019. Particularly, the research trend shows that the integration of 5G mmWave communications into

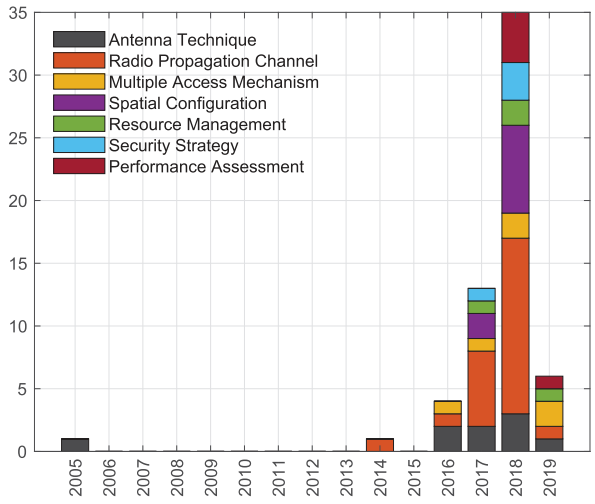

FIGURE 24. The time distribution graph of existing research works in 5G mmWave communications for UAV-assisted wireless networks.

UAV-assisted wireless networks has been recognized as one of the research hotspots in research community recently.

B. CHALLENGES AND OPEN ISSUES

1) mmWave BEAM ALIGNMENT AND BEAM SWITCHING

As a consequence of the decrease of mmWave beamwidth and the mobility of ground UEs, a main challenge in our considered scenario is to effectively steer and align the mmWave beams between TX and RX sides at the beginning of communications [111]–[114]. Efficient beam alignment together with highly directional beamforming can achieve a large directional gain to combat their stronger atmospheric attenuation and higher free space path loss. Therefore, 5G mmWave communications for UAV-assisted wireless networks need to require advanced beam alignment techniques, e.g., beam tracking, beam training, hierarchical beam codebook design, beam search, accurate estimation of the channel, etc. Among them, there are lots of issues need to be resolved, but one important issue is to mitigate the beam alignment overhead. Moreover, an alternative solution to perform a proper beam switching is also required when conventional beam alignment schemes by using beam sweeping become inefficient if not impossible [188]. In practical scenarios, both TX and RX sides cannot purely guarantee perfect beam alignment due to time-varying channel conditions and inaccurate beam tracking. As such, by considering the beam alignment errors, the impact of imperfect beam alignment between TX and RX sides on the system performance and directional gain should further be analyzed and evaluated.

2) DYNAMIC RESOURCE ALLOCATION BY INTEGRATING CONTENT CACHING AND COMPUTATION OFFLOADING

In practical environment, both the users and the UEs on the ground are always moving continuously, and even quickly, e.g., vehicle nodes. Meanwhile, the UAVs' spatial positions and trajectories are also changing overtime in a dynamic time-varying state especially for the fixed-wing UAVs. Apparently, it will be far more realistic to dynamically manage and schedule network resources according to the current instant time in the dynamic scenario. That is, we should perform dynamic resource allocation in which the network resource will be allocated in a continuous-time manner. This kind of continuous-time resource allocation differs from traditional resource allocation by assuming that the finite time horizon is divided into fixed time slots in a discrete way [19], [33], [189], [190]. By using the edge caching, the popular social contents can be cached at the edge of network during off-hours, to reduce backhaul loading at peak-hours. With the help of the MEC, the resource-limited UEs can offload their computation tasks to closer computation servers, to obtain multiple benefits, e.g., reduced latency, alleviated backhaul congestion, and enhanced user experience. Current research efforts have been targeted at content caching and computation offloading from/to the sky [17], [34]–[36], [191]–[193], but not well investigated in UAV-assisted wireless networks with mmWave communications. Therefore, one potential issue that needs to be resolved is to achieve joint dynamic resource allocation for content caching and computation offloading.

3) CROSS-LAYER OPTIMIZATION FRAMEWORK FOR ROUTING AND DISTRIBUTED RESOURCE ALLOCATION

Instead of using one single UAV, multiple UAVs have potentials to bring many benefits to assist wireless networks by creating drone swarm, such as high scalability, enhanced fault tolerance capability, longer network lifetime, improved multitasking ability, and so forth [74]–[76], [194]. Meanwhile, information exchange and transfer among multiple UAVs can be achieved by using the multi-hop drone interconnection via A2A mmWave links. In comparison with the lower layer solutions explored by existing research efforts, recent work indicates that there are many new challenges to routing problem at the network layer in our considered scenario. Several characteristics and constraints that affect the design of routing mechanism should be well incorporated, e.g., large scale spatial distribution, high degree of mobility, high dynamic network topology, possible blockage effect, etc. In addition, with a joint cross-layer optimization, other layer is able to share its information and configuration about its core function with the network layer without breaking the hierarchical structure of the layered architecture. The cross-layer design perspective can improve network performance and efficiency through the cross-layer coupling between network layer and other layers. As a result, joint cross-layer optimization for routing and distributed resource allocation is not only desirable, but also necessary.

4) JOINT OPTIMIZATION OF 3D BEAMFORMING AND AN PROJECTION IN DIRECTIONAL MODULATION

As a transmitter side security technique, the DM is used to project the modulated signals of the confidential mes-

sages into one or more desired spatial directions with the definite constellation patterns. In our considered scenario, by adopting the 3D beamforming architecture with multi-beam antenna array, the UAV serves as the DM transmitter to provide the secure communications at the physical layer for ground legitimate receivers. Nevertheless, existing works only take single desired legitimate receiver into account [177], [181]. That is, only one mmWave beam generated by the DM transmitter through modulating the confidential messages can be securely conveyed along a desired spatial direction. As such, one of the key challenges is to extend single legitimate receiver to multiple receivers by projecting multiple modulated signal of the confidential messages along multiple different spatial directions simultaneously. Additionally, as a spatial direction-dependent transmission, secure mmWave communications via the DM depends directly on the predefined spatial direction, i.e., DOA, for ground legitimate receiver. For the eavesdroppers, the same modulated signals will be particularly scrambled like the AN projection due to their different spatial directions. However, the eavesdroppers and legitimate receiver can be located in the same region. More seriously, one of the eavesdroppers has the chance to move inside the direction of the main beam of the desired receiver. Hence, efficient and adaptive spatial direction measurement and adjustment mechanisms for the 3D beamforming are required to provide more accurate control of DOAs for ground legitimate receivers.

C. POTENTIAL RESEARCH DIRECTIONS

1) UAV-ASSISTED WIRELESS POWER TRANSFER WITH mmWave COMMUNICATIONS

A challenging issue in UAV-assisted wireless networks is that no matter ground UEs or UAVs usually have limited energy storage for normal operations. To prolong the operational time of energy-constrained

UEs and UAVs, a straightforward and effective approach is to apply wireless power transfer to provide a controllable and sustainable energy supply [195]–[197]. For our considered scenario, on the one hand, UAVs are employed as mobile energy transmitters over the air to deliver wireless energy towards ground UEs. On the other hand, UAVs can be recharged by other power source, e.g., the solar energy by installing solar panels on UAVs [198] and the RF-enabled wireless power transfer performed by other UAVs or ground fixed energy transmitters. It is believed that wireless power transfer can be incorporated with mmWave communications for UAV-assisted wireless networks, where further research is needed.

2) mmWave COMMUNICATIONS FOR AERIAL ACCESS NETWORKS

To achieve the 3D ubiquitous super-connectivity in the global scale, the traditional terrestrial network architecture should be fully integrated with various non-terrestrial platforms, including UAVs, balloons, airships, and very low Earth orbit (VLEO) satellites [199]–[201]. The integration of these platforms has substantially boosted the prospect of implementing the aerial access networks (AANs) by extending the spatial scale of UAVs at low-altitude to higher altitudes. As the emerging radio access platforms, the AANs has attracted growing attentions from both academia and industry as a key enabler for future sixth generation (6G) systems of the 2030s. In addition, as a very promising way to sustain ultra-high-speed transmission, we can also apply mmWave communications in the AANs to make global access more robust and reliable [22]. More investigation is needed in this direction to address key technique challenges, e.g., 3D channel models, hybrid altitude optimization, deployment of multiple heterogeneous aerial platforms, cooperative access control, etc.

3) NETWORK FUNCTIONS VIRTUALIZATION FOR UAV-ASSISTED WIRELESS NETWORKS WITH mmWave COMMUNICATIONS

It is generally difficult to effectively manage different network services and various emerging applications, by identifying specific service for each networking entity, e.g., ground UEs and aerial BSs, running on our considered network architecture. There is a urgent need to build up a highly flexible network architecture with enhanced intelligence and improved resilience for our considered scenario [21], [202]–[204]. Network Functions Virtualization (NFV) provides an efficient paradigm to optimize network resource utility by virtualizing network services [205]–[207]. Such virtualization enables deployment of new network services and elastic network scaling to reduce maintenance costs and make network more flexible, scalable and cost-effective. It is firmly anticipated that the use of NFV in UAV-assisted wireless networks with mmWave communications will certainly make the network configuration interesting and valuable for both academia and industry studies.

4) INTEGRATION OF FAR-REACHING APPLICATIONS WITH mmWave COMMUNICATIONS FOR USER-CENTRIC UAV-ASSISTED WIRELESS NETWORKS

As already stated, mmWave communications have indeed paved the way into the widespread use of UAVs to enable wireless communications and networking, with the target to provide ultra-high-speed transmission for 5G and beyond applications. However, current achievements by linking UAV-assisted wireless networks and mmWave communications together are primarily focused on conventional services and applications. With the pervasiveness of Internet of Everything (IoE), the time has come for an unprecedented proliferation of newly emerging applications, e.g., boundless mobile eXtended reality (XR), autonomous driving, haptics, etc [208]–[210], to improve the QoE objective with the center of ground and aerial users. Particularly, the original 5G vision of enabling short-packet and sensing-based massive URLLC services will be disrupted due to these IoE

applications [208]. Further research is especially warranted to address this challenging issue of how to integrate the far-reaching applications with 5G mmWave communications for user-centric UAV-assisted wireless networks.

5) MmWave COMMUNICATIONS FOR UAV-ASSISTED WIRELESS NETWORKS WITH MACHINE LEARNING

MmWave communications for UAV-assisted wireless networks not only have a substantial potential to achieve higher transmission efficiency with enhanced coverage and capacity, but also support a wide variety of 5G and B5G wireless applications. These innovative applications are expected to unleash a massive IoT ecosystem with huge data throughput, high wireless bandwidth, super-fast speeds, ultra-low latency, and increased connectivity. With exciting opportunities, the design, control and optimization of UAV-assisted wireless networks with mmWave communications become very challenging and complex. The significant challenges require us to configure, manage, and control networks in a smarter and more agile manner. Inspired by the trends, machine learning is needed to enable adaptive learning and intelligent decision making, due to its capability to achieve the convergence of computing power, algorithm improvement, and data proliferation [211]–[214]. Future potential research will be strongly expected to apply machine learning technique, e.g., multi-agent deep reinforcement learning [215], federated learning [216], concept drift learning [217], in our considered scenario, to overcome the challenges of resource allocation, cross-layer optimization, physical layer security, etc.

VI. CONCLUSION

In this paper, we have presented a comprehensive literature survey focusing on the current state-of-the-art achievements in the integration of 5G mmWave communications into UAV-assisted wireless networks. By analyzing and reviewing the existing research efforts, we first introduced a novel taxonomy to categorize the cutting-edge solutions from seven aspects. We then reviewed existing articles related to UAV-assisted wireless networks and communications as well as 5G mmWave communications, and further compared our survey with them. Subsequently, we provided a brief overview of key technical advantages and challenges as well as potential applications in 5G mmWave communications for UAV-assisted wireless networks. With the devised taxonomy, we surveyed in detail the state-of-the-art issues, solutions, and open challenges of integrating mmWave communications into UAV-assisted wireless networks. We also derived several lessons learned from these research activities. Finally, we pinpointed several open issues and outlined promising research directions. We hope that this survey is timely and useful for the interested researchers and practitioners to concentrate their research activities on this area for the development of next generation wireless networks.

REFERENCES

[1] S. Hayat, E. Yanmaz, and R. Muzaffar, "Survey on unmanned aerial vehicle networks for civil applications: A communications viewpoint," *IEEE Commun. Surveys Tuts.*, vol. 18, no. 4, pp. 2624–2661, 4th Quart., 2016.
[2] M. Erdelj, E. Natalizio, K. R. Chowdhury, and I. F. Akyildiz, "Help from the sky: Leveraging UAVs for disaster management," *IEEE Pervasive Comput.*, vol. 16, no. 1, pp. 24–32, Jan. 2017.
[3] H. Chao, Y. Cao, and Y. Chen, "Autopilots for small unmanned aerial vehicles: A survey," *Int. J. Control Autom. Syst.*, vol. 8, no. 1, pp. 36–44, Feb. 2010.
[4] S. A. R. Naqvi, S. A. Hassan, H. Pervaiz, and Q. Ni, "Drone-aided communication as a key enabler for 5G and resilient public safety networks," *IEEE Commun. Mag.*, vol. 56, no. 1, pp. 36–42, Jan. 2018.
[5] C. Zhang and J. M. Kovacs, "The application of small unmanned aerial systems for precision agriculture: A review," *Precis. Agricult.*, vol. 13, no. 6, pp. 693–712, Dec. 2012.
[6] N. H. Motlagh, T. Taleb, and O. Arouk, "Low-altitude unmanned aerial vehicles-based Internet of Things services: Comprehensive survey and future perspectives," *IEEE Internet Things J.*, vol. 3, no. 6, pp. 899–922, Dec. 2016.
[7] Shipware. (Nov. 2018). *What Amazon Effect Means for the Shipping Industry*. [Online]. Available: https://www.shipware.com/what-the-amazon-effect-means-for-the-shipping-
[8] M. Mozaffari, W. Saad, M. Bennis, Y.-H. Nam, and M. Debbah, "A tutorial on UAVs for wireless networks: Applications, challenges, and open problems," *IEEE Commun. Surveys Tuts.*, to be published. doi: 10.1109/COMST.2019.2902862.
[9] Y. Zeng, R. Zhang, and T. J. Lim, "Wireless communications with unmanned aerial vehicles: Opportunities and challenges," *IEEE Commun. Mag.*, vol. 54, no. 5, pp. 36–42, May 2016.
[10] Z. Xiao, P. Xia, and X.-G. Xia, "Enabling UAV cellular with millimeter-wave communication: Potentials and approaches," *IEEE Commun. Mag.*, vol. 54, no. 5, pp. 66–73, May 2016.
[11] A. Fotouhi, H. Qiang, M. Ding, M. Hassan, L. G. Giordano, and A. García-Rodríguez, and J. Yuan, "Survey on uav cellular communications: Practical aspects, standardization advancements, regulation, and security challenges," *IEEE Commun. Surveys Tuts.*, to be published. doi: 10.1109/COMST.2019.2906228.
[12] S. Sekander, H. Tabassum, and E. Hossain, "Multi-tier drone architecture for 5G/B5G cellular networks: Challenges, trends, and prospects," *IEEE Commun. Mag.*, vol. 56, no. 3, pp. 96–103, Mar. 2018.
[13] Y. Zeng, Q. Wu, and R. Zhang, "Accessing from the sky: A tutorial on UAV communications for 5G and beyond," Mar. 2019, *arXiv:1903.05289*. [Online]. Available: http://arxiv.org/abs/1903.05289
[14] E. Vinogradov, H. Sallouha, S. D. Bast, M. M. Azari, and S. Pollin, "Tutorial on UAV: A blue sky view on wireless communication," Jan. 2019, *arXiv:1901.02306*. [Online]. Available: http://arxiv.org/abs/1901.02306
[15] H. Hellaoui, O. Bekkouche, M. Bagaa, and T. Taleb, "Aerial control system for spectrum efficiency in UAV-to-cellular communications," *IEEE Commun. Mag.*, vol. 56, no. 10, pp. 108–113, Oct. 2018.
[16] V. Sharma, K. Srinivasan, H.-C. Chao, K.-L. Hua, and W.-H. Cheng, "Intelligent deployment of UAVs in 5G heterogeneous communication environment for improved coverage," *J. Netw. Comput. Appl.*, vol. 85, pp. 94–105, May 2017.
[17] H. Wu, X. Tao, N. Zhang, and X. Shen, "Cooperative UAV cluster-assisted terrestrial cellular networks for ubiquitous coverage," *IEEE J. Sel. Areas Commun.*, vol. 36, no. 9, pp. 2045–2058, Sep. 2018.
[18] P. Yang, X. Cao, C. Yin, Z. Xiao, X. Xi, and D. Wu, "Proactive drone-cell deployment: Overload relief for a cellular network under flash crowd traffic," *IEEE Trans. Intell. Transp. Syst.*, vol. 18, no. 10, pp. 2877–2892, Oct. 2017.
[19] H. Wang, J. Wang, G. Ding, L. Wang, T. A. Tsiftsis, and P. K. Sharma, "Resource allocation for energy harvesting-powered D2D communication underlaying UAV-assisted networks," *IEEE Trans. Green Commun. Netw.*, vol. 2, no. 1, pp. 14–24, Mar. 2018.
[20] C.-M. Cheng, P.-H. Hsiao, H. T. Kung, and D. Vlah, "Maximizing throughput of UAV-relaying networks with the load-carry-and-deliver paradigm," in *Proc. IEEE Wireless Commun. Netw. Conf.*, Hong Kong, Mar. 2007, pp. 4417–4424.
[21] I. Bor-Yaliniz and H. Yanikomeroglu, "The new frontier in RAN heterogeneity: Multi-tier drone-cells," *IEEE Commun. Mag.*, vol. 54, no. 11, pp. 48–55, Nov. 2016.
[22] Y. Huo, X. Dong, T. Lu, W. Xu, and M. Yuen, "Distributed and multi-layer UAV network for the next-generation wireless communi-

cation," *IEEE Internet Things J.*, to be published. doi: 10.1109/JIOT.2019.2914414.

[23] D. Kim, J. Lee, and T. Q. S. Quek, "Multi-layer unmanned aerial vehicle networks: Modeling and performance analysis," Apr. 2019, *arXiv:1904.01167*. [Online]. Available: https://arxiv.org/abs/1904.01167

[24] I. Bekmezci, O. K. Sahingoz, and . Temel, "Flying ad-hoc networks (FANETs): A survey," *Ad Hoc Netw.*, vol. 11, no. 3, pp. 1254–1270, 2013.

[25] L. Gupta, R. Jain, and G. Vaszkun, "Survey of important issues in UAV communication networks," *IEEE Commun. Surveys Tuts.*, vol. 18, no. 2, pp. 1123–1152, 2nd Quart., 2016.

[26] S. Rosati, K. Kru elecki, G. Heitz, D. Floreano, and B. Rimoldi, "Dynamic routing for flying ad hoc networks," *IEEE Trans. Veh. Technol.*, vol. 65, no. 3, pp. 1690–1700, Mar. 2016.

[27] M. Gharibi, R. Boutaba, and S. L. Waslander, "Internet of drones," *IEEE Access*, vol. 4, pp. 1148–1162, Mar. 2016.

[28] G. Choudhary, V. Sharma, and I. You, "Sustainable and secure trajectories for the military Internet of drones (IoD) through an efficient medium access control (MAC) protocol," *Comput. Elect. Eng.*, vol. 74, pp. 59–73, Mar. 2019.

[29] J. Gong, T.-H. Chang, C. Shen, and X. Chen, "Flight time minimization of UAV for data collection over wireless sensor networks," *IEEE J. Sel. Areas Commun.*, vol. 36, no. 9, pp. 1942–1954, Sep. 2018.

[30] W. Shi, H. Zhou, J. Li, W. Xu, N. Zhang, and X. Shen, "Drone assisted vehicular networks: Architecture, challenges and opportunities," *IEEE Netw.*, vol. 32, no. 3, pp. 130–137, May 2018.

[31] M. Mozaffari, W. Saad, M. Bennis, and M. Debbah, "Mobile unmanned aerial vehicles (UAVs) for energy-efficient Internet of Things communications," *IEEE Trans. Wireless Commun.*, vol. 16, no. 11, pp. 7574–7589, Nov. 2017.

[32] P. Zhou, X. Fang, Y. Fang, R. He, Y. Long, and G. Huang, "Beam management and self-healing for mmWave UAV mesh networks," *IEEE Trans. Veh. Technol.*, vol. 68, no. 2, pp. 1718–1732, Feb. 2019.

[33] S. Yin, Y. Zhao, and L. Li, "UAV-assisted cooperative communications with time-sharing SWIPT," in *Proc. IEEE Int. Conf. Commun. (ICC)*, Kansas City, MO, USA, May 2018, pp. 1–6.

[34] N. Zhao, F. Cheng, F. R. Yu, J. Tang, Y. Chen, G. Gui, and H. Sari, "Caching UAV assisted secure transmission in hyper-dense networks based on interference alignment," *IEEE Trans. Commun.*, vol. 66, no. 5, pp. 2281–2294, May 2018.

[35] F. Zhou, Y. Wu, R. Q. Hu, and Y. Qian, "Computation rate maximization in uav-enabled wireless-powered mobile-edge computing systems," *IEEE J. Sel. Areas Commun.*, vol. 36, no. 9, pp. 1927–1941, Sep. 2018.

[36] L. Zhang, Z. Zhao, Q. Wu, H. Zhao, H. Xu, and X. Wu, "Energy-aware dynamic resource allocation in UAV assisted mobile edge computing over social Internet of vehicles," *IEEE Access*, vol. 6, pp. 56700–56715, Oct. 2018.

[37] M. Chen, M. Mozaffari, W. Saad, C. Yin, M. Debbah, and C. S. Hong, "Caching in the sky: Proactive deployment of cache-enabled unmanned aerial vehicles for optimized quality-of-experience," *IEEE J. Sel. Areas Commun.*, vol. 35, no. 5, pp. 1046–1061, May 2017.

[38] S. Zhang and J. Liu, "Analysis and optimization of multiple unmanned aerial vehicle-assisted communications in post-disaster areas," *IEEE Trans. Veh. Technol.*, vol. 67, no. 12, pp. 12049–12060, Dec. 2018.

[39] Y. Saleem, M. H. Rehmani, and S. Zeadally, "Integration of cognitive radio technology with unmanned aerial vehicles: Issues, opportunities, and future research challenges," *J. Netw. Comput. Appl.*, vol. 50, pp. 15–31, Apr. 2015.

[40] L. Liang, W. Xu, and X. Dong, "Low-complexity hybrid precoding in massive multiuser MIMO systems," *IEEE Wireless Commun. Lett.*, vol. 3, no. 6, pp. 653–656, Dec. 2014.

[41] X. Hong, J. Wang, C.-X. Wang, and J. Shi, "Cognitive radio in 5G: A perspective on energy-spectral efficiency trade-off," *IEEE Commun. Mag.*, vol. 52, no. 7, pp. 46–53, Jul. 2014.

[42] N. Bhushan, J. Li, D. Malladi, R. Gilmore, D. Brenner, A. Damnjanovic, R. Sukhavasi, C. Patel, and S. Geirhofer, "Network densification: The dominant theme for wireless evolution into 5G," *IEEE Commun. Mag.*, vol. 52, no. 2, pp. 82–89, Feb. 2014.

[43] Z. Ding, X. Lei, G. K. Karagiannidis, R. Schober, J. Yuan, and V. Bhargava, "A survey on non-orthogonal multiple access for 5G networks: Research challenges and future trends," *IEEE J. Sel. Areas Commun.*, vol. 35, no. 10, pp. 2181–2195, Oct. 2017.

[44] J. Wang, A. Jin, D. Shi, L. Wang, H. Shen, D. Wu, L. Hu, L. Gu, L. Lu, Y. Chen, J. Wang, Y. Saito, A. Benjebbour, and Y. Kishiyama, "Spectral efficiency improvement with 5G technologies: Results from field tests," *IEEE J. Sel. Areas Commun.*, vol. 35, no. 8, pp. 1867–1875, Aug. 2017.

[45] E. M. Yeh and R. A. Berry, "Throughput optimal control of cooperative relay networks," *IEEE Trans. Inf. Theory*, vol. 53, no. 10, pp. 3827–3833, Oct. 2007.

[46] A. Ghosh, T. A. Thomas, M. C. Cudak, R. Ratasuk, P. Moorut, F. W. Vook, T. S. Rappaport, G. R. MacCartney, S. Sun, and S. Nie, "Millimeter-wave enhanced local area systems: A high-data-rate approach for future wireless networks," *IEEE J. Sel. Areas Commun.*, vol. 32, no. 6, pp. 1152–1163, Jun. 2014.

[47] P. Wang, Y. Li, L. Song, and B. Vucetic, "Multi-gigabit millimeter wave wireless communications for 5G: From fixed access to cellular networks," *IEEE Commun. Mag.*, vol. 53, no. 1, pp. 168–178, Jan. 2015.

[48] M. Xiao, S. Mumtaz, Y. Huang, L. Dai, Y. Li, M. Matthaiou, G. K. Karagiannidis, E. Bjornson, K. Yang, C.-L. I, and A. Ghosh, "Millimeter wave communications for future mobile networks," *IEEE J. Sel. Areas Commun.*, vol. 35, no. 9, pp. 1909–1935, Sep. 2017.

[49] Y. Niu, Y. Li, D. Jin, L. Su, and A. V. Vasilakos, "A survey of millimeter wave communications (mmWave) for 5G: Opportunities and challenges," *Wireless Netw.*, vol. 21, no. 8, pp. 2657–2676, Nov. 2015.

[50] T. S. Rappaport, S. Sun, R. Mayzus, H. Zhao, Y. Azar, K. Wang, G. N. Wong, J. K. Schulz, M. Samimi, and F. Gutierrez, "Millimeter wave mobile communications for 5G cellular: It will work!" *IEEE Access*, vol. 1, pp. 335–349, May 2013.

[51] W. Roh, J.-Y. Seol, J. Park, B. Lee, J. Lee, Y. Kim, J. Cho, K. Cheun, and F. Aryanfar, "Millimeter-wave beamforming as an enabling technology for 5G cellular communications: Theoretical feasibility and prototype results," *IEEE Commun. Mag.*, vol. 52, no. 2, pp. 106–113, Feb. 2014.

[52] X. Wang, L. Kong, F. Kong, F. Qiu, M. Xia, S. Arnon, and G. Chen, "Millimeter wave communication: A comprehensive survey," *IEEE Commun. Surveys Tuts.*, vol. 20, no. 3, pp. 1616–1653, 3rd Quart., 2018.

[53] *Use of Multiple Gigabit Wireless Systems in Frequencies Around 60 GHz*, document M.2227-2, Mobile, Radiodetermination, Amateur and Related Satellite Services, Jan. 2018, pp. 1–30.

[54] S.-Y. Lien, S.-L. Shieh, Y. Huang, B. Su, Y.-L. Hsu, and H.-Y. Wei, "5G new radio: Waveform, frame structure, multiple access, and initial access," *IEEE Commun. Mag.*, vol. 55, no. 6, pp. 64–71, Jun. 2017.

[55] M. Shafi, A. F. Molisch, P. J. Smith, T. Haustein, P. Zhu, P. D. Silva, F. Tufvesson, A. Benjebbour, and G. Wunder, "5G: A tutorial overview of standards, trials, challenges, deployment, and practice," *IEEE J. Sel. Areas Commun.*, vol. 35, no. 6, pp. 1201–1221, Jun. 2017.

[56] H. Ji, S. Park, J. Yeo, Y. Kim, J. Lee, and B. Shim, "Ultra-reliable and low-latency communications in 5G downlink: Physical layer aspects," *IEEE Wireless Commun.*, vol. 25, no. 3, pp. 124–130, Jun. 2018.

[57] W. Khawaja, O. Ozdemir, and I. Guvenc, "UAV air-to-ground channel characterization for mmWave systems," in *Proc. IEEE 86th Veh. Technol. Conf. (VTC-Fall)*, Toronto, ON, Canada, Sep. 2017, pp. 1–5.

[58] J. Zhao, F. Gao, L. Kuang, Q. Wu, and W. Jia, "Channel tracking with flight control system for UAV mmWave MIMO communications," *IEEE Commun. Lett.*, vol. 22, no. 6, pp. 1224–1227, Jun. 2018.

[59] J. Bao, D. Sprinz, and H. Li, "Blockage of millimeter wave communications on rotor UAVs: Demonstration and mitigation," in *Proc. IEEE Mil. Commun. Conf. (MILCOM)*, Baltimore, MD, USA, Oct. 2017, pp. 768–774.

[60] Z. Xiao, X. G. Xia, D. Jin, and N. Ge, "Iterative eigenvalue decomposition and multipath-grouping Tx/Rx joint beamformings for millimeter-wave communications," *IEEE Trans. Wireless Commun.*, vol. 14, no. 3, pp. 1595–1607, Mar. 2015.

[61] Z. Xiao, P. Xia, and X.-G. Xia, "Full-duplex millimeter-wave communication," *IEEE Wireless Commun.*, vol. 24, no. 6, pp. 136–143, Dec. 2017.

[62] Z. Xiao, "Suboptimal spatial diversity scheme for 60 GHz millimeter-wave WLAN," *IEEE Commun. Lett.*, vol. 17, no. 9, pp. 1790–1793, Sep. 2013.

[63] M. Gapeyenko, A. Samuylov, M. Gerasimenko, D. Moltchanov, S. Singh, E. Aryafar, S.-P. Yeh, N. Himayat, S. Andreev, and Y. Koucheryavy, "Analysis of human-body blockage in urban millimeter-wave cellular communications," in *Proc. IEEE Int. Conf. Commun. (ICC)*, Kuala Lumpur, Malaysia, May 2016, pp. 1–7.

[64] M. Gapeyenko, I. Bor-Yaliniz, S. Andreev, H. Yanikomeroglu, and Y. Koucheryavy, "Effects of blockage in deploying mmWave drone base stations for 5G networks and beyond," in *Proc. IEEE Int. Conf. Com-*

mun. Workshops (ICC Workshops), Kansas City, MO, USA, May 2018, pp. 1–6.
[65] M. Gapeyenko, V. Petrov, D. Moltchanov, S. Andreev, N. Himayat, and Y. Koucheryavy, "Flexible and reliable UAV-assisted backhaul operation in 5G mmWave cellular networks," *IEEE J. Sel. Areas Commun.*, vol. 36, no. 11, pp. 2486–2496, Nov. 2018.
[66] B. Li, Z. Fei, and Y. Zhang, "UAV communications for 5G and beyond: Recent advances and future trends," *IEEE Internet Things J.*, vol. 6, no. 2, pp. 2241–2263, Dec. 2018.
[67] H. Wang, H. Zhao, J. Zhang, D. Ma, J. Li, and J. Wei, "Survey on unmanned aerial vehicle networks: A cyber physical system perspective," Dec. 2018, *arXiv:1812.06821*. [Online]. Available: http://arxiv.org/abs/1812.06821
[68] J. Sánchez-García, J. García-Campos, M. Arzamendia, D. Reina, S. Toral, and D. Gregor, "A survey on unmanned aerial and aquatic vehicle multi-hop networks: Wireless communications, evaluation tools and applications," *Comput. Commun.*, vol. 119, pp. 43–65, Apr. 2018.
[69] S. Rangan, T. S. Rappaport, and E. Erkip, "Millimeter-wave cellular wireless networks: Potentials and challenges," *Proc. IEEE*, vol. 102, no. 3, pp. 366–385, Mar. 2014.
[70] I. A. Hemadeh, K. Satyanarayana, M. El-Hajjar, and L. Hanzo, "Millimeter-wave communications: Physical channel models, design considerations, antenna constructions, and link-budget," *IEEE Commun. Surveys Tuts.*, vol. 20, no. 2, pp. 870–913, 2nd Quart., 2018.
[71] T. S. Rappaport, Y. Xing, G. R. MacCartney, A. F. Molisch, E. Mellios, and J. Zhang, "Overview of millimeter wave communications for fifth-generation (5G) wireless networks—With a focus on propagation models," *IEEE Trans. Antennas Propag.*, vol. 65, no. 12, pp. 6213–6230, Dec. 2017.
[72] P. Zhou, K. Cheng, X. Han, X. Fang, Y. Fang, R. He, Y. Long, and Y. Liu, "IEEE 802.11ay-based mmWave WLANs: Design challenges and solutions," *IEEE Commun. Surveys Tuts.*, vol. 20, no. 3, pp. 1654–1681, 3rd Quart., 2018.
[73] F. Jameel, S. Wyne, S. J. Nawaz, and Z. Chang, "Propagation channels for mmWave vehicular communications: State-of-the-art and future research directions," *IEEE Wireless Commun.*, vol. 26, no. 1, pp. 144–150, Feb. 2019.
[74] J. Jiang and G. Han, "Routing protocols for unmanned aerial vehicles," *IEEE Commun. Mag.*, vol. 56, no. 1, pp. 58–63, Jan. 2018.
[75] O. S. Oubbati, A. Lakas, F. Zhou, M. Günes, and M. B. Yagoubi, "A survey on position-based routing protocols for flying ad hoc networks (FANETs)," *Veh. Commun.*, vol. 10, pp. 29–56, Oct. 2017.
[76] M. Y. Arafat and S. Moh, "A survey on cluster-based routing protocols for unmanned aerial vehicle networks," *IEEE Access*, vol. 7, pp. 498–516, Jan. 2019.
[77] A. A. Khuwaja, Y. Chen, N. Zhao, M.-S. Alouini, and P. Dobbins, "A survey of channel modeling for UAV communications," *IEEE Commun. Surveys Tuts.*, vol. 20, no. 4, pp. 2804–2821, 4th Quart., 2018.
[78] H. Shakhatreh, A. Sawalmeh, A. I. Al-Fuqaha, Z. Dou, E. Almaita, I. Khalil, N. S. Othman, A. Khreishah, and M. Guizani, "Unmanned aerial vehicles (UAVs): A survey on civil applications and key research challenges," *IEEE Access*, vol. 7, pp. 48572–48634, Apr. 2019.
[79] M. Lu, M. Bagheri, A. P. James, and T. Phung, "Wireless charging techniques for UAVs: A review, reconceptualization, and extension," *IEEE Access*, vol. 6, pp. 29865–29884, May 2018.
[80] M. E. Mkiramweni, C. Yang, J. Li, and Z. Han, "Game-theoretic approaches for wireless communications with unmanned aerial vehicles," *IEEE Wireless Commun.*, vol. 25, no. 6, pp. 104–112, Dec. 2018.
[81] P. Adhikari, "Understanding millimeter wave wireless communication," Loea Corp., San Diego, CA, USA, White Paper L1104-WP, Jun. 2008.
[82] *5G Spectrum Public Policy Position*, Huawei Technol., Shenzhen, China, 2017.
[83] H. Mehrpouyan, M. R. Khanzadi, M. Matthaiou, A. M. Sayeed, R. Schober, and Y. Hua, "Improving bandwidth efficiency in E-band communication systems," *IEEE Commun. Mag.*, vol. 52, no. 3, pp. 121–128, Mar. 2014.
[84] S. Yost, "mmWave: Battle of the bands," Nat. Instrum., Austin, TX, USA, Tech. Rep., Mar. 2019.
[85] *5G Spectrum Recommendations*, 5G Amer., Bellevue, WA, USA, Apr. 2017.
[86] *QTM052 Mmwave Antenna Modules*, Qualcomm Technol., San Diego, CA, USA, Oct. 2018. [Online]. Available: https://www.qualcomm.com/products/qtm052-mmwave-antenna-modules
[87] J. Johnson and M. P. Raja, "A study on millimeter-wave vehicular communication," *Int. J. Innov. Res. Sci., Eng. Technol.*, vol. 7, no. 10, pp. 10425–10431, Oct. 2018.
[88] T. K. Vu, C.-F. Liu, M. Bennis, M. Debbah, M. Latva-Aho, and C. S. Hong, "Ultra-reliable and low latency communication in mmWave-enabled massive MIMO networks," *IEEE Commun. Lett.*, vol. 21, no. 9, pp. 2041–2044, Sep. 2017.
[89] B. He and H. Jafarkhani, "Low-complexity reconfigurable MIMO for millimeter wave communications," *IEEE Trans. Commun.*, vol. 66, no. 11, pp. 5278–5291, Nov. 2018.
[90] L. Yang, Y. Zeng, and R. Zhang, "Channel estimation for millimeter-wave MIMO communications with lens antenna arrays," *IEEE Trans. Veh. Technol.*, vol. 67, no. 4, pp. 3239–3251, Apr. 2018.
[91] R. Sun, C. A. Gentile, J. Senic, P. Vouras, P. B. Papazian, N. T. Golmie, and K. A. Remley, "Millimeter-wave radio channels vs. synthetic beamwidth," *IEEE Commun. Mag.*, vol. 56, no. 12, pp. 53–59, Dec. 2018.
[92] A. T. Nassar, A. I. Sulyman, and A. Alsanie, "Radio capacity estimation for millimeter wave 5G cellular networks using narrow beamwidth antennas at the base stations," *Int. J. Antennas Propag.*, vol. 2015, Jun. 2015, Art. no. 878614.
[93] Q. Xue, P. Zhou, X. Fang, and M. Xiao, "Performance analysis of interference and eavesdropping immunity in narrow beam mmWave networks," *IEEE Access*, vol. 6, pp. 67611–67624, Oct. 2018.
[94] S. K. Islam and M. R. Haider, *Sensors and Low Power Signal Processing*. New York, NY, USA: Springer, 2010.
[95] H. T. Friis, "A note on a simple transmission formula," *Proc. IRE*, vol. 34, no. 5, pp. 254–256, May 1946.
[96] T. S. Rappaport, K. Blankenship, and H. Xu, "Propagation and radio system design issues in mobile radio systems for the glomo project," Virginia Polytechn. Inst. State Univ., Blacksburg, VA, USA, Tech. Rep., 1997.
[97] G. Yue, Z. Wang, L. Chen, L. Cheng, J. Tang, X. Zou, Y. Zeng, and L. Li, "Demonstration of 60 GHz millimeter-wave short-range wireless communication system at 3.5 Gbps over 5 m range," *Sci. China Inf. Sci.*, vol. 60, no. 8, Jun. 2017, Art. no. 080306.
[98] I. F. Akyildiz, C. Han, and S. Nie, "Combating the distance problem in the millimeter wave and terahertz frequency bands," *IEEE Commun. Mag.*, vol. 56, no. 6, pp. 102–108, Jun. 2018.
[99] A. Benjebbour, M. Iwabuchi, Y. Kishiyama, W. Guangjian, L. Gu, Y. Cui, and T. Takada, "Outdoor experimental trials of long range mobile communications using 39 GHz," in *Proc. IEEE 87th Veh. Technol. Conf. (VTC Spring)*, Porto, Portugal, Jun. 2018, pp. 1–5.
[100] M. B. Majed and T. A. Rahman, "Propagation path loss modeling and coverage measurements in urban microcell in millimeter wave frequency bands," *ARPN J. Eng. Appl. Sci.*, vol. 13, no. 8, pp. 2882–2887, Apr. 2018.
[101] G. A. Siles, J. M. Riera, and P. Garcia-del-Pino, "Atmospheric attenuation in wireless communication systems at millimeter and THz frequencies [wireless corner]," *IEEE Antennas Propag. Mag.*, vol. 57, no. 1, pp. 48–61, Feb. 2015.
[102] Y. Banday, G. M. Rather, and G. R. Begh, "Effect of atmospheric absorption on millimetre wave frequencies for 5G cellular networks," *IET Commun.*, vol. 13, no. 3, pp. 265–270, Feb. 2019.
[103] T. L. Frey, "The effects of the atmosphere and weather on the performance of a mm-wave communication link," *Appl. Microw. Wireless*, vol. 11, pp. 76–81, Feb. 1999.
[104] P. Nagaraj, "Impact of atmospheric impairments on mmwave based outdoor communication," Jun. 2018, *arXiv:1806.05176*. [Online]. Available: https://arxiv.org/abs/1806.05176
[105] D. Nandi and A. Maitra, "Study of rain attenuation effects for 5G mm-wave cellular communication in tropical location," *IET Microw., Antennas Propag.*, vol. 12, no. 9, pp. 1504–1507, Jul. 2018.
[106] I. K. Jain, R. Kumar, and S. S. Panwar, "The impact of mobile blockers on millimeter wave cellular systems," *IEEE J. Sel. Areas Commun.*, vol. 37, no. 4, pp. 854–868, Apr. 2019.
[107] Z. Pi and F. Khan, "An introduction to millimeter-wave mobile broadband systems," *IEEE Commun. Mag.*, vol. 49, no. 6, pp. 101–107, Jun. 2011.
[108] T. Bai and R. W. Heath, Jr., "Coverage and rate analysis for millimeter-wave cellular networks," *IEEE Trans. Wireless Commun.*, vol. 14, no. 2, pp. 1100–1114, Feb. 2015.
[109] C. Slezak, V. Semkin, S. Andreev, Y. Koucheryavy, and S. Rangan, "Empirical effects of dynamic human-body blockage in 60 GHz communications," *IEEE Commun. Mag.*, vol. 56, no. 12, pp. 60–66, Dec. 2018.
[110] J. G. Andrews, T. Bai, M. Kulkarni, A. Alkhateeb, A. Gupta, and R. W. Heath, Jr., "Modeling and analyzing millimeter wave cellular systems," *IEEE Trans. Commun.*, vol. 65, no. 1, pp. 403–430, Jan. 2017.

[111] J. Wildman, P. H. J. Nardelli, M. Latva-Aho, and S. Weber, "On the joint impact of beamwidth and orientation error on throughput in directional wireless Poisson networks," *IEEE Trans. Wireless Commun.*, vol. 13, no. 12, pp. 7072–7085, Dec. 2014.

[112] X. Yu, J. Zhang, M. Haenggi, and K. B. Letaief, "Coverage analysis for millimeter wave networks: The impact of directional antenna arrays," *IEEE J. Sel. Areas Commun.*, vol. 35, no. 7, pp. 1498–1512, Jul. 2017.

[113] M. Hashemi, A. Sabharwal, C. E. Koksal, and N. B. Shroff, "Efficient beam alignment in millimeter wave systems using contextual bandits," in *Proc. IEEE INFOCOM*, Apr. 2018, pp. 2393–2401.

[114] H. Hassanieh, O. Abari, M. Rodriguez, M. Abdelghany, D. Katabi, and P. Indyk, "Fast millimeter wave beam alignment," in *Proc. Conf. ACM Special Interest Group Data Commun. (SIGCOMM)*, Budapest, Hungary, Aug. 2018, pp. 432–445.

[115] Z. Xiao, T. He, P. Xia, and X.-G. Xia, "Hierarchical codebook design for beamforming training in millimeter-wave communication," *IEEE Trans. Wireless Commun.*, vol. 15, no. 5, pp. 3380–3392, May 2016.

[116] L. Yang and W. Zhang, "Hierarchical codebook and beam alignment for UAV communications," in *Proc. IEEE Globecom Workshops (GC Wkshps)*, Abu Dhabi, United Arab Emirates, Dec. 2018, pp. 1–6.

[117] C. Liu, M. Li, S. V. Hanly, I. B. Collings, and P. Whiting, "Millimeter wave beam alignment: Large deviations analysis and design insights," *IEEE J. Sel. Areas Commun.*, vol. 35, no. 7, pp. 1619–1631, Jul. 2017.

[118] A. Alkhateeb, J. Mo, N. Gonzalez-Prelcic, and R. W. Heath, Jr., "MIMO precoding and combining solutions for millimeter-wave systems," *IEEE Commun. Mag.*, vol. 52, no. 12, pp. 122–131, Dec. 2014.

[119] B. Gao, Z. Xiao, C. Zhang, L. Su, D. Jin, and L. Zeng, "Double-link beam tracking against human blockage and device mobility for 60-GHz WLAN," in *Proc. IEEE Wireless Commun. Netw. Conf. (WCNC)*, Istanbul, Turkey, Apr. 2014, pp. 323–328.

[120] J. Lee, M.-D. Kim, J.-J. Park, and Y. J. Chong, "Field-measurement-based received power analysis for directional beamforming millimeter-wave systems: Effects of beamwidth and beam misalignment," *ETRI J.*, vol. 40, no. 1, pp. 26–38, Feb. 2018.

[121] T. Nitsche, A. B. Flores, E. W. Knightly, and J. Widmer, "Steering with eyes closed: Mm-wave beam steering without in-band measurement," in *Proc. IEEE Conf. Comput. Commun.*, Hong Kong, Apr. 2015, pp. 2416–2424.

[122] N. Rupasinghe, Y. Yapıcı, I. Güvenç, and Y. Kakishima, "Non-orthogonal multiple access for mmwave drone networks with limited feedback," *IEEE Trans. Commun.*, vol. 67, no. 1, pp. 762–777, Jan. 2019.

[123] Y. Zhu, G. Zheng, and M. Fitch, "Secrecy rate analysis of UAV-enabled mmWave networks using Matérn hardcore point processes," *IEEE J. Sel. Areas Commun.*, vol. 36, no. 7, pp. 1397–1409, Jul. 2018.

[124] R. Taori and A. Sridharan, "Point-to-multipoint in-band mmwave backhaul for 5G networks," *IEEE Commun. Mag.*, vol. 53, no. 1, pp. 195–201, Jan. 2015.

[125] *Use of Spectrum Bands Above 24 GHz for Mobile Radio Services*, document GN 14-177, FCC, Feb. 2019.

[126] *Revision of Part 15 of the Commission's Rules Regarding Operation in the 57-64 GHz Band*, document FCC-13-112, FCC, Aug. 2013.

[127] L. Zhu, J. Zhang, Z. Xiao, X. Cao, D. O. Wu, and X.-G. Xia, "3-D beamforming for flexible coverage in millimeter-wave UAV communications," *IEEE Wireless Commun. Lett.*, vol. 8, no. 3, pp. 837–840, Jun. 2019.

[128] W. Zhong, L. Xu, Q. Zhu, X. Chen, and J. Zhou, "MmWave beamforming for UAV communications with unstable beam pointing," *China Commun.*, vol. 16, no. 1, pp. 37–46, Jan. 2019.

[129] H. Tsuji, M. Oodo, R. Miura, and M. Suzuki, "The development of intelligent beamforming antenna systems for stratospheric platforms in the millimeter-wave band," *Wireless Pers. Commun.*, vol. 32, nos. 3–4, pp. 237–255, Feb. 2005.

[130] S. S. Siddiq, G. S. Karthikeya, T. Tanjavur, and N. Agnihotri, "Microstrip dual band millimeter-wave antenna array for UAV applications," in *Proc. Int. Conf. Microw., Radar Wireless Commun.*, Krakow, Poland, May 2016, pp. 1–4.

[131] Y. Huo and X. Dong, "Millimeter-wave for unmanned aerial vehicles networks: Enabling multi-beam multi-stream communications," Oct. 2018, *arXiv:1810.06923*. [Online]. Available: http://arxiv.org/abs/1810.06923

[132] K. Heimann, J. Tiemann, S. Boecker, and C. Wietfeld, "On the potential of 5G mmwave pencil beam antennas for UAV communications: An experimental evaluation," in *Proc. Int. ITG Workshop Smart Antennas*, Bochum, Germany, Mar. 2018, pp. 1–6.

[133] J. Li, Y. Sun, L. Xiao, S. Zhou, and C. E. Koksal, "Analog beam tracking in linear antenna arrays: Convergence, optimality, and performance," in *Proc. Asilomar Conf. Signals, Syst., Comput.*, Pacific Grove, CA, USA, Oct. 2017, pp. 1193–1198.

[134] J. Li, Y. Sun, L. Xiao, S. Zhou, and C. E. Koksal, "Fast analog beam tracking in phased antenna arrays: Theory and performance," Jun. 2017, *arXiv:1710.07873*. [Online]. Available: http://arxiv.org/abs/1710.07873

[135] W. Zhong, L. Xu, X. Lu, and L. Wang, "Research on millimeter wave communication interference suppression of UAV based on beam optimization," in *Proc. Int. Conf. Mach. Learn. Intell. Commun. (MLICOM)*, Hangzhou, China, Jul. 2018, pp. 472–481.

[136] S. Kutty and D. Sen, "Beamforming for millimeter wave communications: An inclusive survey," *IEEE Commun. Surveys Tuts.*, vol. 18, no. 2, pp. 949–973, 2nd Quart., 2016.

[137] T. He and Z. Xiao, "Suboptimal beam search algorithm and codebook design for millimeter-wave communications," *Mobile Netw. Appl.*, vol. 20, no. 1, pp. 86–97, Feb. 2015.

[138] W. Khawaja, O. Ozdemir, and I. Guvenc, "Temporal and spatial characteristics of mm wave propagation channels for UAVs," in *Proc. IEEE Global Symp. Millim. Waves (GSMM)*, Boulder, CO, USA, May 2018, pp. 1–6.

[139] M. R. Akdeniz, Y. Liu, M. K. Samimi, S. Sun, S. Rangan, T. S. Rappaport, and E. Erkip, "Millimeter wave channel modeling and cellular capacity evaluation," *IEEE J. Sel. Areas Commun.*, vol. 32, no. 6, pp. 1164–1179, Jun. 2014.

[140] S. Meng, X. Su, Z. Wen, X. Dai, Y. Zhou, and W. Yang, "Robust drones formation control in 5G wireless sensor network using mmWave," *Wireless Commun. Mobile Computing*, vol. 2018, May 2018, Art. no. 5253840.

[141] J. Rodriguez-Fernandez, N. González-Prelcic, and R. W. Heath, Jr., "Position-aided compressive channel estimation and tracking for millimeter wave multi-user MIMO air-to-air communications," in *Proc. IEEE Int. Conf. Commun. Workshops (ICC Workshops)*, Kansas City, MO, USA, May 2018, pp. 1–6.

[142] J. Zhao and W. Jia, "Channel transmission strategy for mmWave hybrid UAV communications with blockage," *Electron. Lett.*, vol. 54, no. 2, pp. 74–76, Jan. 2018.

[143] N. Rupasinghe, Y. Yapıcı, and . Güvenç, "Performance of limited feedback based NOMA transmission in mmWave drone networks," in *Proc. IEEE Int. Conf. Commun. Workshops (ICC Workshops)*, Kansas City, MO, USA, May 2018, pp. 1–6.

[144] N. Rupasinghe, Y. Yapıcı, . Güvenç, and Y. Kakishima, "Non-orthogonal multiple access for mmwave drones with multi-antenna transmission," in *Proc. 51st Asilomar Conf. Signal, Syst., Comput.*, Pacific Grove, CA, USA, Oct. 2017, pp. 958–963.

[145] N. Rupasinghe, Y. Yapıcı, . Güvenç, and Y. Kakishima, "Comparison of limited feedback schemes for NOMA transmission in mmWave drone networks," in *Proc. IEEE 19th Int. Workshop Signal Process. Adv. Wireless Commun. (SPAWC)*, Kalamata, Greece, Jun. 2018, pp. 1–5.

[146] J. Talvitie, M. Valkama, G. Destino, and H. Wymeersch, "Novel algorithms for high-accuracy joint position and orientation estimation in 5G mmWave systems," in *Proc. IEEE Globecom Workshops (GC Wkshps)*, Singapore, Dec. 2017, pp. 1–7.

[147] J. Zhao and W. Jia, "Efficient channel tracking strategy for mmWave UAV communications," *Electron. Lett.*, vol. 54, no. 21, pp. 1218–1220, Oct. 2018.

[148] A. Prokes, J. Vychodil, T. Mikulasek, J. Blumenstein, E. Zochmann, H. Groll, C. F. Mecklenbrauker, M. Hofer, D. Loschenbrand, L. Bernado, T. Zemen, S. Sangodoyin, and A. Molisch, "Time-domain broadband 60 GHz channel sounder for vehicle-to-vehicle channel measurement," in *Proc. IEEE Veh. Netw. Conf. (VNC)*, Taipei, Taiwan, Dec. 2018, pp. 1–7.

[149] S. M. Abuelenin, "On the similarity between Nakagami-m fading distribution and the Gaussian ensembles of random matrix theory," Apr. 2018, *arXiv:1803.08688*. [Online]. Available: http://arxiv.org/abs/1803.08688

[150] S. Panic, M. Stefanovic, J. Anastasov, and P. Spalevic, *Fading and Interference Mitigation in Wireless Communications*. Boca Raton, FL, USA: CRC Press, Dec. 2013.

[151] T. S. Rappaport, *Wireless Communications: Principles and Practice*, 2nd ed. Upper Saddle River, NJ, USA: Prentice-Hall, 2002.

[152] T. S. Rappaport, F. Gutierrez, Jr., E. Ben-Dor, J. N. Murdock, Y. Qiao, and J. I. Tamir, "Broadband millimeter-wave propagation measurements and

models using adaptive-beam antennas for outdoor urban cellular communications," *IEEE Trans. Antennas Propag.*, vol. 61, no. 4, pp. 1850–1859, Apr. 2013.
[153] J. Li, Y. Sun, L. Xiao, S. Zhou, and A. Sabharwal, "How to mobilize mmwave: A joint beam and channel tracking approach," in *Proc. IEEE Int. Conf. Acoust., Speech Signal Process. (ICASSP)*, Calgary, AB, Canada, Apr. 2018, pp. 3624–3628.
[154] H. Yan, S. Chaudhari, and D. Cabric, "Wideband channel tracking for mmWave MIMO system with hybrid beamforming architecture," in *Proc. IEEE Int. Workshop Comput. Adv. Multi-Sensor Adapt. Process. (CAMSAP)*, Curacao, Dutch Antilles, Dec. 2017, pp. 1–5.
[155] L. Song, Y. Li, Z. Ding, and H. V. Poor, "Resource management in non-orthogonal multiple access networks for 5G and beyond," *IEEE Netw.*, vol. 31, no. 4, pp. 8–14, Jul. 2017.
[156] Z. Ding, Y. Liu, J. Choi, Q. Sun, M. Elkashlan, C.-L. I, and H. V. Poor, "Application of non-orthogonal multiple access in LTE and 5G networks," *IEEE Commun. Mag.*, vol. 55, no. 2, pp. 185–191, Feb. 2017.
[157] Z. Xiao, L. Zhu, J. Choi, P. Xia, and X.-G. Xia, "Joint power allocation and beamforming for non-orthogonal multiple access (NOMA) in 5G millimeter wave communications," *IEEE Trans. Wireless Commun.*, vol. 17, no. 5, pp. 2961–2974, May 2018.
[158] W. Tan, S. Li, C. He, W. Tan, X. Gu, and Z. Shi, "Achievable rate of UAV-based communication with uniform circular arrays in Ricean fading," *Phys. Commun.*, vol. 32, pp. 185–191, Feb. 2019.
[159] L. Kong, L. Ye, F. Wu, M. Tao, G. Chen, and A. V. Vasilakos, "Autonomous relay for millimeter-wave wireless communications," *IEEE J. Sel. Areas Commun.*, vol. 35, no. 9, pp. 2127–2136, Sep. 2017.
[160] G. S. Thomas and C. S. Chandran, "A review on autonomous relay for millimeter wave wireless communications," *IOP Conf. Ser., Mater. Sci. Eng.*, vol. 396, Aug. 2018, Art. no. 012043.
[161] S. Fu, L. Zhao, Z. Su, and X. Jian, "UAV based relay for wireless sensor networks in 5G systems," *Sensors*, vol. 18, no. 8, p. 2413, Jul. 2018.
[162] H. Ghazzai, M. B. Ghorbel, A. Kassler, and M. J. Hossain, "Trajectory optimization for cooperative dual-band UAV swarms," in *Proc. IEEE Global Commun. Conf. (GLOBECOM)*, Abu Dhabi, United Arab Emirates, Dec. 2018, pp. 1–7.
[163] Z. Khosravi, M. Gerasimenko, S. Andreev, and Y. Koucheryavy, "Performance evaluation of UAV-assisted mmWave operation in mobility-enabled urban deployments," in *Proc. Int. Conf. Telecommun. Signal Process. (TSP)*, Athens, Greece, Jul. 2018, pp. 150–153.
[164] E. Castañeda, A. Silva, A. Gameiro, and M. Kountouris, "An overview on resource allocation techniques for multi-user MIMO systems," *IEEE Commun. Surveys Tuts.*, vol. 19, no. 1, pp. 239–284, 1st Quart., 2017.
[165] N. C. Luong, P. Wang, D. Niyato, Y. Wen, and Z. Han, "Resource management in cloud networking using economic analysis and pricing models: A survey," *IEEE Commun. Surveys Tuts.*, vol. 19, no. 2, pp. 954–1001, 2nd Quart., 2017.
[166] B. Li, Z. Fei, X. Xu, and Z. Chu, "Resource allocations for secure cognitive satellite-terrestrial networks," *IEEE Wireless Commun. Lett*, vol. 7, no. 1, pp. 78–81, Feb. 2018.
[167] S. Li, Q. Ni, Y. Sun, G. Min, and S. Al-Rubaye, "Energy-efficient resource allocation for industrial cyber-physical IoT systems in 5G era," *IEEE Trans. Ind. Informat.*, vol. 14, no. 6, pp. 2618–2628, Jun. 2018.
[168] M. Liu, F. R. Yu, Y. Teng, V. C. M. Leung, and M. Song, "Distributed resource allocation in blockchain-based video streaming systems with mobile edge computing," *IEEE Trans. Wireless Commun.*, vol. 18, no. 1, pp. 695–708, Jan. 2019.
[169] J. Chakareski, S. Naqvi, N. Mastronarde, J. Xu, F. Afghah, and A. Razi, "An energy efficient framework for UAV-assisted millimeter wave 5G heterogeneous cellular networks," *IEEE Trans. Green Commun. Netw.*, vol. 3, no. 1, pp. 37–44, Mar. 2019.
[170] S. Naqvi, J. Chakareski, N. Mastronarde, J. Xu, F. Afghah, and A. Razi, "Energy efficiency analysis of UAV-assisted mmWave HetNets," in *Proc. IEEE Int. Conf. Commun. (ICC)*, Kansas City, MO, USA, May 2018, pp. 1–6.
[171] M. Chen, W. Saad, and C. Yin, "Echo-liquid state deep learning for 360° content transmission and caching in wireless VR networks with cellular-connected UAVs," *IEEE Trans. Commun.*, to be published. doi: 10.1109/TCOMM.2019.2917440.
[172] Y. Zou, J. Zhu, X. Wang, and L. Hanzo, "A survey on wireless security: Technical challenges, recent advances, and future trends," *Proc. IEEE*, vol. 104, no. 9, pp. 1727–1765, Sep. 2016.
[173] G. Zhang, Q. Wu, M. Cui, and R. Zhang, "Securing UAV communications via joint trajectory and power control," *IEEE Trans. Wireless Commun.*, vol. 18, no. 2, pp. 1376–1389, Feb. 2019.
[174] H. Liu, S.-J. Yoo, and K. S. Kwak, "Opportunistic relaying for low-altitude UAV swarm secure communications with multiple eavesdroppers," *J. Commun. Netw.*, vol. 20, no. 5, pp. 496–508, Oct. 2018.
[175] Z. Li, M. Chen, C. Pan, N. Huang, Z. Yang, and A. Nallanathan, "Joint trajectory and communication design for secure UAV networks," *IEEE Wireless Commun. Lett.*, vol. 23, no. 4, pp. 636–639, Apr. 2019.
[176] C. Liu, T. Q. S. Quek, and J. Lee, "Secure UAV communication in the presence of active eavesdropper," in *Proc. Int. Conf. Wireless Commun. Signal Process. (WCSP)*, Nanjing, China, Oct. 2017, pp. 1–6.
[177] F. Shu, Y. Qin, R. Chen, L. Xu, T. Shen, S. Wan, S. Jin, J. Wang, and X. You, "Directional modulation: A secure solution to 5G and beyond mobile networks," Mar. 2018, *arXiv:1803.09938*. [Online]. Available: http://arxiv.org/abs/1803.09938
[178] J. Hu, S. Yan, F. Shu, J. Wang, J. Li, and Y. Zhang, "Artificial-noise-aided secure transmission with directional modulation based on random frequency diverse arrays," *IEEE Access*, vol. 5, pp. 1658–1667, 2017.
[179] F. Shu, X. Wu, J. Hu, J. Li, R. Chen, and J. Wang, "Secure and precise wireless transmission for random-subcarrier-selection-based directional modulation transmit antenna array," *IEEE J. Sel. Areas Commun.*, vol. 36, no. 4, pp. 890–904, Apr. 2018.
[180] F. Shu, S. Wan, Y. Wu, S. Yan, R. Chen, J. Li, and J. Lu, "Secure directional modulation to enhance physical layer security in IoT networks," Jan. 2017, *arXiv:1712.02104*. [Online]. Available: http://arxiv.org/abs/1712.02104
[181] Y. Ding and V. Fusco, "A review of directional modulation technology," *Int. J. Microw. Wireless Technol.*, vol. 8, no. 7, pp. 981–993, Jul. 2015.
[182] T. Xie, J. Zhu, and Y. Li, "Artificial-noise-aided zero-forcing synthesis approach for secure multi-beam directional modulation," *IEEE Commun. Lett.*, vol. 22, no. 2, pp. 276–279, Feb. 2018.
[183] J. Xiong, S. Y. Nusenu, and W.-Q. Wang, "Directional modulation using frequency diverse array for secure communications," *Wireless Pers. Commun.*, vol. 95, no. 3, pp. 2679–2689, Aug. 2017.
[184] W. Yi, Y. Liu, E. L. Bodanese, A. Nallanathan, and G. K. Karagiannidis, "A unified spatial framework for UAV-aided mmwave networks," Jan. 2019, *arXiv:1901.01432*. [Online]. Available: http://arxiv.org/abs/1901.01432
[185] B. Galkin, J. Kibilda, and L. A. DaSilva, "Backhaul for low-altitude UAVs in urban environments," in *Proc. IEEE Int. Conf. Commun. (ICC)*, Kansas City, MO, USA, May 2018, pp. 1–6.
[186] R. Kovalchukov, D. Moltchanov, A. Samuylov, A. Ometov, S. Andreev, Y. Koucheryavy, and K. Samouylov, "Analyzing effects of directionality and random heights in drone-based mmWave communication," *IEEE Trans. Veh. Technol.*, vol. 67, no. 10, pp. 10064–10069, Oct. 2018.
[187] D. S. Vasiliev, A. Abilov, I. A. Kaysina, and D. S. Meitis, "Simulation-based assesment of quality of service in UAV-assisted mmWave system in crowded area," in *Proc. IEEE Conf. Open Innov. Assoc. (FRUCT)*, Helsinki, Finland, Nov. 2018, pp. 391–397.
[188] V. Va, X. Zhang, and R. W. Heath, Jr., "Beam switching for millimeter wave communication to support high speed trains," in *Proc. IEEE 82nd Veh. Technol. Conf. (VTC-Fall)*, Boston, MA, USA, Sep. 2015, pp. 1–5.
[189] Y. Zeng, R. Zhang, and T. J. Lim, "Throughput maximization for UAV-enabled mobile relaying systems," *IEEE Trans. Commun.*, vol. 64, no. 12, pp. 4983–4996, Dec. 2016.
[190] M. F. Sohail, C. Y. Leow, and S. Won, "Non-orthogonal multiple access for unmanned aerial vehicle assisted communication," *IEEE Access*, vol. 6, pp. 22716–22727, Apr. 2018.
[191] N. Cheng, W. Xu, W. Shi, Y. Zhou, N. Lu, H. Zhou, and X. Shen, "Air-ground integrated mobile edge networks: Architecture, challenges, and opportunities," *IEEE Commun. Mag.*, vol. 56, no. 8, pp. 26–32, Aug. 2018.
[192] X. Lin, J. Xia, and Z. Wang, "Probabilistic caching placement in UAV-assisted heterogeneous wireless networks," *Phys. Commun.*, vol. 33, pp. 54–61, Apr. 2019.
[193] M. Chen, W. Saad, and C. Yin, "Liquid state machine learning for resource allocation in a network of cache-enabled LTE-U UAVs," in *Proc. IEEE Global Commun. Conf. (GLOBECOM)*, Singapore, Dec. 2017, pp. 1–6.
[194] M. H. Tareque, M. S. Hossain, and M. Atiquzzaman, "On the routing in flying ad hoc networks," in *Proc. Federated Conf. Comput. Sci. Inf. Syst.*, Lodz, Poland, Oct. 2015, pp. 1–9.

[195] S. Bi, C. K. Ho, and R. Zhang, "Wireless powered communication: Opportunities and challenges," *IEEE Commun. Mag.*, vol. 53, no. 4, pp. 117–125, Apr. 2015.

[196] Y. Wu, L. Qiu, and J. Xu, "UAV-enabled wireless power transfer with directional antenna: A two-user case," in *Proc. Int. Symp. Wireless Commun. Syst. (ISWCS)*, Lisbon, Portugal, Aug. 2018, pp. 1–6.

[197] J. Park, H. Lee, S. Eom, and I. Lee, "Wireless powered communication networks aided by an unmanned aerial vehicle," in *Proc. IEEE 88th Veh. Technol. Conf. (VTC-Fall)*, Chicago, IL, USA, Aug. 2018, pp. 1–5.

[198] Y. Sun, D. W. K. Ng, D. Xu, L. Dai, and R. Schober, "Resource allocation for solar powered UAV communication systems," in *Proc. IEEE Int. Workshop Signal Process. Adv. Wireless Commun. (SPAWC)*, Kalamata, Greece, Jun. 2018, pp. 1–5.

[199] H. Yanikomeroglu, "Integrated terrestrial/non-terrestrial 6G networks for ubiquitous 3D super-connectivity," in *Proc. ACM Int. Conf. Modeling, Anal. Simulation Wireless Mobile Syst.*, Oct. 2018, pp. 3–4.

[200] X. Cao, P. Yang, M. Alzenad, X. Xi, D. Wu, and H. Yanikomeroglu, "Airborne communication networks: A survey," *IEEE J. Sel. Areas Commun.*, vol. 36, no. 10, pp. 1907–1926, Sep. 2018.

[201] E. C. Strinati, S. Barbarossa, J. L. Gonzalez-Jimenez, D. Kténas, N. Cassiau, and C. Dehos, "6G: The next frontier," May 2019, *arXiv:1901.03239*. [Online]. Available: https://arxiv.org/abs/1901.03239

[202] J. Liu, Y. Shi, Z. M. Fadlullah, and N. Kato, "Space-air-ground integrated network: A survey," *IEEE Commun. Surveys Tuts.*, vol. 20, no. 4, pp. 2714–2741, 4th Quart., 2018.

[203] K. J. White, E. Denney, M. D. Knudson, A. K. Mamerides, and D. P. Pezaros, "A programmable SDN+NFV-based architecture for UAV telemetry monitoring," in *Proc. 14th IEEE Annu. Consum. Commun. Netw. Conf. (CCNC)*, Las Vegas, NV, USA, Jan. 2017, pp. 522–527.

[204] C. Rametta and G. Schembra, "Designing a softwarized network deployed on a fleet of drones for rural zone monitoring," *Future Internet*, vol. 9, no. 1, p. 8, Mar. 2017.

[205] R. Mijumbi, J. Serrat, J.-L. Gorricho, N. Bouten, F. D. Turck, and R. Boutaba, "Network function virtualization: State-of-the-art and research challenges," *IEEE Commun. Surveys Tuts.*, vol. 18, no. 1, pp. 236–262, 1st Quart., 2016.

[206] X. Cheng, Y. Wu, G. Min, and A. Y. Zomaya, "Network function virtualization in dynamic networks: A stochastic perspective," *IEEE J. Sel. Areas Commun.*, vol. 36, no. 10, pp. 2218–2232, Oct. 2018.

[207] B. Yi, X. Wang, S. K. Das, K. Li, and M. Huang, "A comprehensive survey of network function virtualization," *Comput. Netw.*, vol. 133, pp. 212–262, Mar. 2018.

[208] W. Saad, M. Bennis, and M. Chen, "A vision of 6G wireless systems: Applications, trends, technologies, and open research problems," Feb. 2019, *arXiv:1902.10265*. [Online]. Available: http://arxiv.org/abs/1902.10265

[209] F. Tariq, M. R. A. Khandaker, K. Wong, M. A. Imran, M. Bennis, and M. Debbah, "A speculative study on 6G," Feb. 2019, *arXiv:1902.06700*. [Online]. Available: http://arxiv.org/abs/1902.06700

[210] T. Braud, F. H. Bijarbooneh, D. Chatzopoulos, and P. Hui, "Future networking challenges: The case of mobile augmented reality," in *Proc. IEEE Int. Conf. Distrib. Comput. Syst. (ICDCS)*, Atlanta, GA, USA, Jun. 2017, pp. 1796–1807.

[211] C. Jiang, H. Zhang, Y. Ren, Z. Han, K.-C. Chen, and L. Hanzo, "Machine learning paradigms for next-generation wireless networks," *IEEE Wireless Commun.*, vol. 24, no. 2, pp. 98–105, Apr. 2017.

[212] M. Chen, U. Challita, W. Saad, C. Yin, and M. Debbah, "Machine learning for wireless networks with artificial intelligence: A tutorial on neural networks," Oct. 2017, *arXiv:1710.02913*. [Online]. Available: http://arxiv.org/abs/1710.02913

[213] Y. Sun, M. Peng, Y. Zhou, Y. Huang, and S. Mao, "Application of machine learning in wireless networks: Key techniques and open issues," *IEEE Commun. Surveys Tuts.*, to be published. doi: 10.1109/COMST.2019.2924243.

[214] C. Zhang, P. Patras, and H. Haddadi, "Deep learning in mobile and wireless networking: A survey," *IEEE Commun. Surveys Tuts.*, to be published. doi: 10.1109/COMST.2019.2904897.

[215] R. Lowe, Y. Wu, A. Tamar, J. Harb, O. P. Abbeel, and I. Mordatch, "Multi-agent actor-critic for mixed cooperative-competitive environments," in *Proc. Adv. Neural Info. Process. Syst.*, Long Beach, CA, USA, Dec. 2017, pp. 6379–6390.

[216] X. Wang, Y. Han, C. Wang, Q. Zhao, X. Chen, and M. Chen, "In-edge AI: Intelligentizing mobile edge computing, caching and communication by federated learning," *IEEE Netw.*, to be published. doi: 10.1109/MNET.2019.1800286.

[217] Y. Xu, R. Xu, W. Yan, and P. Ardis, "Concept drift learning with alternating learners," in *Proc. Int. Joint Conf. Neural Netw. (IJCNN)*, Anchorage, AK, USA, May 2017, pp. 2104–2111.

LONG ZHANG received the B.E. degree in communication engineering from the China University of Geosciences, Wuhan, China, in 2006, and the Ph.D. degree in communication and information systems from the University of Science and Technology Beijing, Beijing, China, in 2012. In 2017, he was a Visiting Scholar with the School of Computing, Tokyo Institute of Technology, Tokyo, Japan. He is currently an Associate Professor with the School of Information and Electrical Engineering, Hebei University of Engineering, Handan, China, and a Visiting Postdoctoral Fellow with the Department of Electrical and Computer Engineering, University of Houston, Houston, TX, USA. His research interests include cognitive radio, vehicular networks, UAV-assisted wireless networks, network functions virtualization, fog/edge computing, deep space communications, space–terrestrial integrated networks, AI-enabled networks, radio resource allocation, machine learning, and hypergraph for wireless networking.

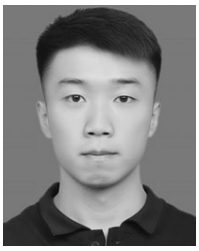

HUI ZHAO received the B.E. degree in information and computing science from Shijiazhuang University, Shijiazhuang, China, in 2017. He is currently pursuing the M.S. degree in computer science and technology with the Department of Communication Engineering, School of Information and Electrical Engineering, Hebei University of Engineering, Handan, China. His current research interests include UAV-assisted wireless networks, resource allocation, physical-layer security, mmWave communications, federated reinforcement learning, and big data.

SHUAI HOU received the M.S. degree in control theory and control engineering and the Ph.D. degree in material processing engineering from Northeastern University, Shenyang, China, in 2009 and 2015, respectively. He is currently an Associate Professor of automation technology with the School of Information and Electrical Engineering, Hebei University of Engineering, Handan, China. His current research interests include stochastic modeling, data mining, UAV topology control, edge caching, and compact deep neural networks.

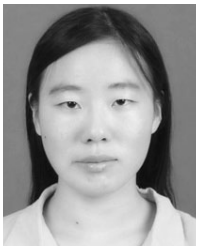

ZHEN ZHAO received the B.E. degree in communication engineering from the Qingdao Institute of Technology, Qingdao, China, in 2018. She is currently pursuing the M.S. degree in computer science and technology with the Department of Communication Engineering, School of Information and Electrical Engineering, Hebei University of Engineering, Handan, China. Her current research interests include UAV-enabled networks, wireless power transfer, multi-access edge computing, resource allocation, and multi-agent deep reinforcement learning.

HAITAO XU received the B.E. degree in communication engineering from Sun Yat-sen University, Guangzhou, China, in 2007, the M.E. degree in communication system and signal processing from the University of Bristol, U.K., in 2009, and the Ph.D. degree in communication and information systems from the University of Science and Technology Beijing, Beijing, China, in 2014. He was a Postdoctoral Fellow with the University of Science and Technology Beijing, where he is currently an Associate Professor. He held a Visiting Professor position at the ECE Department, University of Houston, USA, from 2016 to 2017. His research interests include wireless communication, cognitive radio, game theory, secure communications, and mobile edge computing.

XIAOBO WU received the Ph.D. degree in communication and information systems from the Department of Communication Engineering, School of Computer and Communication Engineering, University of Science and Technology Beijing, Beijing, China, in 2013. He is currently a Senior Engineer with the China Academy of Transportation Sciences. His research interests include the Internet of Vehicles, UAV-aided vehicular networks, transportation informatization, vehicle trajectory optimization, intelligent transport systems, and AI-enabled vehicular networks.

QIWU WU received the B.E. degree in computer science and technology from Hunan Normal University, Changsha, China, in 2005, and the Ph.D. degree in communication and information systems from the University of Science and Technology Beijing, Beijing, China, in 2010. He was a Postdoctoral Fellow with the School of Electrical and Information Engineering, Xi'an Jiaotong University, Xi'an, China. He is currently an Associate Professor with the Engineering University of PAP, Xi'an. His research interests include the Internet of Things, UAV networking, secure communications, millimeter-wave communications, visible light communications, and optical networks.

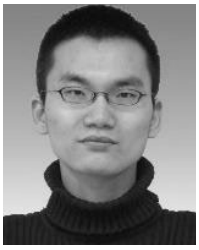

RONGHUI ZHANG received the B.Sc. (Eng.) degree from the Department of Automation Science and Electrical Engineering, Hebei University, Baoding, China, in 2003, the M.S. degree in vehicle application engineering from Jilin University, Changchun, China, in 2006, and the Ph.D. (Eng.) degree in mechanical and electrical engineering from the Changchun Institute of Optics, Fine Mechanics and Physics, Chinese Academy of Sciences, Changchun, in 2009. He finished his Postdoctoral Research Work at INRIA, Paris, France, in 2011. He is currently a Research Fellow with the Guangdong Key Laboratory of Intelligent Transportation System, School of intelligent systems engineering, Sun Yat-sen University, Guangzhou, China. He has published more than 20 papers in international journals. His current research interests include computer vision, intelligent control, and intelligent transportation systems.